THE REE MINERALS OF THE BASTNÄS-TYPE DEPOSITS, SOUTH-CENTRAL SWEDEN

Dan HOLTSTAM[§]

Department of Mineralogy, Swedish Museum of Natural History, Box 50007, SE–104 05 Stockholm, Sweden

Ulf B. ANDERSSON[ⴶ]

GeoforschungsZentrum, P.B. 4.1, Telegrafenberg, D-14473 Potsdam, Germany

Abstract

On the basis of characteristic assemblages, the Bastnäs-type Fe–(Cu–)REE skarn deposits in the Bergslagen mining region of south-central Sweden can be divided into two subtypes: one almost exclusively with LREE enrichment (subtype 1, mainly in the Riddarhyttan–Bastnäs area), and another showing enrichment of both LREE and Y + HREE (subtype 2, Norberg District). New data have been collected on twenty REE species including three unnamed ones, using electron-microprobe analysis, X-ray diffraction and Mössbauer spectroscopy. Cerite-(Ce) is, together with ferriallanite-(Ce), the most important REE mineral at Bastnäs, but less common at the subtype-2 deposits. Compared to other occurrences worldwide, the present samples of cerite-(Ce) are poor in Ca and enriched in Mg and F. Calcium and (REE + Y) in the samples are negatively correlated, and the upper limit for Ca is close to 1 *apfu*. Iron ranges from 0.01 to 0.30 *apfu*, and is mainly in the trivalent state. Cerite-(Ce) is a major carrier of Y (up to 3.5 wt.% Y_2O_3). Fluorbritholite is found only in the subtype-2 deposits, and is low in P, Na and the actinides compared to other major occurrences in the world. Significant inter- and intrasample variations in REE and Y occur, ranging from fluor-britholite-(Ce) to the unaccredited member "fluorbritholite-(Y)". Fluorbritholite is non-stoichiometric, with Ca < 2 and (REE + Y) > 3 *apfu*. Västmanlandite-(Ce) is another important host for the REE in subtype 2. By means of the substitutions Mg^{2+} + $F^- \rightarrow Fe^{3+} + O^{2-}$ and $Mg^{2+} \rightarrow Fe^{2+}$, it forms solid solutions with an unnamed Fe-dominant member that is found in the subtype-1 deposits. Dollaseite-(Ce), which forms a partial solid-solution series with dissakisite-(Ce), is restricted to subtype 2. Gadolinite is very rare at the subtype-1 deposits, and more widespread in the Norberg District. All samples have a significant hingganite component in solid solution (0.10–0.35 molar fraction). Single crystals are commonly zoned with respect to REE and Y, with compositions corresponding to gadolinite-(Ce), gadolinite-(Y) and an Nd-dominant member. The substantial fractionation of REE and Y on a local scale within the Bastnäs-type deposits is dependent both on crystal-chemical factors and on fluctuations in fluid composition during crystallization. The initial precipitation of REE silicates in type-1 and type-2 deposits (mainly cerite and fluorbritholite, respectively) was a reaction between relatively acidic solutions carrying major amounts of REE complexed mainly by ligands of F and Si, and dolomitic host-rocks.

Keywords: REE minerals, cerite, dollaseite, fluorbritholite, gadolinite, törnebohmite, västmanlandite, Bastnäs, Norberg, Sweden.

[§]   *Present address*: Swedish Research Council, SE–103 78 Stockholm, Sweden. *E-mail address*: dan.holtstam@vr.se
[ⴶ]   *Formerly at:* Department of Mineralogy, Swedish Museum of Natural History, Box 50007, SE–104 05 Stockholm, Sweden

Sommaire

A la lumière des assemblages caractéristiques, on peut diviser les gisements de skarns à Fe–(Cu–)TR (terres rares) du type Bastnäs dans le camp minier de Bergslagen, partie centre-sud de la Suède, en deux sous-types: le sous-type 1, avec exemples surtout dans la région de Riddarhyttan–Bastnäs, montre presqu'exclusivement un enrichissement en terres rares légères, tandis que le sous-type 2, avec exemples dans le district de Norberg, montre à la fois un enrichissement dans les terres rares légères et lourdes et en yttrium. Nous présentons des données nouvelles (microsonde électronique, diffraction X et spectroscopie de Mössbauer) pour vingt espèces minérales contenant les terres rares, y compris trois sans nom. La cérite-(Ce) et la ferriallanite-(Ce) seraient les deux minéraux de TR les plus importants à Bastnäs; ils sont moins importants dans les gisements de sous-type 2. Comparés aux autres exemples ailleurs au monde, nos échantillons de cérite-(Ce) ont une faible teneur en Ca, et ils sont enrichis en Mg et F. Les teneurs en Ca et en TR + Y montrent une corrélation négative, et la limite supérieure des teneurs en Ca est proche de 1 *apfu*. La teneur en fer va de 0.01 à 0.30 *apfu*, et le fer serait surtout à l'état trivalent. La cérite-(Ce) est l'hôte principal de Y (jusqu'à 3.5% Y$_2$O$_3$, poids). La fluorbritholite n'est présente que dans les gisements du sous-type 2, et elle est faible en P, Na et les actinides par rapport aux exemples connus de cette espèce à l'échelle mondiale. On note des variations importantes en TR et en Y entre échantillons et à l'intérieur d'un seul échantillon; ceux-ci varient de fluorbritholite-(Ce) au pôle non homologué "fluorbritholite-(Y)". La fluorbritholite est non-stoechiométrique, avec Ca < 2 et (TR + Y) > 3 *apfu*. La västmanlandite-(Ce) serait un autre hôte important des TR dans les gisements de sous-type 2. Grâce aux substitutions Mg^{2+} + F$^-$ → Fe^{3+} + O^{2-} et Mg^{2+} → Fe^{2+}, elle forme une solution solide avec un membre à dominance de Fe, sans nom, dans les gisements du sous-type 1. La dollaséite-(Ce), qui forme une solution solide partielle avec la dissakisite-(Ce), n'est présente que dans les gisements du sous-type 2. La gadolinite est très rare dans les gisements du sous-type 1, et davantage répandue dans le district de Norberg. Tous les échantillons montrent une proportion importante de la composante hingganite en solution solide (fraction molaire entre 0.10 et 0.35). Les monocristaux sont généralement zonés par rapport aux TR et à Y, avec des compositions correspondant à gadolinite-(Ce), gadolinite-(Y) et un pôle ayant Nd dominant. L'enrichissement relatif local marqué en TR et en Y au sein des gisements de type Bastnäs dépend à la fois des facteurs critallochimiques et des fluctuations dans la composition de la phase fluide au cours de la cristallisation. La précipitation initiale d'un silicate de TR dans les gisements de type 1 et 2 (principalement cérite et fluorbritholite, respectivement) est due à la réaction entre des solutions relativement acides porteuses de quantités importantes de TR complexées par des ligands contenant F et Si, et des roches hôtes dolomitiques.

(Traduit par la Rédaction)

Mots-clés: minéraux de terres rares, cérite, dollaséite, fluorbritholite, gadolinite, törnebohmite, västmanlandite, Bastnäs, Norberg, Suède.

Introduction

The Bastnäs Fe–Cu–REE deposit belongs to the Riddarhyttan ore field, Skinnskatteberg District, Sweden, where mining, primarily for iron, was pursued already in late medieval times (Carlborg 1923). The scientific study of this remarkable locality commenced when Cronstedt (1751) described a "flesh-colored, heavy rock" called *Bastnäs tungsten*, which had been found in a small copper mine at Bastnäs, known as S:t Göransgruvan ("St. George's mine"). This material is presently known as the mineral cerite-(Ce), from which Hisinger & Berzelius (1804) extracted previously unknown oxides. They named the corresponding metal cerium, and subsequent discoveries of other rare-earth elements (REE) and new mineral species have made the locality prominent in the history of natural science.

Geijer (1961) introduced the generic term "Bastnäs type" by including other Fe deposits, all strongly enriched in REE and with a putatively common origin, situated mainly in the Norberg District, *ca*. 30 km northeast of Bastnäs. The present work also includes the Rödbergsgruvan deposit in the Nora District, 50 km to the southwest, where the characteristic REE mineralization with, *e.g.*, cerite-(Ce), was not recognized until the 1980s.

Researchers have paid little attention to the Bastnäs-type deposits in recent times, and few primary data have been collected since the 1920s. Here we present new mineral-chemical and some paragenetic data for the REE minerals. A second paper (Holtstam *et al.*, in prep.) focuses on the genetic aspects of these unique deposits.

Geological Setting and Mineral Assemblages of the Deposits

The Bastnäs-type deposits are restricted to a northeast-trending narrow carbonate-bearing zone within early Svecofennian (1.91–1.88 Ga) supracrustal rocks, mainly felsic metavolcanic rocks and marble, situated in the northwestern part of the Bergslagen mining region, central southern Sweden (Fig. 1). The metavolcanic sequences have undergone extensive synvolcanic hydrothermal alteration, causing metasomatic enrichments in K, Na, and Mg in successive pulses and areas (*e.g.,* Geijer 1923, Trägårdh 1991, Hallberg 2003). In the areas of the Bastnäs-type deposits, Mg metasomatism is most prominent in the country rocks, and the supracrustal sequences later became metamorphosed under amphibolite-facies conditions (Trägårdh 1988).

Allen *et al.* (1996) provided a synthesis of the volcano-tectonic history of Bergslagen.

The supracrustal units were intruded by at least two generations of plutonic rocks. The older, early Svecofennian (1.90–1.86 Ga) intrusions range from gabbro through tonalite and granodiorite to granite in composition, and are normally deformed and metamorphosed along with the supracrustal units (*e.g.,* Lindh & Persson 1990). Rocks of the younger, late Svecofennian (1.81–1.75 Ga) group vary from undeformed, homogeneous granites to migmatites (Andersson & Öhlander 2004, and references therein). Overlapping in time with the latter (1.82–1.78 Ga, Romer & Smeds 1997), numerous pegmatite dykes and bodies cut the early Svecofennian rocks in Bergslagen (*e.g.,* Ambros 1983). Later tectonic stresses caused fracturing and faulting, affecting all types of rock in the area.

In the Norberg District, typical REE mineralization has been reported from a few iron mines, now abandoned. The deposits consist of disseminated to massive magnetite–amphibole skarn replacements in dominantly dolomitic marbles (Geijer 1936). Fluorine-rich minerals, such as norbergite, chondrodite, fluorian phlogopite and fluorite, are commonly associated with the REE minerals (Geijer 1927). Sulfide mineralization, with mainly pyrite, molybdenite and chalcopyrite, is locally important. Samples used in the present investigation originate from the mines Östanmossagruvan (60°5'N, 15°56'E), Södra Hackspikgruvan (*ca.* 60°4'N, 15°57'E; now inaccessible), Johannagruvan (60°4'N, 15°55'E) and Malmkärragruvan (60°4'N, 15°51'E).

At the Bastnäs (strictly *Nya* Bastnäs) deposit (59°51'N, 15°35'E), quartz-banded hematite ore is juxtaposed with a magnetite-skarn ore that has more or less completely replaced a dolomite marble horizon (Geijer 1921). The dominant country-rock is a metasomatized volcanic rock, essentially quartz-rich, commonly cordierite-bearing mica schist (Ambros 1983). The REE mineralization is associated with amphibole skarns and was encountered in two shallow mines at a maximum depth of 30 m, where it formed restricted zones up to 0.6 m thick and less than 10 m long (Geijer 1921). Talc and quartz appear locally. Sulfide minerals, dominantly chalcopyrite, bismuthinite and molybdenite, are closely associated with the REE minerals, and commonly interstitial to them. Minor opaque phases detected are carrollite, bornite, covellite, wittichenite, emplectite, hodrushite, tetradymite, kupčíkite, native copper, native bismuth and gold–silver alloys; uranium oxide is locally found within blebs of solidified bitumens (Holtstam & Enserö 2002, Enserö 2003). Although originally mined as a copper and iron deposit, about 160 metric tonnes of REE ore produced from Bastnäs was sold over the period 1860–1919 (Carlborg 1923).

The Rödbergsgruvan deposit (59°30'N, 14°53'E) is at the southern end of the zone described above. It consists of a quartz-rich magnetite ore with sulfide impregnations (mainly pyrite), associated with diversi-fied skarn-type assemblages comprising, *e.g.,* tremolite, cummingtonite, almandine, talc, micas and chlorite minerals (Geijer & Magnusson 1944). The REE mineralization has not been described from an *in situ* occurrence in this case. In the mine dumps, sporadic finds of magnetite–amphibole skarn associated with REE silicates and sulfides have been made (K. Gatedal, pers. commun., 2002).

On the basis of composition and paragenesis of REE minerals, the deposits have been subdivided into two subtypes (Holtstam & Andersson 2002): one almost exclusively enriched in LREE (subtype 1; Bastnäs and Rödbergsgruvan), and another showing enrichment of LREE and HREE + Y (subtype 2; Norberg area). Both are characterized in detail below.

METHODS

About forty polished thin sections were prepared from representative specimens of REE-mineral assemblages and examined under a polarizing microscope. Scanning electron microscopy studies were performed on carbon-coated sections using a field-emission instrument (Hitachi S4300), fitted with a back-scattered electron (BSE) detector, and an energy-dispersive X-ray (EDX) micro-analyzer (Oxford Instruments) that was used as an aid in mineral identification (qualitative analyses).

The chemical composition of the REE minerals was determined using wavelength-dispersion analyses on a Cameca SX50 electron microprobe (EMP) at GeoForschungsZentrum in Potsdam. The acceleration voltage was 20 kV, with a beam current of 40 nA and a beam diameter of 3 μm. As standards, we used pure synthetic REE phosphates (REE$L\alpha$ for La, Ce, Yb, Lu; REE$L\beta$ for the remaining REE), YPO$_4$, (Y$L\alpha$), PrPO$_4$ (P$K\alpha$), Fe$_2$O$_3$ (Fe$K\alpha$), wollastonite (Ca$K\alpha$, Si$K\alpha$), MgO (Mg$K\alpha$), Al$_2$O$_3$ (Al$K\alpha$), tugtupite (Cl$K\alpha$) and LiF (F$K\alpha$). Each peak was measured during 30 or 50 s (10 and 25 s for the background, respectively). Data reduction was made using a Cameca version of the PAP (Pouchou & Pichoir 1991) routine.

The concentration of fluorine was calculated by empirical correction for the interference of Ce$L\alpha$ on F$K\alpha$. The elements Mn, Ti, Ba, Sr, Na, Th and U were routinely monitored, but found to be below the limit of detection ($\leq$ 0.05 wt.%) in most REE minerals analyzed. A few complementary analyses were done at the Department of Earth Sciences, Uppsala University, with the same kind of instrument and with similar settings and standards (Ho, Yb, Lu were not measured in these sessions). However, F$K\alpha$ was measured using a TAP crystal (PC1 in Potsdam), resulting in a considerably higher level of detection (ca. 0.4 wt.% instead of 0.1 wt.%) and poorer analytical precision. Note that the concentration of Eu cannot be measured with the technique employed here owing to interference with some of the LREE. The chondrite-normalized REE patterns
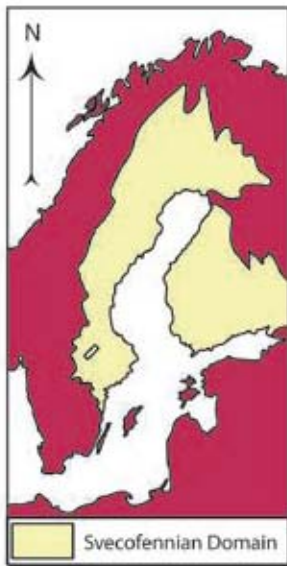
Fe oxide deposit with REE mineralization (Bastnäs type)

Granite, ≤ 1800 Ma

Gabbro etc.

Granite-granodiorite-tonalite, ≥ 1850 Ma (deformed)

Metacarbonate

Supracrustal, mainly felsic metavolcanic, rock

presented in this paper, based on the EMP results, were plotted using the chondrite abundance-values of Boynton (1984). Element ratios in the text (*e.g.,* Y/Ce) are given on a molar (atomic) basis.

X-ray powder-diffraction data for selected samples were recorded with step (0.02° per 2.5 s) scans in the 2θ range 3 to 70° on an automated Philips PW1710 diffractometer using graphite-monochromatized Cu$K\alpha$ radiation (PW1830 generator operated at 40 kV and 40 mA). Peak positions were determined with the X'Pert Graphics & Identify program, and 2θ was corrected against an external silicon standard. Unit-cell dimensions were determined using reflections equivalent in number to at least five times the number of refined parameters, and a least-squares program (Novak & Colville 1989).

Mössbauer ^{57}Fe absorption spectra were obtained at room temperature for a few iron-bearing samples that could be purified, following crushing and sieving, by hand-picking under a binocular microscope. A ^{57}Co(Rh) source (nominally 1.8 w × 10^9 Bq) was used as a source of γ radiation, and velocity calibration was done against a 25 μm thick foil of α-Fe. The powdered samples (corresponding to an absorber thickness of maximum 5 mg/cm^2), were run at magic-angle geometry (54.7°) using a constant-acceleration spectrometer and stored in a 1024-channel analyzer. Spectral analyses, assuming a "thin" absorber and a Lorentzian line-shape, were carried out using the software developed by Jernberg & Sundqvist (1983). The centroid shift (CS), quadrupole splitting (QS) and line width (Γ) are parameters used to characterize the absorption doublets.

RESULTS: CHARACTERISTICS OF THE REE MINERALS

Fluocerite

Fluocerite, (Ce,La)F$_3$, is known from the Bastnäs deposit (Geijer 1921), where it is a relatively rare constituent of the cerite ore. Fresh grains, normally less than 1 mm across, are irregular in outline and in direct contact with cerite-(Ce) or bastnäsite-(Ce). The mineral is partly altered (Fig. 2A). In cases where alteration is complete, only a very fine-grained, turbid and partly porous material remains. We have identified bastnäsite-(La) and

cerianite as the principal products of its breakdown (see below). Ten-point analyses of sample #02+ 0052 gave, on average: Ce$_2$O$_3$ 36.51 (range 32.90–38.92), La$_2$O$_3$ 39.82 (34.10–48.67), Nd$_2$O$_3$ 5.85 (4.77–6.42), Pr$_2$O$_3$ 2.18 (1.91–2.45), Sm$_2$O$_3$ 0.13 (0.10–0.22), Gd$_2$O$_3$ 0.25 (0.08–0.43), SiO$_2$ 0.09 (0.00–0.16), CaO 0.05 (0.01–0.10), F 24.76 (21.83–27.95), O = F –10.42, sum 99.22 (all in wt.%). The range of La/ (La + Ce) values is 0.49–0.57 (mean 0.52), indicating that the mineral is essentially fluocerite-(La). As the analyses correspond to only 0.80–0.91 mole fractions of the (REE)F$_3$ component, the deficiency in the F contents relative to the ideal formula of fluocerite might possibly be explained by an as yet unproven substitution of OH$^-$ or O^{2-} for F$^-$. The unit-cell parameters of the analyzed sample, determined by powder XRD, are a 7.155(6), c 7.290(5) Å, V 323.2(6) Å^3 (hexagonal cell).

The breakdown of fluocerite to bastnäsite has been documented from several occurrences (*e.g.,* Styles & Young 1983, Lahti & Suominen 1988, Beukes *et al.* 1991, Imaoka & Nakashima 1994). This is generally believed to occur by reaction with carbonic aqueous fluids: (Ce,La)F$_3$ + CO$_2$ (aq) + H$_2$O → (Ce,La)(CO$_3$) F + 2 HF (aq). The presence of cerianite in association with altered fluocerite has been ascribed to a late oxidation of Ce (*e.g.,* Van Wambeke 1977, Lahti & Suominen 1988). However, we note a decrease of Ce/ La in the secondary bastnäsite relative to that of fluocerite in our samples (Fig. 3). A reaction representing the alteration process, which takes the approximate composition of the reactants and products into account, could then be: (La$_{0.5}$Ce$_{0.5}$)F$_3$ + 0.83 CO$_2$ + 1.17 H$_2$O → 0.83 (La$_{0.6}$Ce$_{0.4}$)(CO$_3$)F + 0.17 CeO$_2$ (cerianite) + 2.17 HF + 0.08 H$_2$.

Cerianite

Cerianite, ideally CeO$_2$, is a product of the alteration of fluocerite in the Bastnäs deposit. It exists as microscopic grains less than 20 μm across (Fig. 2B), and the small volumes of sample presented difficulties in the analyses. Concentrations (wt.%) obtained from measurements of two grains in #A37 that produced reasonably high totals are: CeO$_2$ 91.70, 92.32, La$_2$O$_3$ 1.08, 1.03, Nd$_2$O$_3$ 2.75, 1.79, Sm$_2$O$_3$ 0.26, 0.22, Gd$_2$O$_3$ 0.11, 0.08, SiO$_2$ 0.13, 1.14, CaO 0.22, 0.23, F 0.98, 0.84, Cl 0.05, 0.06, O = F,Cl –0.42, –0.36, sum 97.86, 97.35, which yield an average formula Ce$^{4+}_{0.93}$Nd$_{0.02}$La$_{0.01}$ Si$_{0.02}$Ca$_{0.01}$O$_{1.92}$F$_{0.08}$ on the basis of one cation. We believe that the significant contents of F obtained are real; the monovalent anion balances the minor amounts of REE^{3+} and Ca^{2+}. Note that CeO$_2$ and the oxyfluoride CeOF are isostructural compounds, with a fluorite-type atomic arrangement (Strunz & Nickel 2001); thus limited solid-solution is not unexpected. The refined unit-cell parameter of cerianite in this sample, a 5.411(3) Å, is identical to the literature value for the pure synthetic dioxide, 5.41134(12) Å (PDF 34–394).

FIG. 1. Geological map (position indicated by small rectangle in the inset map) of the area with location of Bastnäs-type deposits, based on work by the Geological Survey of Sweden (Ambros 1983, 1988, Lundström & Koark 1979). R: Rödbergsgruvan, B: Bastnäs field (subtype 1). Malmkärra (M), Johannagruvan (J), S. Hackspikgruvan (H) and Östanmossa (Ö) are located near the town of Norberg (subtype 2).
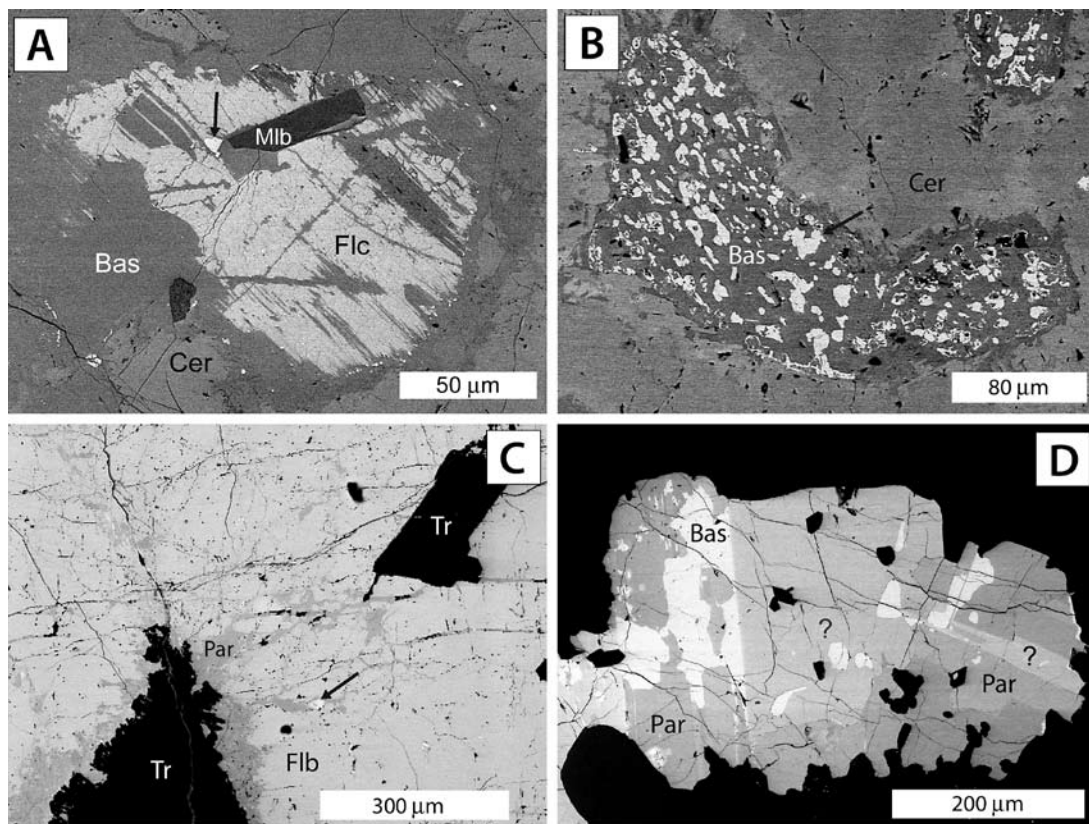
FIG. 2. BSE images of assemblages of REE minerals from Bastnäs-type deposits. (A) Sample #02+0052 from Bastnäs, with fluocerite (Flc), bastnäsite (Bas), cerite (Cer) and molybdenite (Mlb). Some alteration to cerianite (arrow) has occurred. (B) Sample #A37, Bastnäs, with fluocerite grains broken down completely to bastnäsite-(La) and cerianite (arrow). (C) Sample #430644 from Östanmossa with tremolite (Tr) and fluorbritholite (Flb), the latter mineral partly altered to parisite (Par) and bastnäsite. (D) Sample #540155 from Östanmossa with a grain of intergrown fluorocarbonates. Phases of intermediate grey-scale level and compositions are indicated by ?.

Håleniusite-(La)

Håleniusite-(La), (La, Ce)OF, is a secondary mineral formed by alteration of primary bastnäsite-(La), most likely *via* a decarbonation reaction, (La, Ce)CO$_3$F → (La, Ce)OF + CO$_2$ (Holtstam *et al.* 2004). It is quite common in the Bastnäs deposit; considering the variations in La/Ce encountered in bastnäsite (see below), it is expected that a Ce-dominant analogue exists there as well.

Parisite-(Ce)

Parisite-(Ce), CaCe$_2$(CO$_3$)$_3$F$_2$, has been identified in a few samples from the Östamossa mine (subtype 2). In sample #430644, this fluorocarbonate occurs in large grains of "fluorbritholite-(Y)", where it partly replaces the host mineral along edges and fractures (Fig. 2C). Individual grains of parisite-(Ce) may reach 200 μm across, and occasionally the mineral occurs in parallel intergrowth lamellae (20–40 μm wide) with an unknown fluorocarbonate with lower Ca and F contents. Locally, parisite-(Ce) also is found in direct contact with bastnäsite-(Ce). In #540155, aggregates (0.2–1 mm) of fluorocarbonates are distributed in a matrix of tremolite, calcite, dolomite, dollaseite-(Ce) and magnetite. From the results of the EMP analyses (Table 1), we conclude that the patchily to regularly intergrown phases (Fig. 2D) consist of parisite-(Ce), bastnäsite-(Ce) and an intermediate (on the gray scale of BSE images), unnamed mineral. Tremolite is euhedral toward the fluorocarbonate minerals, which occasionally also incorporate small crystals of an amphibole and magnetite.
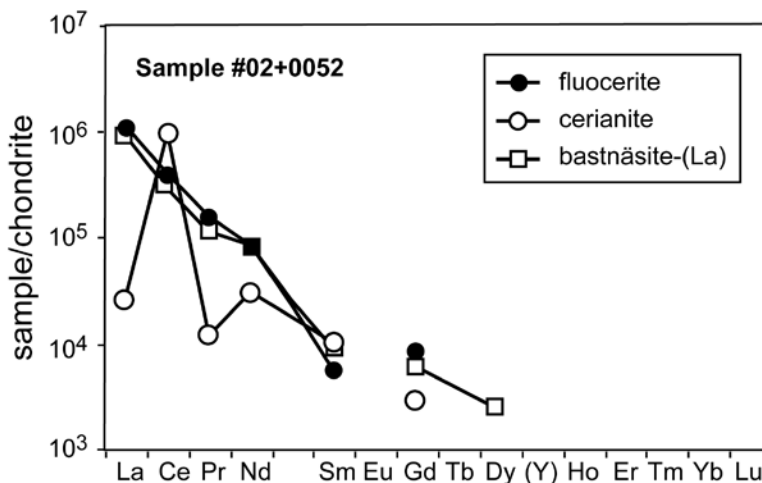
FIG. 3. Chondrite-normalized REE patterns of fluocerite and its alteration products, from the Bastnäs deposit.

Parisite-(Ce) differs from most samples of bastnäsite, the dominant fluorocarbonate at these deposits, in its high concentration of Nd (Nd > La for most points analyzed) and Y (0.8–5.6% Y_2O_3). Refinement of powder XRD data for #430644 indexed on a hexagonal unit-cell gave a 7.099(2), c 28.12(2) Å (representing a pseudocell of a monoclinic polytype, or the true unit-cell of a hexagonal variety; *cf*. Ni *et al*. 2000).

Bastnäsite-(Ce) – bastnäsite-(La)

Bastnäsite, $(Ce,La)CO_3F$, was first described from the type locality by Hisinger (1838). It is a ubiquitous although subordinate component of the cerite ore, where it occurs normally as small grains (≤0.2 mm) interstitial to the REE-bearing silicates. In all sections of this material, one can observe that cerite-(Ce), and törnebohmite-(Ce) to some extent, are replaced by bastnäsite as fine grains. Coarse-grained homogeneous masses of bastnäsite are less common in the Bastnäs deposit. In sample #882234, the mineral fills cavities in a mass of ferriallanite-(Ce), which is distinctly euhedral toward the bastnäsite. Rare, minute grains of cerite-(Ce) are found in bastnäsite. Molybdenite and quartz occupy minor parts of the cavities, and euhedral crystals of bastnäsite are occasionally seen enclosed in the latter mineral.

In the Norberg District, bastnäsite is generally less common and, in some instances, it is found mainly as a microscopic phase in association with fluorbritholite-(Ce) or cerite-(Ce). However, in S. Hackspikgruvan, here represented by sample #381132, elongate, slightly bent crystals of bastnäsite-(Ce) up to 20 mm in length appear in fibrous amphibole skarn. Small, subhedral grains of dollaseite-(Ce), fluorbritholite-(Ce) and fluorian phlogopite occur sporadically along the contact between amphibole and the bastnäsite-(Ce). The sample is rich in fluorite, as selvages around bastnäsite, as fracture infillings and inclusions in the latter mineral, and as significant impregnations in the amphibole mass (Fig. 4A).

Lanthanum, Ce and Nd are the dominant REE in all samples of bastnäsite, amounting to 94–98 atom % for subtype 1 and 89–97 atom % for subtype 2 (Table 2, Fig. 5). The Nd contents are in the range of 0.05–0.14 atoms per formula unit (*apfu*); two samples from Östanmossa, coexisting with Nd-rich parisite-(Ce), are exceptional in having >0.20 *apfu* Nd. The ratio Ce/(Ce + La) lies in the range 0.43–0.67, corresponding to an intermediate part of the bastnäsite-(La)–bastnäsite-(Ce) solid-solution series. The compositional heterogeneity can also be significant within a sample. A total of 36 point analyses were collected along a 2-mm traverse on the coarse-grained material in #882234; Ce/(Ce + La) ranges from 0.472 to 0.577, with a mean of 0.496 ± 0.003. The parameters for this sample are a 7.142(2) and c 9.788(2) Å (hexagonal cell). Ni *et al*. (1993) gave a 7.118, c 9.762 Å for a bastnäsite-(Ce) specimen slightly poorer in La. For most samples, the F content does not significantly deviate from the stoichiometric value of 1 *apfu*, considering the analytical uncertainty. A few analyses, however, suggest a component of hydroxylbastnäsite, $(Ce,La)CO_3(OH)$, in solid solution with bastnäsite (samples ##060375, 970319).

TABLE 1. CHEMICAL COMPOSITION OF FLUOROCARBONATES

Sample#	430644 Ö parisite						540155 Ö zoned grain					
point	a p2	a p3	a p8	a p9	b p7	b p8	p1	p2	p3	p4	p5	p6
$La_2(CO_3)_3$ wt%	12.65	11.76	18.72	19.40	15.83	19.25	19.30	17.59	16.83	18.34	17.57	21.92
$Ce_2(CO_3)_3$	33.54	32.89	39.14	39.86	37.72	38.28	40.00	37.24	34.81	38.03	35.10	43.01
$Pr_2(CO_3)_3$	4.58	4.61	4.65	4.65	4.76	4.27	5.21	4.65	4.36	5.07	4.49	5.15
$Nd_2(CO_3)_3$	21.73	22.80	19.46	19.91	20.74	17.49	24.05	23.19	20.52	23.15	20.64	23.08
$Sm_2(CO_3)_3$	4.14	4.46	2.38	2.36	2.75	2.12	3.39	3.31	3.26	3.60	3.15	2.89
$Gd_2(CO_3)_3$	2.93	2.98	1.08	1.06	1.57	1.34	1.02	1.03	1.49	1.27	1.26	0.76
$Tb_2(CO_3)_3$	0.14	0.15	0.04	0.00	0.03	0.00	n.d.	n.d.	n.d.	n.d.	n.d.	n.d.
$Dy_2(CO_3)_3$	0.42	0.48	0.00	0.00	0.00	0.04	0.10	0.10	0.23	0.04	0.10	0.14
$Ho_2(CO_3)_3$	0.07	0.14	0.05	0.00	0.06	0.00	n.d.	n.d.	n.d.	n.d.	n.d.	n.d.
$Er_2(CO_3)_3$	0.20	0.04	0.15	0.18	0.09	0.01	n.d.	n.d.	n.d.	n.d.	n.d.	n.d.
$Yb_2(CO_3)_3$	0.05	0.04	0.03	0.00	0.00	0.04	n.d.	n.d.	n.d.	n.d.	n.d.	n.d.
$Lu_2(CO_3)_3$	0.00	0.00	0.00	0.00	0.00	0.00	n.d.	n.d.	n.d.	n.d.	n.d.	n.d.
$Y_2(CO_3)_3$	5.31	5.65	0.81	0.90	1.16	1.17	0.58	0.60	1.11	0.46	0.59	0.34
$CaCO_3$	18.40	18.19	15.96	16.75	17.73	17.76	10.53	10.15	14.91	7.99	14.72	0.01
$PbCO_3$	0.00	0.00	0.02	0.00	0.00	0.00	n.d.	n.d.	n.d.	n.d.	n.d.	n.d.
$FeCO_3$	0.00	0.07	0.01	0.05	0.00	0.32	0.00	0.00	0.00	0.00	0.00	0.00
F	6.22	6.26	7.12	6.01	6.88	6.95	4.98	5.76	5.24	6.01	5.75	6.66
Cl	0.04	0.05	0.04	0.06	0.05	0.03	n.d.	n.d.	n.d.	n.d.	n.d.	n.d.
$CO_3 \approx F$	-9.82	-9.88	-11.25	-9.49	-10.87	-10.98	-7.87	-9.09	-8.27	-9.48	-9.08	-10.52
Total	100.57	100.67	98.41	101.69	98.49	98.10	101.29	94.53	94.48	94.48	94.29	93.45
La *apfu*	0.30	0.28	0.46	0.46	0.38	0.46	0.83	0.80	0.44	1.03	0.46	0.23
Ce	0.78	0.77	0.95	0.94	0.90	0.92	1.70	1.68	0.90	2.12	0.90	0.44
Pr	0.11	0.11	0.11	0.11	0.11	0.10	0.22	0.21	0.11	0.28	0.12	0.05
N.d.	0.50	0.52	0.47	0.46	0.49	0.41	1.01	1.03	0.52	1.26	0.52	0.23
Sm	0.09	0.10	0.06	0.05	0.06	0.05	0.14	0.14	0.08	0.19	0.08	0.03
Gd	0.06	0.06	0.02	0.02	0.03	0.03	0.04	0.04	0.04	0.07	0.03	0.01
Tb	0.00	0.00	0.00	0.00	0.00	0.00						
Dy	0.01	0.01	0.00	0.00	0.00	0.00	0.00	0.00	0.01	0.00	0.00	0.00
Ho	0.00	0.00	0.00	0.00	0.00	0.00						
Er	0.00	0.00	0.00	0.00	0.00	0.00						
Yb	0.00	0.00	0.00	0.00	0.00	0.00						
Lu	0.00	0.00	0.00	0.00	0.00	0.00						
Y	0.16	0.17	0.03	0.03	0.04	0.04	0.03	0.03	0.04	0.03	0.02	0.00
Ca	0.99	0.97	0.90	0.91	0.98	0.98	1.03	1.05	0.88	1.02	0.87	0.00
Pb	0.00	0.00	0.00	0.00	0.00	0.00						
Fe	0.00	0.00	0.00	0.00	0.00	0.02	0.00	0.00	0.00	0.00	0.00	0.00
F	1.76	1.77	2.10	1.72	2.00	2.01	2.57	3.15	1.63	4.04	1.79	0.83
Cl	0.01	0.01	0.01	0.01	0.01	0.01						
Σ cations	3.00	3.00	3.00	3.00	3.00	3.00	5.00	5.00	3.00	6.00	3.00	1.00

n.d.: not determined. Ö: Östanmossa.

Lanthanite-(*Ce*)

Lanthanite-(Ce), $Ce_2(CO_3)_3 \cdot 8H_2O$, is a secondary mineral formed at low temperatures (<100°C), and appears locally as a coating on cerite–ferriallanite ore. Crystals are lath-like to platy in habit and normally less than 1 mm across. The accredited type-locality for lanthanite-(Ce) is the Britannia mine in North Wales (Bevins *et al*. 1985). However, lanthanite-(Ce) from Bastnäs was first described and analyzed by Berzelius (1825). The crystal structure of the mineral was determined on material from the original type-locality (Dal Negro *et al*. 1977). Atencio *et al*. (1989) determined the composition of a single sample from Bastnäs to show that it is clearly Ce-dominant. This is supported by EDX analyses performed by us on four specimens (#g10778,

g30592, 23:0475, 221690), that consistently have Ce > La ≈ Nd > Pr > Sm. A more complete chemical analysis of this mineral with the EMP proved to be difficult due to violent degassing under the electron beam.

Cerite-(*Ce*)

Cerite-(Ce), $(Ce,La,Ca)_9(Mg,Fe)(SiO_4)_6(SiO_3OH)$ $(OH,F)_3$, is locally rock-forming at Bastnäs. It occurs in medium-grained (0.2–1 mm) masses; individual crystals are normally anhedral. Replacement veins of ferriallanite-(Ce) ± törnebohmite-(Ce) commonly transect the cerite ore, in many cases to such an extent that cm-sized "islands" of cerite-(Ce) are completely surrounded by these minerals. Quartz occurs sporadically as an interstitial phase. Small grains of sulfide (chalcopyrite,
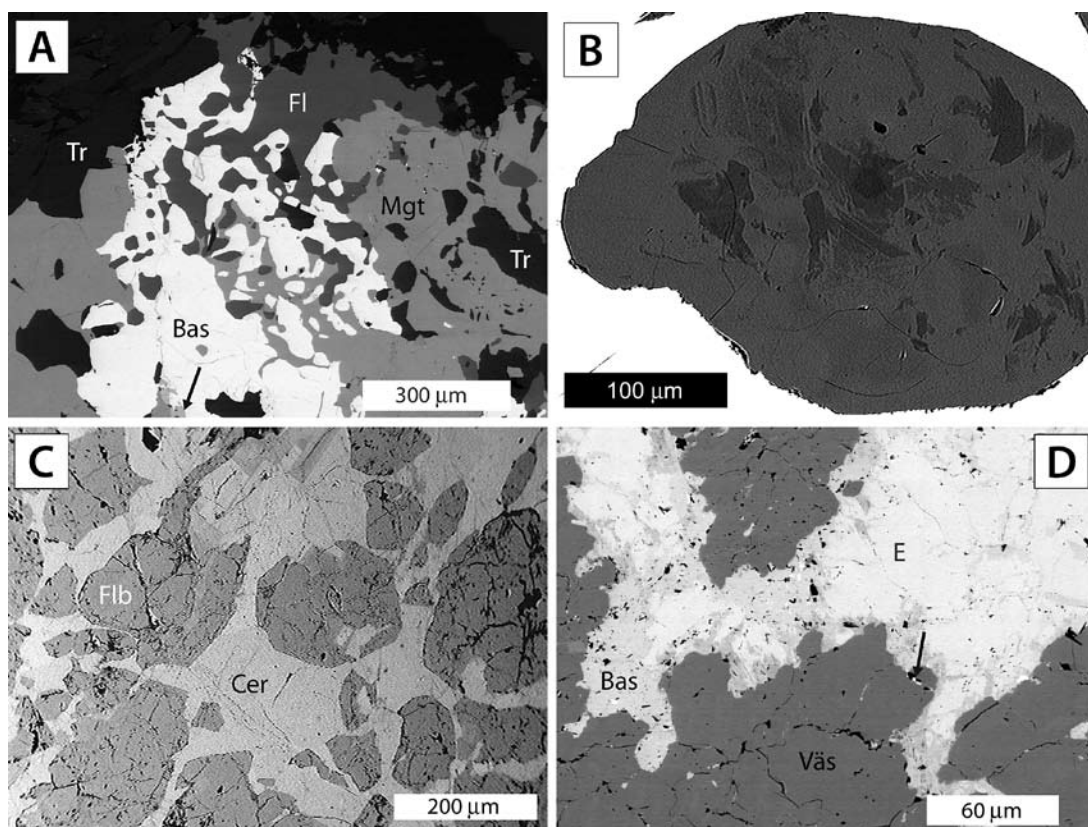
FIG. 4.   BSE images of REE mineral assemblages from Bastnäs-type deposits. (A) Sample #381132 from S. Hackspikgruvan with bastnäsite (Bas), tremolite (Tr), fluorite (Fl), magnetite (Mgt) and västmanlandite (arrow). (B) Sample #390477, Bastnäs, with a heterogeneous grain of cerite-(Ce) enclosed by bismuthinite. (C) Sample #03+0029 from Malmkärra with fluorbritholite (Flb) and cerite (Cer). (D) Sample #UU318/77, Malmkärra, with unnamed mineral E partly altered to bastnäsite, and västmanlandite (Väs). The arrow points to a small grain of scheelite.

molybdenite) are occasionally found dispersed in the cerite-(Ce) masses. Rarely, *e.g.,* in sample #390477, subhedral crystals of cerite-(Ce) are found embedded in massive bismuthinite (Fig. 4B) associated with subordinate chalcopyrite and molybdenite. Locally (in S:t Göransgruvan), here represented by sample #LK4838, cerite-(Ce) forms layers up to 5 cm thick sandwiched between fibrous masses of actinolite, with the amphibole crystals oriented perpendicular to the cerite-(Ce) layers. Ferriallanite-(Ce), törnebohmite-(Ce) and talc have developed extensively at the layer boundaries.

At Rödbergsgruvan (#880072), cerite-(Ce) constitutes deformed lenses up to 2 cm thick, within coarse-grained aggregates of a calcic amphibole (actinolite–edenite in composition); the two minerals are separated by a zone 0.5–1 mm wide of mainly ferriallanite-(Ce) + the Fe analogue of västmanlandite-(Ce). Bastnäsite-(Ce), amphibole and ferriallanite-(Ce) also occur within the cerite-(Ce) mass.

In the subtype-2 deposits of the Norberg area, cerite-(Ce) is subordinate in relation to fluorbritholite-(Ce), which has a similar megascopic appearance. Sample #660298 from Malmkärra is a lump of REE silicates with amphibole as a minor constituent. A few veinlets of pyrite up to 2 mm thick transect the specimen. Cerite-(Ce) forms aggregates of anhedral grains (with an average size of *ca.* 0.5 mm), in contact with subhedral grains of västmanlandite-(Ce) up to 1 mm across, and minor amounts of anhedral bastnäsite-(Ce). Chalcopyrite is found as small grains interstitial to the REE minerals. In #490216 from Johannagruvan, cerite-(Ce) and bastnäsite-(La) occur as patches up to 10 mm across surrounded by a thick margin of dollaseite-(Ce), in a matrix of dense amphibole skarn. Bastnäsite-(Ce) forms larger, coherent areas, whereas cerite-(Ce) occurs as fine-grained aggregates with an irregular outline. Subhedral grains of västmanlandite up to 0.5 mm wide occur close to the contact between

TABLE 2. CHEMICAL COMPOSITION OF BASTNÄSITE

Sample #	A37 B			LK4838 B				g10778 B			060375 B	381132 H		
point	a p6	a p11	b p5	p11	p12	p14	p15	b p2	b p3	b p5	b p6	a p1	b p10	b p17
La$_2$(CO$_3$)$_3$ wt%	34.21	43.03	51.44	49.18	54.55	49.43	50.95	42.92	48.94	39.06	41.25	42.99	43.64	43.09
Ce$_2$(CO$_3$)$_3$	48.58	45.58	43.33	43.97	40.55	44.18	43.00	47.25	44.84	49.70	46.73	46.89	46.57	46.83
Pr$_2$(CO$_3$)$_3$	3.98	3.18	2.23	2.58	1.96	2.64	2.42	3.21	2.58	3.68	3.15	3.12	3.18	3.12
Nd$_2$(CO$_3$)$_3$	14.42	9.87	6.24	6.99	5.57	7.06	6.50	10.11	7.88	11.70	11.33	9.53	9.38	9.44
Sm$_2$(CO$_3$)$_3$	1.09	0.57	0.20	0.25	0.16	0.25	0.17	0.57	0.36	0.83	0.88	0.41	0.23	0.38
Gd$_2$(CO$_3$)$_3$	0.53	0.20	0.03	0.19	0.27	0.04	0.09	0.30	0.26	0.12	0.39	0.23	0.12	0.20
Tb$_2$(CO$_3$)$_3$	0.00	0.06	0.00	0.00	0.00	0.00	0.00	0.14	0.03	0.00	0.00	0.00	0.00	0.00
Dy$_2$(CO$_3$)$_3$	0.03	0.00	0.00	0.00	0.00	0.00	0.00	0.02	0.03	0.00	0.00	0.01	0.01	0.00
Ho$_2$(CO$_3$)$_3$	0.00	0.17	0.05	0.03	0.05	0.00	0.00	0.00	0.03	0.00	0.00	0.05	0.00	0.05
Er$_2$(CO$_3$)$_3$	0.11	0.06	0.10	0.00	0.05	0.02	0.06	0.00	0.00	0.00	0.08	0.00	0.00	0.00
Yb$_2$(CO$_3$)$_3$	0.00	0.01	0.00	0.00	0.03	0.01	0.00	0.00	0.00	0.06	0.00	0.04	0.01	0.00
Lu$_2$(CO$_3$)$_3$	0.00	0.00	0.00	0.00	0.00	0.04	0.00	0.00	0.00	0.01	0.01	0.00	0.00	0.00
Y$_2$(CO$_3$)$_3$	0.17	0.06	0.05	0.06	0.02	0.05	0.01	0.17	0.32	0.15	0.15	0.01	0.03	0.04
CaCO$_3$	0.06	0.02	0.11	0.06	0.03	0.04	0.02	0.03	0.09	0.04	0.04	0.02	0.06	0.02
PbCO$_3$	0.07	0.06	0.00	0.00	0.00	0.07	0.07	0.01	0.00	0.00	0.01	0.00	0.00	0.03
FeCO$_3$	0.01	0.00	0.00	0.00	0.01	0.05	0.00	0.00	0.00	0.00	0.00	0.00	0.00	0.00
F	8.23	8.37	8.01	8.41	8.46	8.45	8.28	7.38	7.45	7.51	4.22	8.62	8.43	8.42
Cl	0.03	0.02	0.03	0.02	0.02	0.02	0.02	0.02	0.02	0.03	0.03	0.02	0.03	0.03
CO$_3$=F	-13.0	-13.2	-12.6	-13.3	-13.4	-13.3	-13.1	-11.7	-11.8	-11.9	-6.7	-13.6	-13.3	-13.3
Total	98.50	98.03	99.18	98.47	98.37	99.00	98.51	100.5	101.1	101.0	101.6	98.34	98.38	98.36
La *apfu*	0.333	0.421	0.497	0.478	0.530	0.477	0.495	0.412	0.466	0.373	0.399	0.418	0.425	0.420
Ce	0.471	0.443	0.416	0.425	0.392	0.424	0.416	0.451	0.424	0.472	0.449	0.454	0.451	0.454
Pr	0.038	0.031	0.021	0.025	0.019	0.025	0.023	0.031	0.024	0.035	0.030	0.030	0.031	0.030
Nd	0.137	0.094	0.059	0.066	0.053	0.067	0.062	0.095	0.073	0.109	0.107	0.091	0.089	0.090
Sm	0.010	0.005	0.002	0.002	0.002	0.002	0.002	0.005	0.003	0.008	0.008	0.004	0.002	0.003
Gd	0.005	0.002	0.000	0.002	0.002	0.000	0.001	0.003	0.002	0.001	0.004	0.002	0.001	0.002
Tb	0.000	0.001	0.000	0.000	0.000	0.000	0.000	0.001	0.000	0.000	0.000	0.000	0.000	0.000
Dy	0.000	0.000	0.000	0.000	0.000	0.000	0.000	0.000	0.000	0.000	0.000	0.000	0.000	0.000
Ho	0.000	0.001	0.000	0.000	0.000	0.000	0.000	0.000	0.000	0.000	0.000	0.000	0.000	0.000
Er	0.001	0.000	0.001	0.000	0.000	0.000	0.001	0.000	0.000	0.000	0.001	0.000	0.000	0.000
Yb	0.000	0.000	0.000	0.000	0.000	0.000	0.000	0.000	0.000	0.000	0.000	0.000	0.000	0.000
Lu	0.000	0.000	0.000	0.000	0.000	0.000	0.000	0.000	0.000	0.000	0.000	0.000	0.000	0.000
Y	0.002	0.001	0.001	0.001	0.000	0.001	0.000	0.002	0.004	0.002	0.002	0.000	0.000	0.000
Ca	0.001	0.000	0.002	0.001	0.001	0.001	0.000	0.001	0.002	0.001	0.001	0.000	0.001	0.000
Pb	0.001	0.001	0.000	0.000	0.000	0.001	0.001	0.000	0.000	0.000	0.000	0.000	0.000	0.000
Fe	0.000	0.000	0.000	0.000	0.000	0.001	0.000	0.000	0.000	0.000	0.000	0.000	0.000	0.000
F	0.966	0.985	0.932	0.984	0.991	0.983	0.970	0.853	0.854	0.864	0.491	1.011	0.988	0.987
Cl	0.002	0.001	0.002	0.002	0.001	0.001	0.001	0.001	0.001	0.002	0.002	0.001	0.002	0.002

B: Bastnäs, H: S. Hackspikgruvan. The compositional data are first expressed in wt%, then in *apfu*, calculated on the basis of one cation.

dollaseite-(Ce) and cerite-(Ce). In #03+0029 from Malmkärra, cerite-(Ce) occurs in close association with fluorbritholite-(Ce), where it locally has replaced the latter mineral (Fig. 4C). This material in part displays a sector-like pattern of zonation on BSE images, related to variations in Ca and REE concentrations between the zones.

The crystal structure of cerite-(Ce) was solved on material from Mountain Pass, California (Moore & Shen 1983). There are three non-equivalent positions in the structure, occupied mainly by REE, each coordinated to (8 O + 1 OH). The REE polyhedra are connected to form rods, to which isolated SiO$_4$ tetrahedra are attached. A second type of parallel rods consists of SiO$_3$OH tetrahedra and (Mg,Fe)O$_6$ octahedra. Calcium enters the REE sites plus a six-coordinated site with low occupancy, Ca(x), and possibly also the *M* sites. On the basis of bond-valence calculations, Pakhomovsky *et al.* (2002) suggested a modified structural formula with a higher number of OH groups for cerite-(La), (La,Ce,Ca)$_9$(Fe,Ca,Mg)(SiO$_4$)$_3$[SiO$_3$(OH)]$_4$(OH)$_3$. Cerite is thus structurally complex, and shows a significant compositional variability.

Compared to other occurrences worldwide (Förster 2000, and references therein), the present material is poor in Ca and enriched in Mg and F (Tables 3a, b).

TABLE 2 (cont'd). CHEMICAL COMPOSITION OF BASTNÄSITE

Sample #	430 644 Ö	880072 R	882234 B								970319 M
point	b p6	p5	a p6	a p7	b tr	b tr	b tr	b tr	b tr	b tr	c p3	v14
$La_2(CO_3)_3$	23.65	37.63	45.80	35.93	48.47	48.49	47.50	45.37	44.83	44.55	47.98	34.33
$Ce_2(CO_3)_3$	48.63	48.93	45.00	49.32	43.53	43.83	44.09	45.29	45.31	46.04	43.63	48.78
$Pr_2(CO_3)_3$	5.28	3.50	2.77	3.82	2.72	2.50	2.81	2.89	2.83	2.96	2.79	4.01
$Nd_2(CO_3)_3$	21.31	10.62	8.64	12.75	7.62	7.78	8.04	8.98	8.62	9.02	7.82	13.57
$Sm_2(CO_3)_3$	2.22	0.57	0.46	0.77	0.39	0.39	0.28	0.56	0.45	0.49	0.33	0.93
$Gd_2(CO_3)_3$	1.02	0.12	0.14	0.39	0.18	0.18	0.13	0.12	0.21	0.28	0.12	0.50
$Tb_2(CO_3)_3$	0.02	0.00	0.00	0.00	0.00	0.01	0.00	0.00	0.00	0.00	0.00	0.00
$Dy_2(CO_3)_3$	0.00	0.00	0.00	0.00	0.00	0.07	0.00	0.02	0.00	0.03	0.06	0.06
$Ho_2(CO_3)_3$	0.00	0.03	0.09	0.00	0.00	0.00	0.00	0.12	0.07	0.00	0.05	0.00
$Er_2(CO_3)_3$	0.10	0.00	0.02	0.12	0.00	0.10	0.08	0.00	0.04	0.08	0.02	0.01
$Yb_2(CO_3)_3$	0.05	0.00	0.04	0.00	0.03	0.00	0.00	0.03	0.02	0.03	0.00	0.00
$Lu_2(CO_3)_3$	0.00	0.00	0.04	0.00	0.01	0.00	0.00	0.05	0.04	0.00	0.03	0.04
$Y_2(CO_3)_3$	0.53	0.17	0.12	0.15	0.09	0.10	0.10	0.08	0.10	0.08	0.08	0.46
$CaCO_3$	0.12	0.04	0.03	0.04	0.04	0.03	0.02	0.04	0.06	0.08	0.15	0.08
$PbCO_3$	0.00	0.00	0.05	0.00	0.00	0.00	0.05	0.00	0.06	0.00	0.02	0.04
$FeCO_3$	0.00	0.00	0.00	0.00	0.00	0.03	0.00	0.01	0.02	0.00	0.00	0.04
F	8.42	8.54	7.94	7.89	8.34	8.34	8.44	8.38	8.42	8.40	7.77	6.62
Cl	0.05	0.03	0.04	0.02	0.03	0.03	0.03	0.02	0.04	0.02	0.03	0.04
$CO_3=F$	-13.3	-13.5	-12.5	-12.5	-13.2	-13.2	-13.3	-13.2	-13.3	-13.3	-12.3	-10.5
Total	98.11	96.71	98.66	98.73	98.27	98.70	98.22	98.73	97.79	98.81	98.59	99.05
La *apfu*	0.231	0.372	0.446	0.350	0.472	0.470	0.463	0.440	0.438	0.432	0.467	0.335
Ce	0.473	0.481	0.436	0.478	0.422	0.423	0.427	0.437	0.441	0.444	0.422	0.474
Pr	0.051	0.034	0.027	0.037	0.026	0.024	0.027	0.028	0.027	0.028	0.027	0.039
Nd	0.204	0.103	0.082	0.121	0.072	0.074	0.076	0.085	0.082	0.085	0.074	0.129
Sm	0.021	0.005	0.004	0.007	0.004	0.004	0.003	0.005	0.004	0.004	0.003	0.009
Gd	0.009	0.001	0.001	0.003	0.002	0.002	0.001	0.001	0.002	0.002	0.001	0.004
Tb	0.000	0.000	0.000	0.000	0.000	0.000	0.000	0.000	0.000	0.000	0.000	0.000
Dy	0.000	0.000	0.000	0.000	0.000	0.001	0.000	0.000	0.000	0.000	0.001	0.001
Ho	0.000	0.000	0.001	0.000	0.000	0.000	0.000	0.001	0.001	0.000	0.000	0.000
Er	0.001	0.000	0.000	0.001	0.000	0.001	0.001	0.000	0.000	0.001	0.000	0.000
Yb	0.000	0.000	0.000	0.000	0.000	0.000	0.000	0.000	0.000	0.000	0.000	0.000
Lu	0.000	0.000	0.000	0.000	0.000	0.000	0.000	0.000	0.000	0.000	0.000	0.000
Y	0.007	0.002	0.002	0.002	0.001	0.001	0.001	0.001	0.001	0.001	0.001	0.006
Ca	0.003	0.001	0.001	0.001	0.001	0.001	0.000	0.001	0.001	0.002	0.003	0.002
Pb	0.000	0.000	0.000	0.000	0.000	0.000	0.000	0.000	0.001	0.000	0.000	0.000
Fe	0.000	0.000	0.000	0.000	0.000	0.001	0.000	0.000	0.000	0.000	0.000	0.001
F	0.993	1.017	0.931	0.926	0.978	0.975	0.990	0.980	0.992	0.980	0.911	0.779
Cl	0.003	0.002	0.002	0.001	0.002	0.002	0.001	0.002	0.001	0.002	0.002	0.002

B: Bastnäs, M: Malmkärra, Ö: Östanmossa, R: Rödbergsgruvan. The compositional data are first expressed in wt%, then in *apfu*, calculated on the basis of one cation.

The sums (Ca + REE + Y) are in the range 8.94–9.18 (mean 9.05) *apfu*. However, the Ca content is normally below 1 *apfu* (mostly 0.4–0.9) and negatively correlated with REE + Y (Fig. 6), indicating that the fraction of Ca atoms entering the *M* or the Ca(x) sites is minor in our samples. Iron ranges from 0.01 to 0.30 *apfu*, with lower values associated with specimens from the subtype-2 localities. Mössbauer spectra obtained on two samples from Bastnäs (#060375, #A37) reveal that Fe is dominantly in the trivalent state in cerite-(Ce), corresponding to *ca.* 80% of the total amount. The CS values, 0.33–0.35 mm/s, are consistent with Fe^{3+} ions being located at an octahedral site. The hyperfine parameters for the minor Fe^{2+} fraction, CS and QS both in the range 1.2–1.3 mm/s, suggest a coordination number of 6 or higher. There is a clear negative correlation between Mg and Fe for the present sample-population. Possible exchange-mechanisms to explain this trend would be $Fe^{3+} + Ca^{2+} = Mg^{2+} + REE^{3+}$ or $Fe^{3+} + O^{2-} = Mg^{2+} + F^-$, but so far they lack support from direct structural evidence.

Generally, cerite-(Ce) is homogeneous with respect to the concentration of SiO_2, corresponding to a narrow range with 6.83 to 7.07 Si *apfu*. In one sample (#390477), there are, however, rare grains with irregular patches (dark on BSE images; Fig. 4B) that show large fluctuations in (SiO_2 17–24 wt.%) and low totals. Cerite-(Ce) is a major carrier of Y, with up to 2.1 and 3.5 wt.% Y_2O_3 at the subtype-1 and subtype-2 deposits, respectively. The chondrite-normalized

curves for the mineral are quite distinct from those of associated epidote-group minerals and fluorocarbonates (Fig. 7); the cerite curves have an upward convex shape related to a relative enrichment of Nd, Sm and Gd, in particular, compared with the coexisting REE minerals. Cerite-(Ce) shows significant and variable F contents, corresponding to 1.18–1.72 *apfu*; nothing is known at present, however, about the structural role of the anion. Note that most REE-bearing silicates at the Bastnäs-type deposit contain no detectable Cl; however,

low concentrations of this element, 0.04 to 0.09 wt.%, are found in cerite-(Ce) (the estimated detection-level at 3σ is *ca.* 0.02 wt.% for Cl) .

The hexagonal unit-cell for two samples yield the parameters *a* 10.737(6), *c* 37.81(2) Å, *V* 3775 Å^3 (#060375) and *a* 10.763(8), *c* 37.89(3) Å, *V* 3802 Å^3 (#03+0029), respectively. Moore & Shen (1983) gave *a* 10.779, *c* 38.06 Å, *V* 3830 Å^3 for cerite-(Ce) from Mountain Pass, and Pakhomovsky *et al.* (2002) reported *a* 10.749, *c* 38.318 Å, *V* 3834 Å^3 for cerite-(La) from
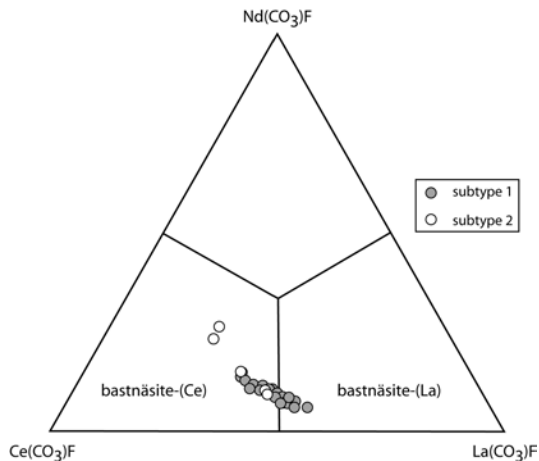
FIG. 5.   Compositional diagram for the dominant REE in bastnäsite.
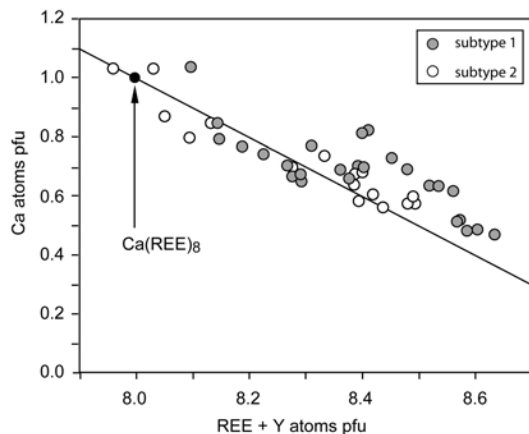
FIG. 6.   Compositional diagram showing the variation of Ca *versus* (REE + Y) in cerite-(Ce). The straight line corresponds to an ideal REE+ Y + Ca = 9 *apfu*.
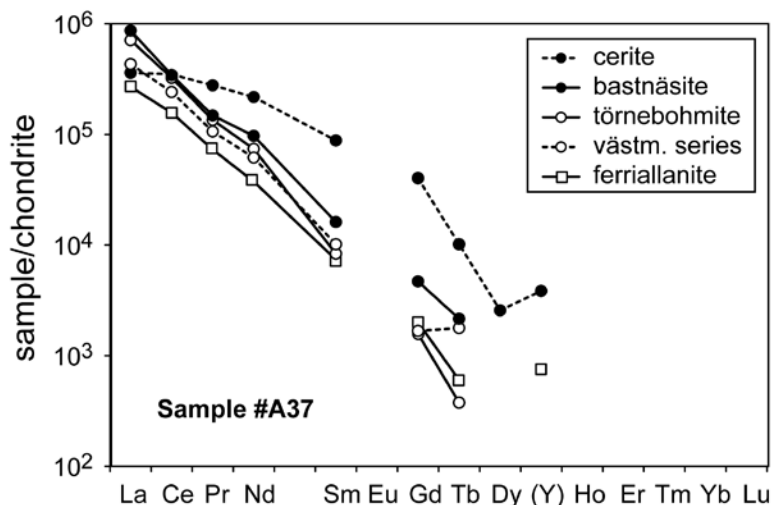
FIG. 7.   Chondrite-normalized patterns for coexisting REE minerals from Bastnäs (a selected typical sample).

Khibina, Kola Peninsula. The larger unit-cell volume in the latter case, as compared to the Bastnäs-type material, might be explained by significant difference in Ce/La between cerite from the two localities.

On the basis of an examination of the relatively small amount of modern chemical data (EMP) that presently exist, it seems plausible that the term "cerite" embraces more than one distinct species, if variations in the M-type cations were to be considered in the nomenclature. All samples analyzed in the present study have Mg > Fe [0.69 < Mg/(Mg + Fe) < 0.99], whereas Al is generally at or below the limit of detection. The material from the Niederbobritzsch granite (Erzgebirge, Germany) analyzed by Förster (2000) contains significant Al (up to 1.04 $apfu$), little Fe and no Mg. Chakhmouradian & Zaitsev (2002) reported another Mg-free variety, from the Afrikanda Complex, Kola Peninsula, displaying some variations in Fe and Al [0.50 < Fe/(Fe + Al) < 0.76]. In the type specimen of cerite-(La), Fe is the dominant cation at the M site, which is also inferred to contain significant Ca (0.30 $apfu$; Pakhomovsky et al. 2002). Note that all examples of cerite referred to here have elevated concentrations of Ca, with a range from 4.42 wt.% (Khibina) to 9.33 wt.% CaO (Afrikanda), compared to our material (maximum 3.0 wt.% CaO). Clearly, new crystal-structure refinements of cerite from several localities, combined with

TABLE 3a. CHEMICAL COMPOSITION OF CERITE FROM BASTNÄS AND RÖDBERGSGRUVAN

Sample#	A37		LK4838					52:414		060375				
point	a p5	a p12	p6	p7	p8	p9	p10	b p2	b p5	b p5	b p9	b v2	b v4	b v14
La$_2$O$_3$ wt%	13.22	12.99	16.79	15.93	17.99	17.58	17.43	11.40	16.03	14.72	13.95	14.45	14.10	13.73
Ce$_2$O$_3$	34.19	31.89	34.21	35.03	33.89	34.30	34.22	34.66	31.99	31.93	31.62	31.72	31.14	30.98
Pr$_2$O$_3$	3.98	3.93	3.64	3.64	3.37	3.45	3.61	4.14	3.64	3.65	3.58	3.70	3.61	3.42
Nd$_2$O$_3$	15.06	15.38	12.86	13.30	12.22	12.46	12.41	16.60	13.81	14.70	14.53	14.44	14.30	14.04
Sm$_2$O$_3$	1.80	2.18	1.52	1.59	1.45	1.35	1.48	1.95	1.84	2.49	2.68	2.43	2.66	2.73
Gd$_2$O$_3$	1.02	1.38	0.99	0.70	0.76	0.71	0.83	0.71	0.98	1.50	1.80	1.71	1.93	2.03
Dy$_2$O$_3$	0.04	0.15	0.09	0.00	0.00	0.00	0.11	0.00	0.14	0.16	0.23	0.13	0.39	0.42
Ho$_2$O$_3$	0.00	0.00	0.00	0.08	0.00	0.01	0.01	0.03	0.00	0.02	0.00	0.08	0.00	0.17
Er$_2$O$_3$	0.07	0.04	0.00	0.04	0.01	0.00	0.23	0.08	0.02	0.13	0.02	0.15	0.12	0.12
Yb$_2$O$_3$	0.00	0.00	0.00	0.05	0.00	0.09	0.00	0.03	0.03	0.00	0.00	0.00	0.00	0.01
Lu$_2$O$_3$	0.02	0.00	0.00	0.00	0.00	0.00	0.00	0.02	0.01	0.00	0.00	0.00	0.00	0.00
Y$_2$O$_3$	0.81	1.24	0.72	0.55	0.63	0.62	0.69	0.33	0.96	0.83	1.13	0.93	1.49	1.74
CaO	1.89	1.94	1.35	1.36	1.44	1.46	1.31	1.77	1.96	1.77	1.93	1.87	1.94	1.92
Fe$_2$O$_3$	0.97	0.83	1.05	0.72	1.00	1.20	0.99	0.77	1.13	0.74	0.67	0.73	0.71	0.70
MgO	1.53	1.57	1.50	1.57	1.46	1.33	1.46	1.61	1.42	1.63	1.67	1.66	1.59	1.62
Al$_2$O$_3$	0.03	0.02	0.04	0.02	0.02	0.04	0.03	0.01	0.03	0.01	0.00	0.00	0.00	0.00
SiO$_2$	21.30	21.37	20.85	20.87	20.80	20.82	20.78	20.37	21.10	20.48	20.45	21.68	21.83	21.79
P$_2$O$_5$	0.03	0.00	0.02	0.02	0.00	0.05	0.02	0.07	0.04	0.00	0.02	0.00	0.00	0.00
F	1.51	1.46	1.60	1.53	1.51	1.50	1.53	1.38	1.41	1.12	1.12	1.16	1.11	1.15
Cl	0.06	0.09	0.04	0.05	0.06	0.05	0.04	0.05	0.04	0.09	0.07	0.08	0.06	0.08
O=F	-0.64	-0.61	-0.67	-0.64	-0.64	-0.63	-0.64	-0.58	-0.59	-0.47	-0.47	-0.49	-0.47	-0.49
O=Cl	-0.01	-0.02	-0.01	-0.01	-0.01	-0.01	-0.01	-0.01	-0.01	-0.02	-0.02	-0.02	-0.01	-0.02
Total	96.88	95.83	96.57	96.38	95.95	96.39	96.51	95.40	95.97	95.48	94.99	96.40	96.49	96.16
La $apfu$	1.59	1.59	2.05	1.95	2.21	2.15	2.14	1.41	1.95	1.81	1.72	1.74	1.69	1.65
Ce	4.09	4.09	4.15	4.26	4.13	4.17	4.17	4.25	3.85	3.90	3.86	3.78	3.70	3.69
Pr	0.47	0.47	0.44	0.44	0.41	0.42	0.44	0.50	0.44	0.44	0.44	0.44	0.43	0.41
Nd	1.76	1.76	1.52	1.58	1.45	1.48	1.47	1.98	1.62	1.75	1.73	1.68	1.66	1.63
Sm	0.20	0.20	0.17	0.18	0.17	0.15	0.17	0.22	0.21	0.29	0.31	0.27	0.30	0.31
Gd	0.11	0.11	0.11	0.08	0.08	0.08	0.09	0.08	0.11	0.17	0.20	0.18	0.21	0.22
Dy	0.00	0.00	0.01	0.00	0.00	0.00	0.01	0.00	0.01	0.02	0.02	0.01	0.04	0.04
Ho	0.00	0.00	0.00	0.01	0.00	0.00	0.00	0.00	0.00	0.00	0.00	0.01	0.00	0.02
Er	0.01	0.01	0.00	0.00	0.00	0.00	0.02	0.01	0.00	0.01	0.00	0.01	0.01	0.01
Yb	0.00	0.00	0.00	0.00	0.00	0.01	0.00	0.00	0.00	0.00	0.00	0.00	0.00	0.00
Lu	0.00	0.00	0.00	0.00	0.00	0.00	0.00	0.00	0.00	0.00	0.00	0.00	0.00	0.00
Y	0.14	0.14	0.13	0.10	0.11	0.11	0.12	0.06	0.17	0.15	0.20	0.16	0.26	0.30
Ca	0.66	0.66	0.48	0.49	0.51	0.52	0.47	0.64	0.69	0.63	0.69	0.65	0.67	0.67
Fe^{3+}	0.24	0.24	0.26	0.18	0.25	0.30	0.25	0.19	0.28	0.19	0.17	0.18	0.17	0.17
Mg	0.74	0.74	0.74	0.78	0.72	0.66	0.72	0.80	0.69	0.81	0.83	0.81	0.77	0.78
Al	0.01	0.01	0.01	0.01	0.01	0.02	0.01	0.00	0.01	0.00	0.00	0.00	0.00	0.00
Si	6.96	6.96	6.91	6.94	6.93	6.92	6.91	6.82	6.95	6.83	6.82	7.06	7.09	7.09
P	0.01	0.01	0.01	0.00	0.00	0.01	0.01	0.02	0.01	0.00	0.01	0.00	0.00	0.00
F	1.56	1.56	1.68	1.61	1.59	1.58	1.61	1.46	1.46	1.18	1.18	1.19	1.14	1.19
Cl	0.03	0.03	0.02	0.03	0.04	0.03	0.02	0.03	0.02	0.05	0.04	0.04	0.03	0.04

The compositional data are first expressed in wt%, then in $apfu$, calculated on the basis of 17 cations.

TABLE 3a (cont'd). CHEMICAL COMPOSITION OF CERITE FROM BASTNÄS AND RÖDBERGSGRUVAN

Sample#	390477					882234			02+0052		03+0246				880072 R	
point	p1	p2	p4	p8	A:1	a p1	a p2	a p3	p3	p8	A:1	A:2	A:3	C:1	p1	p2
La$_2$O$_3$ wt%	11.70	9.74	12.07	11.50	10.08	15.10	14.73	11.53	15.59	13.82	9.56	9.50	10.08	11.97	15.95	11.18
Ce$_2$O$_3$	29.67	26.85	29.49	30.22	25.75	31.70	31.49	31.20	35.02	35.70	29.78	27.43	29.85	28.93	32.56	31.43
Pr$_2$O$_3$	3.87	3.77	3.85	3.95	4.17	3.49	3.66	4.04	3.49	3.79	4.53	4.34	4.55	4.17	3.55	3.85
Nd$_2$O$_3$	16.93	17.39	16.83	17.10	19.98	14.19	14.84	16.34	13.55	14.44	19.79	20.46	19.36	18.46	12.98	15.22
Sm$_2$O$_3$	2.70	3.33	2.74	2.82	3.16	2.07	2.14	2.50	1.45	1.59	3.13	3.62	3.27	3.13	1.60	1.88
Gd$_2$O$_3$	1.87	2.33	1.78	1.84	2.27	1.30	1.37	1.76	0.41	0.36	1.85	2.39	1.73	2.18	1.06	1.32
Dy$_2$O$_3$	0.18	0.19	0.25	0.17	0.29	0.17	0.10	0.22	0.07	0.13	0.21	0.29	0.17	0.38	0.21	0.29
Ho$_2$O$_3$	0.01	0.00	0.00	0.03	0.00	0.10	0.00	0.01	n.d.	n.d.	n.d.	n.d.	n.d.	n.d.	0.04	0.03
Er$_2$O$_3$	0.16	0.14	0.15	0.24	0.00	0.04	0.07	0.07	0.00	0.00	0.00	0.00	0.00	0.00	0.09	0.08
Yb$_2$O$_3$	0.01	0.00	0.00	0.00	0.00	0.00	0.02	0.00	n.d.	n.d.	n.d.	n.d.	n.d.	n.d.	0.00	0.07
Lu$_2$O$_3$	0.00	0.00	0.00	0.00	0.00	0.00	0.00	0.00	n.d.	n.d.	n.d.	n.d.	n.d.	n.d.	0.00	0.00
Y$_2$O$_3$	1.42	1.76	1.32	1.30	1.58	1.23	1.07	1.48	1.23	0.94	0.81	1.58	1.06	1.26	1.83	2.45
CaO	2.28	1.97	2.42	2.20	1.82	2.02	1.97	2.13	1.80	1.74	2.19	2.29	2.33	2.00	2.07	2.98
Fe$_2$O$_3$	0.77	1.06	0.82	0.91	1.26	0.90	0.93	0.80	0.78	0.57	0.46	0.38	0.33	0.41	0.95	0.83
MgO	1.61	1.33	1.59	1.55	0.85	1.53	1.53	1.64	1.38	1.45	1.49	1.43	1.42	1.51	1.56	1.61
Al$_2$O$_3$	0.01	0.05	0.01	0.02	0.05	0.01	0.02	0.01	0.00	0.00	0.01	0.00	0.00	0.00	0.01	0.05
SiO$_2$	21.70	24.25	21.49	21.69	17.80	21.59	20.83	21.60	21.24	21.07	21.46	21.05	21.13	21.52	20.73	21.17
P$_2$O$_5$	0.11	0.13	0.12	0.12	0.00	0.09	0.05	0.06	0.05	0.01	0.11	0.08	0.11	0.18	0.01	0.03
F	1.22	1.19	1.20	1.20	1.24	1.39	1.40	1.35	1.72	1.52	1.65	1.48	1.51	1.25	1.60	1.63
Cl	0.05	0.05	0.04	0.06	0.00	0.06	0.05	0.09	n.d.	n.d.	n.d.	n.d.	n.d.	n.d.	0.05	0.06
O=F	-0.51	-0.50	-0.51	-0.50	-0.44	-0.59	-0.59	-0.57	0.73	0.64	0.70	0.62	0.64	0.53	-0.68	-0.69
O=Cl	-0.01	-0.01	-0.01	-0.01	-0.01	-0.01	-0.01	-0.02							-0.01	-0.01
Total	95.75	95.00	95.66	96.39	89.85	96.37	95.65	96.24	98.52	97.77	97.73	96.94	97.53	97.87	96.16	95.46
La $apfu$	1.40	1.15	1.45	1.38	1.35	1.81	1.80	1.38	1.88	1.68	1.16	1.16	1.22	1.44	1.93	1.34
Ce	3.53	3.14	3.51	3.59	3.41	3.78	3.81	3.71	4.20	4.32	3.58	3.32	3.60	3.46	3.92	3.73
Pr	0.46	0.44	0.46	0.47	0.56	0.41	0.44	0.48	0.42	0.46	0.54	0.52	0.55	0.50	0.43	0.45
Nd	1.97	1.98	1.96	1.98	2.64	1.65	1.75	1.90	1.59	1.70	2.32	2.42	2.28	2.15	1.52	1.76
Sm	0.30	0.37	0.31	0.31	0.40	0.23	0.24	0.28	0.16	0.18	0.35	0.41	0.37	0.35	0.18	0.21
Gd	0.20	0.25	0.19	0.20	0.24	0.14	0.15	0.19	0.04	0.04	0.20	0.26	0.19	0.24	0.12	0.14
Dy	0.02	0.02	0.03	0.02	0.03	0.02	0.01	0.02	0.01	0.01	0.02	0.03	0.02	0.04	0.02	0.03
Ho	0.00	0.00	0.00	0.00	0.00	0.01	0.00	0.00	0.00	0.00					0.00	0.00
Er	0.02	0.01	0.02	0.02	0.00	0.00	0.01	0.01	0.00	0.00	0.00	0.00	0.00	0.00	0.01	0.01
Yb	0.00	0.00	0.00	0.00	0.00	0.00	0.00	0.00	0.00	0.01					0.00	0.00
Lu	0.00	0.00	0.00	0.00	0.00	0.00	0.00	0.00	0.00	0.00					0.00	0.00
Y	0.25	0.30	0.23	0.22	0.31	0.21	0.19	0.26	0.21	0.17	0.14	0.28	0.19	0.22	0.32	0.42
Ca	0.79	0.67	0.85	0.77	0.73	0.70	0.70	0.74	0.63	0.62	0.77	0.81	0.82	0.70	0.73	1.03
Fe^{3+}	0.19	0.25	0.20	0.22	0.32	0.22	0.23	0.20	0.19	0.14	0.11	0.09	0.08	0.10	0.23	0.20
Mg	0.78	0.63	0.77	0.75	0.47	0.74	0.76	0.80	0.68	0.72	0.73	0.71	0.70	0.73	0.76	0.78
Al	0.00	0.02	0.00	0.01	0.02	0.01	0.01	0.00	0.00	0.02					0.00	0.02
Si	7.06	7.74	6.99	7.03	6.52	7.02	6.89	7.02	6.96	6.96	7.04	6.96	6.96	7.02	6.81	6.85
P	0.03	0.03	0.03	0.03	0.00	0.02	0.01	0.02	0.01	0.00	0.03	0.02	0.03	0.05	0.00	0.01
F	1.26	1.20	1.24	1.23	1.46	1.43	1.47	1.39	1.79	1.59	1.72	1.55	1.58	1.29	1.67	1.67
Cl	0.03	0.03	0.02	0.03	0.00	0.03	0.03	0.05							0.03	0.03

n.d.: not determined. R = Rödbergsgruvan. The compositional data are first expressed in wt%, then in $apfu$, calculated on the basis of 17 cations.

chemical analyses, are required to fully reveal its crystal-chemical character and variability.

Unnamed mineral E

A chlorine-bearing REE silicate was found in sample #UU318/77 from the Malmkärra mine. It occurs as a greyish pink, cerite-like mass with a greasy luster, in association with mainly västmanlandite-(Ce), talc and phlogopite. Alteration to bastnäsite-(Ce) is pervasive in certain areas (Fig. 4D). Fractured grains of magnetite (≤1 mm), equant to skeletal in outline, occur in contact with both västmanlandite-(Ce) and the unnamed mineral. It is colorless, transparent and nonpleochroic in thin section. The optical character is biaxial (–), with $2V \approx 55°$. Individual grains (100–300 μm) are subhedral

TABLE 3b. CHEMICAL COMPOSITION OF CERITE FROM THE NORBERG DISTRICT

#	490216 J			660298 M					03+0029 M									
point	4:1	2:1	2:2	2:3	p1	p2	p3	p4	p5	p6	p7	p8	p11	p12	p13	p14	p15
La$_2$O$_3$	17.70	9.08	8.78	8.62	11.61	12.85	12.39	14.22	13.60	12.69	11.92	13.81	10.81	10.79	11.53	11.57	9.84
Ce$_2$O$_3$	34.94	27.97	28.09	27.82	31.54	32.77	32.54	31.95	32.57	32.74	31.64	31.59	31.63	31.46	32.74	32.68	30.03
Pr$_2$O$_3$	3.77	3.95	3.95	4.27	4.14	4.18	3.89	3.77	3.93	4.10	4.12	3.83	4.23	4.18	4.13	4.07	4.30
Nd$_2$O$_3$	11.93	18.00	18.59	18.33	16.46	16.09	16.49	14.83	15.40	16.25	16.42	14.88	17.24	17.71	16.98	17.10	18.16
Sm$_2$O$_3$	1.08	3.32	3.44	3.34	3.01	2.49	2.84	2.12	2.39	2.71	2.60	2.37	3.19	2.92	2.87	2.71	3.33
Gd$_2$O$_3$	0.30	1.72	1.79	2.04	1.11	0.60	0.90	0.55	0.69	0.81	0.89	0.67	1.10	1.22	1.09	0.91	1.36
Dy$_2$O$_3$	0.06	0.65	0.79	0.71	0.43	0.36	0.41	0.25	0.27	0.36	0.37	0.15	0.39	0.37	0.38	0.31	0.65
Ho$_2$O$_3$	n.d.	n.d.	n.d.	n.d.	n.d.	n.d.	n.d.	n.d.	n.d.	n.d.	n.d.	n.d.	n.d.	n.d.	n.d.	n.d.	n.d.
Er$_2$O$_3$	0.00	0.07	0.00	0.09	0.02	0.00	0.00	0.00	0.00	0.00	0.00	0.07	0.01	0.00	0.00	0.03	0.00
Yb$_2$O$_3$	n.d.	n.d.	n.d.	n.d.	n.d.	n.d.	n.d.	n.d.	n.d.	n.d.	n.d.	n.d.	n.d.	n.d.	n.d.	n.d.	n.d.
Lu$_2$O$_3$	n.d.	n.d.	n.d.	n.d.	n.d.	n.d.	n.d.	n.d.	n.d.	n.d.	n.d.	n.d.	n.d.	n.d.	n.d.	n.d.	n.d.
Y$_2$O$_3$	0.21	3.41	3.51	3.50	1.47	1.10	1.21	0.85	1.17	0.93	1.45	1.03	1.52	1.46	1.37	1.34	1.87
CaO	1.65	2.32	2.00	2.56	1.94	1.62	1.63	3.00	2.11	1.69	1.91	3.02	1.72	1.82	1.61	1.68	2.47
Fe$_2$O$_3$	0.00	0.04	0.18	0.19	0.03	0.07	0.04	0.92	0.36	0.12	0.03	0.97	0.21	0.15	0.35	0.25	0.32
MgO	1.80	1.76	1.56	1.81	1.71	1.68	1.67	1.30	1.51	1.70	1.71	1.33	1.66	1.68	1.61	1.52	1.59
Al$_2$O$_3$	0.00	0.00	0.00	0.00	0.00	0.00	0.00	0.00	0.00	0.00	0.00	0.00	0.00	0.00	0.00	0.00	0.00
SiO$_2$	21.68	22.51	22.13	22.54	21.39	21.45	21.51	22.06	21.67	21.27	21.36	22.36	21.53	21.64	21.89	21.51	22.40
P$_2$O$_5$	0.08	0.10	0.17	0.15	0.12	0.16	0.11	0.07	0.26	0.16	0.15	0.14	0.18	0.18	0.14	0.23	0.12
F	1.87	1.54	1.33	1.53	1.63	1.55	1.55	1.66	1.41	1.47	1.52	1.57	1.38	1.51	1.47	1.29	1.54
O=F	-0.79	-0.65	-0.56	-0.64	-0.69	-0.65	-0.65	-0.70	-0.60	-0.62	-0.64	-0.66	-0.58	-0.63	-0.62	-0.54	-0.65
Total	96.27	95.77	95.73	96.82	95.92	96.32	96.55	96.86	96.75	96.38	95.45	97.15	96.22	96.45	97.53	96.66	97.33
La *apfu*	2.14	1.08	1.05	1.01	1.41	1.56	1.50	1.68	1.63	1.54	1.45	1.62	1.31	1.30	1.38	1.40	1.16
Ce	4.20	3.29	3.34	3.23	3.80	3.95	3.92	3.75	3.88	3.95	3.82	3.68	3.80	3.77	3.89	3.92	3.51
Pr	0.45	0.46	0.47	0.49	0.50	0.50	0.47	0.44	0.47	0.49	0.50	0.44	0.51	0.50	0.49	0.49	0.50
Nd	1.40	2.06	2.15	2.07	1.93	1.89	1.94	1.70	1.79	1.91	1.93	1.69	2.02	2.07	1.97	2.00	2.07
Sm	0.12	0.37	0.38	0.36	0.34	0.28	0.32	0.23	0.27	0.31	0.30	0.26	0.36	0.33	0.32	0.31	0.37
Gd	0.03	0.18	0.19	0.21	0.12	0.07	0.10	0.06	0.07	0.09	0.10	0.07	0.12	0.13	0.12	0.10	0.14
Dy	0.01	0.07	0.08	0.07	0.05	0.04	0.04	0.03	0.03	0.04	0.04	0.02	0.04	0.04	0.04	0.03	0.07
Er	0.00	0.01	0.00	0.01	0.00	0.00	0.00	0.00	0.00	0.00	0.00	0.01	0.00	0.00	0.00	0.00	0.00
Y	0.04	0.58	0.61	0.59	0.26	0.19	0.21	0.14	0.20	0.16	0.25	0.17	0.27	0.25	0.24	0.23	0.32
Ca	0.58	0.80	0.70	0.87	0.68	0.57	0.58	1.03	0.74	0.60	0.68	1.03	0.60	0.64	0.56	0.59	0.85
Fe^{3+}	0.00	0.01	0.04	0.05	0.01	0.02	0.01	0.22	0.09	0.03	0.01	0.23	0.05	0.04	0.08	0.06	0.08
Mg	0.88	0.84	0.75	0.85	0.84	0.82	0.82	0.62	0.73	0.83	0.84	0.63	0.81	0.82	0.78	0.74	0.76
Al	0.00	0.00	0.00	0.00	0.00	0.00	0.00	0.00	0.00	0.00	0.00	0.00	0.00	0.00	0.00	0.00	0.00
Si	7.12	7.23	7.18	7.14	7.03	7.06	7.07	7.07	7.04	7.00	7.05	7.11	7.06	7.07	7.10	7.05	7.15
P	0.02	0.03	0.05	0.04	0.03	0.05	0.03	0.02	0.07	0.05	0.04	0.04	0.05	0.05	0.04	0.06	0.03
F	1.94	1.56	1.36	1.53	1.70	1.61	1.61	1.68	1.45	1.53	1.59	1.58	1.43	1.56	1.51	1.34	1.56

n.d.: not determined. J: Johannagruvan, M: Malmkärra. The compositional data are first expressed in wt%, then in *apfu*, calculated on the basis of 17 cations.

and display slight undulatory extinction. A small inclusion of fluorbritholite-(Ce) was detected in one of the grains, and minute grains of scheelite are scattered all over the specimen.

A preliminary single-crystal diffraction study indicates that mineral E is monoclinic, with the unit-cell parameters *a* 14.14, *b* 10.74, *c* 15.51 Å, β 106.6°. No precise structural formula can be established at present, but the chemical composition (Table 4), with relatively high and constant Cl contents (2.85–2.97 wt.%), and a unique X-ray powder-diffraction pattern, indicate that this represents a new species (no Ce silicate

with essential Cl is presently known to the scientific community; Mandarino & Back 2004).

The mineral has Ce > Nd > La, *i.e.*, the same order as encountered in fluorbritholite-(Ce) and cerite-(Ce) from the Malmkärra mine. In its overall chemical composition, it is most similar to cerite-(Ce), albeit clearly distinguished by its Cl content. The low totals (94.9–96.2 wt.%) clearly suggest that unanalyzed volatile components are contained in the mineral. A single analyzed grain (<30 μm across) in contact with cerite-(Ce) in a Bastnäs sample (#A37) has a composition similar to that of mineral E, except that it is has Fe > Mg (Table 4).
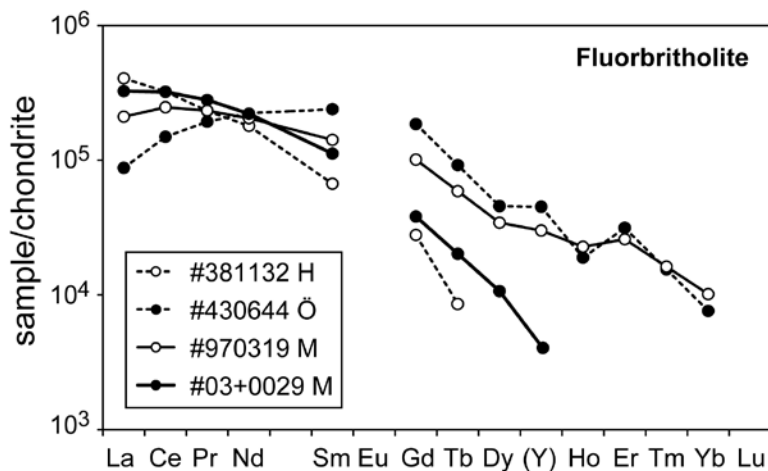
FIG. 8.   Selected chondrite-normalized REE patterns for fluorbritholite samples from the Norberg District.

Minerals of the fluorbritholite group

Fluorbritholite, ideally $REE_3Ca_2[SiO_4]_3F$, is only found in the subtype-2 deposits and was not known to exist there before our studies (Holtstam & Andersson 2002); it is now clear that some occurrences of "cerite" reported earlier (Geijer 1927) are in fact fluorbritholite. Fluorbritholite is isostructural with fluorapatite, and the type material is reported to be hexagonal, $P6_3/m$ (Gu *et al.* 1994). Oberti *et al.* (2001) structurally characterized two samples that were best described in the lower symmetry $P6_3$, and monoclinic–pseudohexagonal varieties may also exist (*e.g., Noe et al.* 1993).

The major occurrences of fluorbritholite-(Ce) are in the Malmkärra deposit, where large masses weighing several kilograms each have been collected. In these samples, fluorbritholite-(Ce) is associated with dollaseite-(Ce), västmanlandite-(Ce), gadolinite, amphibole, dolomite, phlogopite, magnetite and pyrite. A general impression from the textures of this kind of material (*e.g.*, ##970319 and 540027) is that fluorbritholite-(Ce) is the primary, earliest mineral to crystallize; other REE minerals, at least to some extent, seem to have formed during breakdown of the fluorbritholite-(Ce).

In #03+0029, fluorbritholite-(Ce) forms irregular masses up to 2 cm across in a skarn rock of coarse actinolite and magnetite. It is peculiar to this sample that cerite-(Ce) has partly replaced fluorbritholite-(Ce).

An Y-dominant analogue (Table 5) of fluorbritholite-(Ce) occurs in a sample (#430644) from the Östanmossa deposit. Aggregates up to 3 cm across coexist with some tremolite in a coarsely crystalline vein of dolomite transecting dollaseite-bearing amphibole skarn. In #381132 from S. Hackspikgruvan, fluorbritholite-(Ce)

is a subordinate component associated with bastnäsite-(Ce) and fluorite.

Fluorbritholite is low in Ca, P and the actinides compared to most other known ocurrences (*e.g.*, Arden & Halden 1999, Della Ventura *et al.* 1999, Smith *et al.* 2002). Significant inter- and intrasample variations in REE and Y, corresponding to a range from fluorbritholite-(Ce) to the previously unrecognized members "fluorbritholite-(Nd)" and "fluorbritholite-(Y)", occur. Consequently, fluorbritholite samples display large variations in the chondrite-normalized patterns (Fig. 8). The more Y-rich samples (Y > 0.5 *apfu*) are significantly enriched in HREE, Gd–Lu (0.20–0.40 *apfu*).

Fluorbritholite is consistently nonstoichiometric in that Ca < 2 and (REE + Y) > 3 *apfu* (Fig. 9). This finding could theoretically be explained by one of the following mechanisms of substitution, proposed to operate in apatite-type structures (*e.g.*, Pan & Fleet 2002):

$$REE^{3+} + M^+ = 2\ Ca^{2+} \qquad (1)$$

$$REE^{3+} + M^{3+} = Ca^{2+} + Si^{4+} \qquad (2)$$

$$REE^{3+} + O^{2-} = Ca^{2+} + F^- \qquad (3)$$

$$2\ REE^{3+} + \square = 3\ Ca^{2+} \qquad (4)$$
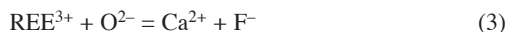
As there are no monovalent cations (*e.g.*, Na^+) present, (1) can be ruled out. Boron, which is an easily overlooked component, was not measured in our samples; B^{3+} partly replacing Si^{4+} at the tetrahedrally coordinated sites has in fact been demonstrated in a sample of fluorbritholite (Oberti *et al.* 2001). However, if (2) was the mechanism responsible, (REE + Y) and Si should be

anticorrelated, which is not the case here. With a few significant exceptions, the deviation from the ideal value of 3 Si *apfu* is explained by a P^{5+}-for-Si^{4+} exchange in our samples (Fig. 10). The observed variations in the F content (0.63–1.02 *apfu*), which could correspond to (3), are uncorrelated with the REE, and are probably simply an expression of a common OH–F substitution in the present material. The calculated formulae, if based on a fixed number of anions (12.5 O), give cation sums below 8 *apfu* for most points, in support of the last mechanism (4). However, there is no physical evidence for cation vacancies (□) in fluorbritholite; further studies clearly are needed to resolve the question of nonstoichiometry in fluorbritholite. Compositionally similar samples of fluorbritholite-(Ce), *i.e.*, with Ca

< 2 and REE > 3 *apfu*, were recently described from nepheline syenite in the Pilansberg alkaline complex, South Africa (Liferovich & Mitchell 2006).

The unit-cell parameters of "fluorbritholite-(Y)" in #430664 was determined to *a* 9.561(1), *c* 6.950(1) Å, *V* 550.2(2) Å³. For two specimens of fluorbritholite-(Ce) (#97319, #03+0029), we found *a* 9.617(2), 9.620(2), *c* 7.010(2), 7.033(2) Å and *V* 561.5(3), 563.7(3) Å³.

Törnebohmite-(*Ce*)

Törnebohmite-(Ce), (Ce, La)$_2$Al[SiO$_4$]$_2$(OH), was first discovered at Bastnäs and carefully described by Geijer (1921). Using plesiotype material, Shen & Moore (1982) solved the crystal structure of this

TABLE 4. AVERAGE COMPOSITION OF UNNAMED MINERALS
FROM BASTNÄS-TYPE DEPOSITS

Sample #	060375 B mineral C *n* = 4	970319 M mineral D *n* = 5	UU318/77 M mineral E *n* = 10	A37 B mineral E *n* = 1
La$_2$O$_3$ wt%	14.58	6.27	11.87	20.04
Ce$_2$O$_3$	23.29	16.17	30.98	35.10
Pr$_2$O$_3$	1.89	1.95	3.99	3.24
Nd$_2$O$_3$	6.13	7.88	17.14	11.37
Sm$_2$O$_3$	0.74	1.87	2.81	0.99
Gd$_2$O$_3$	0.37	2.79	1.15	0.43
Dy$_2$O$_3$	0.03	2.38	0.30	0.00
Ho$_2$O$_3$	0.00	0.48	nd	0.00
Er$_2$O$_3$	0.04	1.65	0.00	0.00
Yb$_2$O$_3$	0.12	1.22	n.d.	0.01
Lu$_2$O$_3$	0.01	0.16	n.d.	0.00
Y$_2$O$_3$	0.22	21.44	1.11	0.21
CaO	0.76	0.02	2.26	0.85
FeO		0.18	0.03	1.99
Fe$_2$O$_3$	12.86			
MgO	2.43	4.36	1.97	0.91
Al$_2$O$_3$	0.73	0.00	0.00	0.10
SiO$_2$	18.16	26.53	19.13	19.30
P$_2$O$_5$	0.00	0.00	0.08	0.01
TiO$_2$	0.09	0.00	0.00	0.00
WO$_3$	15.53	n.d.	n.d.	n.d.
F	0.05	4.36	1.09	1.20
Cl	0.03	0.02	2.89	1.98
O=F	-0.02	-1.83	-0.46	-0.51
O=Cl	-0.01	-0.01	-0.65	-0.45
Total	98.03	97.89	95.70	96.78
La *apfu*	1.50	0.35	1.58	2.69
Ce	2.38	0.89	4.09	4.68
Pr	0.19	0.11	0.52	0.43
Nd	0.61	0.42	2.21	1.48
Sm	0.07	0.10	0.35	0.12
Gd	0.03	0.14	0.14	0.05
Dy	0.00	0.12	0.03	0.00
Ho	0.00	0.02		0.00
Er	0.00	0.08	0.00	0.00
Yb	0.01	0.06		0.00
Lu	0.00	0.01		0.00
Y	0.03	1.72	0.21	0.04
Ca	0.23	0.00	0.87	0.33
Fe^{3+}	2.70			
Fe^{2+}		0.02	0.01	0.61
Mg	1.01	0.98	1.06	0.49
Al	0.24	0.00	0.00	0.04
Si	5.06	3.99	6.90	7.03
P	0.00	0.00	0.02	0.00
Ti	0.02	0.00	0.00	0.00
W	0.92			
F	0.04	2.07	1.24	1.38
Cl	0.01	0.01	1.77	1.22
Σ cations	15.00	9.00	18.00	18.00

n: number of analyses; n.d.: not determined. B: Bastnäs, M: Malmkärra.
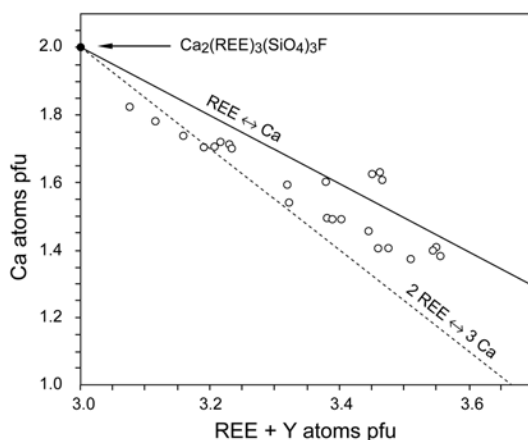
FIG. 9. Compositional diagram showing the variation of Ca *versus* REE + Y in fluorbritholite.
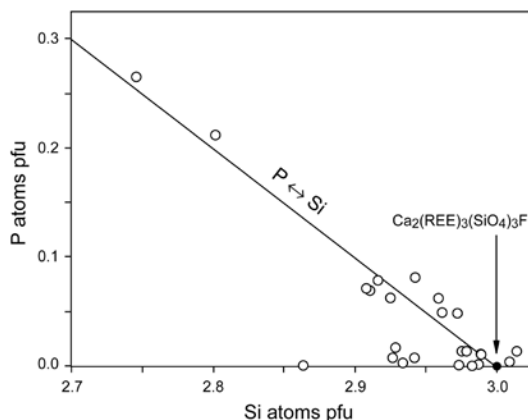
FIG. 10. Compositional diagram showing the variation of P *versus* Si in fluorbritholite.

TABLE 5. CHEMICAL COMPOSITION OF FLUORBRITHOLITE

Sample #	381132 H				430644 Ö						540027 M			
point	a p2	b p9	b p11	b p12	a p1	a p5	a p6	b p3	b p4	b p5	p3	p4	v1	v2
La_2O_3 wt%	12.42	14.34	16.44	15.71	3.33	3.58	3.00	3.03	3.14	3.05	3.96	4.43	3.99	4.55
Ce_2O_3	29.43	31.08	30.77	31.10	13.59	13.66	12.81	13.94	15.22	15.54	16.58	17.56	16.62	17.99
Pr_2O_3	3.49	3.43	3.14	3.18	2.63	2.65	2.71	2.62	2.87	3.10	2.98	3.23	3.21	3.32
Nd_2O_3	14.09	12.78	11.49	11.96	14.93	14.96	15.01	15.69	16.32	16.98	16.82	17.65	16.85	17.75
Sm_2O_3	2.11	1.48	1.28	1.19	5.20	5.32	5.44	5.64	5.30	5.55	5.58	5.37	5.51	5.48
Gd_2O_3	1.31	0.69	0.66	0.66	5.69	5.60	5.82	5.65	5.28	5.17	5.26	5.41	5.30	5.10
Dy_2O_3	0.10	0.18	0.11	0.01	1.77	1.71	1.97	1.68	1.56	1.44	1.64	1.77	1.71	1.91
Ho_2O_3	0.00	0.02	0.03	0.00	0.15	0.18	0.17	0.22	0.15	0.07	0.21	0.20	0.24	0.26
Er_2O_3	0.14	0.10	0.05	0.09	0.88	0.74	0.88	0.65	0.78	0.60	0.65	0.70	0.71	0.54
Yb_2O_3	0.00	0.00	0.06	0.05	0.12	0.23	0.25	0.14	0.15	0.20	0.13	0.14	0.21	0.15
Lu_2O_3	0.00	0.00	0.05	0.00	0.00	0.00	0.00	0.00	0.00	0.00	0.00	0.00	0.00	0.00
Y_2O_3	2.07	1.34	1.11	1.09	12.73	13.13	13.94	11.47	10.98	9.86	6.69	7.02	7.02	7.29
CaO	10.61	10.55	10.35	10.47	11.89	11.97	11.96	12.08	11.83	11.76	12.09	10.67	12.75	10.46
FeO	0.15	0.15	0.12	0.12	0.12	0.12	0.14	0.12	0.11	0.12	0.03	0.00	0.02	0.05
MgO	0.01	0.01	0.01	0.00	0.02	0.02	0.04	0.00	0.01	0.00	0.00	0.00	0.00	0.07
Al_2O_3	0.00	0.00	0.00	0.00	0.00	0.00	0.00	0.00	0.00	0.00	0.00	0.00	0.00	0.00
SiO_2	20.58	19.58	19.58	19.64	21.46	21.55	21.66	21.65	21.75	21.59	20.08	20.55	20.23	21.22
P_2O_5	0.03	0.00	0.00	0.01	0.54	0.62	0.63	0.70	0.42	0.54	1.79	0.66	2.31	0.40
Ba	0.01	0.01	0.04	0.00	0.03	0.03	0.03	0.02	0.01	0.06	0.05	0.04	0.07	0.04
F	2.26	2.31	2.08	2.23	1.80	1.89	1.81	1.81	1.81	1.86	1.36	2.17	1.56	1.90
Cl	0.05	0.04	0.04	0.05	0.05	0.05	0.05	0.05	0.05	0.05	0.33	0.20	0.31	0.18
O=F	-0.95	-0.97	-0.87	-0.94	-0.76	-0.80	-0.76	-0.77	-0.76	-0.78	-0.57	-0.91	-0.65	-0.80
O=Cl	-0.05	-0.04	-0.04	-0.05	-0.05	-0.05	-0.05	-0.05	-0.05	-0.05	-0.33	-0.20	-0.31	-0.18
Total	97.85	97.07	96.48	96.58	96.12	97.14	97.49	96.35	96.93	96.71	95.34	96.65	97.63	97.69
La *apfu*	0.65	0.76	0.88	0.84	0.17	0.18	0.15	0.15	0.16	0.15	0.20	0.23	0.20	0.23
Ce	1.52	1.64	1.63	1.65	0.67	0.67	0.62	0.68	0.75	0.77	0.83	0.90	0.81	0.91
Pr	0.18	0.18	0.17	0.17	0.13	0.13	0.13	0.13	0.14	0.15	0.15	0.16	0.16	0.17
Nd	0.71	0.66	0.59	0.62	0.72	0.71	0.71	0.75	0.78	0.82	0.82	0.88	0.80	0.87
Sm	0.10	0.07	0.06	0.06	0.24	0.24	0.25	0.26	0.25	0.26	0.26	0.26	0.25	0.26
Gd	0.06	0.03	0.03	0.03	0.25	0.25	0.26	0.25	0.24	0.23	0.24	0.25	0.23	0.23
Dy	0.00	0.01	0.00	0.00	0.08	0.07	0.08	0.07	0.07	0.06	0.07	0.08	0.07	0.08
Ho	0.00	0.00	0.00	0.00	0.01	0.01	0.01	0.01	0.01	0.00	0.01	0.01	0.01	0.01
Er	0.01	0.00	0.00	0.00	0.04	0.03	0.04	0.03	0.03	0.03	0.03	0.03	0.03	0.02
Yb	0.00	0.00	0.00	0.00	0.01	0.01	0.01	0.01	0.01	0.01	0.01	0.01	0.01	0.01
Lu	0.00	0.00	0.00	0.00	0.00	0.00	0.00	0.00	0.00	0.00	0.00	0.00	0.00	0.00
Y	0.15	0.10	0.09	0.08	0.91	0.93	0.98	0.82	0.79	0.71	0.49	0.52	0.50	0.53
Ca	1.60	1.63	1.61	1.62	1.72	1.71	1.70	1.74	1.70	1.70	1.78	1.59	1.82	1.54
Fe^{2+}	0.02	0.02	0.01	0.01	0.01	0.01	0.02	0.01	0.01	0.01	0.00	0.00	0.00	0.01
Mg	0.00	0.00	0.00	0.00	0.00	0.00	0.01	0.00	0.00	0.00	0.00	0.00	0.00	0.01
Si	2.90	2.82	2.84	2.84	2.89	2.87	2.87	2.90	2.92	2.92	2.76	2.86	2.70	2.92
Ba	0.00	0.00	0.00	0.00	0.00	0.00	0.00	0.00	0.00	0.00	0.00	0.00	0.00	0.00
P	0.00	0.00	0.00	0.00	0.06	0.07	0.07	0.08	0.05	0.06	0.21	0.08	0.26	0.05
F	1.01	1.05	0.95	1.02	0.77	0.80	0.76	0.78	0.77	0.79	0.59	0.96	0.66	0.82
Cl	0.01	0.01	0.01	0.01	0.01	0.01	0.01	0.01	0.01	0.01	0.08	0.05	0.07	0.04
Σ cat.	7.91	7.94	7.93	7.93	7.91	7.90	7.90	7.90	7.90	7.89	7.87	7.86	7.87	7.85

monoclinic mineral. It consists of straight chains of edge-sharing $AlO_4(OH)_2$ octahedra running along **b**, linked by isolated $[SiO_4]$ tetrahedra. The REE cations occupy cavities with 10-fold coordination (9 O + 1 OH) between the chains.

Törnebohmite-(Ce) belongs to the cerite-(Ce) – ferriallanite-(Ce) association (*i.e.*, the major REE ore) in the Bastnäs deposit (Figs. 11A,B). The mineral grains, recognized in thin section by their characteristic pleochroism (*Y* bluish green), are anhedral, typically slightly elongate, and 0.05 to 1 mm in their longest dimension. Crystal aggregates of törnebohmite-(Ce) may

exceptionally reach 5 mm across. The mineral is most closely associated with ferriallanite-(Ce), with which it commonly is in direct contact or occasionally intergrown. In a few cases, lamellae of törnebohmite-(Ce), *ca.* 20 µm or wider, have been found regularly arranged in a host crystal of ferriallanite-(Ce). In a similar fashion, törnebohmite-(Ce) may contain oriented lamellae of ferriallanite-(Ce), although irregular inclusions of this mineral are more common. There is a structural explanation for this kind of epitaxy; see the paragraph on västmanlandite-(Ce) below. Törnebohmite-(Ce) locally occurs without any particular spatial

TABLE 5 (cont'd). CHEMICAL COMPOSITION OF FLUORBRITHOLITE

Sample#	970319 M						01+0081 M				03+0029 M				
point	p1	p4	p7	p12	v11	v12	p4	p5	p6	p7	A A:1	A A:2	A A:3	B A:1	B C:2
La_2O_3	7.07	7.91	7.68	8.95	7.04	7.25	10.64	10.59	10.52	10.28	12.50	9.32	12.11	12.27	11.07
Ce_2O_3	22.38	21.76	23.14	24.48	24.57	23.96	30.78	31.72	30.95	31.38	29.99	29.41	29.70	30.00	30.16
Pr_2O_3	3.24	2.83	3.45	3.27	3.62	3.58	4.19	4.28	3.95	4.12	4.20	3.97	3.76	4.34
Nd_2O_3	14.24	12.19	13.99	13.82	16.21	15.63	17.45	16.94	17.28	17.72	15.59	16.84	15.28	14.78	15.80
Sm_2O_3	3.55	2.70	2.98	2.84	3.53	3.61	2.66	2.56	3.01	2.62	2.40	3.15	2.24	2.48	2.70
Gd_2O_3	3.71	3.01	2.77	2.61	2.91	3.10	1.34	1.13	1.35	1.33	1.30	1.76	1.31	1.45	1.61
Dy_2O_3	1.57	1.58	1.21	1.20	0.96	1.09	0.01	0.11	0.16	0.03	0.42	0.44	0.41	0.46	0.34
Ho_2O_3	0.29	0.31	0.14	0.22	0.06	0.11	0.00	0.02	0.00	0.04	n.d.	n.d.	n.d.	n.d.	n.d.
Er_2O_3	0.73	0.84	0.66	0.64	0.43	0.43	0.00	0.00	0.00	0.00	0.02	0.02	0.00	0.00	0.00
Yb_2O_3	0.19	0.45	0.27	0.26	0.13	0.15	0.00	0.00	0.05	0.00	n.d.	n.d.	n.d.	n.d.	n.d.
Lu_2O_3	0.00	0.00	0.05	0.03	0.00	0.00	0.00	0.00	0.00	0.00	n.d.	n.d.	n.d.	n.d.	n.d.
Y_2O_3	8.90	11.44	8.09	7.58	5.93	6.14	0.95	0.93	1.08	1.08	0.98	1.07	1.20	1.07	0.92
CaO	9.47	9.95	10.01	9.47	10.05	10.06	9.17	9.15	9.02	9.15	9.59	8.78	9.54	9.49	8.66
FeO	0.15	0.19	0.22	0.09	0.23	0.27	0.00	0.00	0.00	0.00	0.00	0.00	0.00	0.00	0.00
MgO	0.03	0.06	0.03	0.22	0.01	0.04	0.01	0.01	0.00	0.02	0.00	0.00	0.00	0.00	0.00
Al_2O_3	0.00	0.00	0.00	0.00	0.00	0.00	0.00	0.00	0.00	0.00	0.00	0.00	0.00	0.00	0.00
SiO_2	21.14	21.44	21.15	21.13	21.24	21.12	20.05	20.15	20.19	20.80	21.06	20.73	20.97	20.65	20.50
P_2O_5	0.02	0.00	0.00	0.00	0.09	0.12	0.07	0.14	0.07	0.11	0.21	0.10	0.13	0.12	0.07
Ba	0.02	0.02	0.03	0.04	0.04	0.08	0.09	0.10	0.08	0.10	n.d.	n.d.	n.d.	n.d.	n.d.
F	1.38	1.47	1.59	1.85	1.71	1.74	1.80	1.90	1.83	1.86	1.89	1.62	1.56	1.48	1.83
Cl	0.09	0.10	0.13	0.14	0.12	0.10	0.04	0.02	0.04	0.04	n.d.	n.d.	n.d.	n.d.	n.d.
O=F	-0.58	-0.62	-0.67	-0.78	-0.72	-0.73	-0.48	-0.52	-0.49	-0.50	-0.80	-0.68	-0.66	-0.62	-0.77
O=Cl	-0.09	-0.10	-0.13	-0.14	-0.12	-0.10	-0.04	-0.02	-0.04	-0.04	0.00	0.00	0.00	0.00	0.00
Total	97.50	97.53	96.79	97.92	98.04	97.72	98.71	99.21	99.05	100.26	99.29	96.77	97.77	97.40	97.23
La	0.36	0.40	0.39	0.46	0.36	0.37	0.56	0.56	0.55	0.53	0.64	0.64	0.63	0.64	0.59
Ce	1.13	1.09	1.17	1.24	1.24	1.21	1.61	1.65	1.62	1.61	1.53	1.53	1.53	1.56	1.59
Pr	0.16	0.14	0.17	0.16	0.18	0.18	0.22	0.22	0.21	0.22	0.21	0.21	0.20	0.19	0.23
Nd	0.70	0.59	0.69	0.68	0.80	0.77	0.89	0.86	0.88	0.89	0.78	0.78	0.77	0.75	0.81
Sm	0.17	0.13	0.14	0.14	0.17	0.17	0.13	0.13	0.15	0.13	0.12	0.12	0.11	0.12	0.13
Gd	0.17	0.14	0.13	0.12	0.13	0.14	0.06	0.05	0.06	0.06	0.06	0.06	0.06	0.07	0.08
Dy	0.07	0.07	0.05	0.05	0.04	0.05	0.00	0.00	0.01	0.00	0.02	0.02	0.02	0.02	0.02
Ho	0.01	0.01	0.01	0.01	0.00	0.00	0.00	0.00	0.00	0.00					
Er	0.03	0.04	0.03	0.03	0.02	0.02	0.00	0.00	0.00	0.00	0.00	0.00	0.00	0.00	
Yb	0.01	0.02	0.01	0.01	0.01	0.01	0.00	0.00	0.00	0.00					
Lu	0.00	0.00	0.00	0.00	0.00	0.00	0.00	0.00	0.00	0.00					
Y	0.66	0.83	0.60	0.56	0.44	0.45	0.07	0.07	0.08	0.08	0.07	0.07	0.09	0.08	0.07
Ca	1.40	1.45	1.49	1.40	1.49	1.49	1.41	1.40	1.38	1.37	1.43	1.43	1.44	1.44	1.33
Fe^{2+}	0.02	0.02	0.03	0.01	0.03	0.03	0.00	0.00	0.00	0.00	0.00	0.00	0.00	0.00	0.00
Mg	0.01	0.01	0.01	0.05	0.00	0.01	0.00	0.00	0.00	0.00	0.00	0.00	0.00	0.00	0.00
Si	2.92	2.92	2.93	2.92	2.93	2.92	2.87	2.87	2.88	2.91	2.93	2.93	2.95	2.93	2.94
Ba	0.00	0.00	0.00	0.00	0.00	0.00	0.00	0.01	0.00	0.01					
P	0.00	0.00	0.00	0.00	0.01	0.01	0.01	0.02	0.01	0.01	0.02	0.02	0.02	0.01	0.01
F	0.60	0.63	0.70	0.81	0.75	0.76	0.81	0.85	0.82	0.82	0.83	0.83	0.69	0.67	0.83
Cl	0.02	0.02	0.03	0.03	0.03	0.02	0.01	0.00	0.01	0.01					
Σ cat.	7.83	7.85	7.86	7.85	7.85	7.86	7.84	7.83	7.83	7.81	7.82	7.82	7.82	7.83	7.79

n.d.: not determined. H: S. Hackspikgruvan, M: Malmkärra, Ö: Östanmossa. The compositional data are first reported in wt%, then in *apfu*, with the conversion based on 12.5 atoms of oxygen.

relation to ferriallanite-(Ce); it is then surrounded by cerite-(Ce). At rare contacts with patches of bastnäsite, the crystals tend to be subhedral in shape. Törnebohmite is said to have been found in relatively large quantities at S. Hackspikgruvan (Geijer 1936), but such material was not available to us.

The chemical variation within the investigated population of samples is moderate (Table 6). A clear negative correlation between Fe and Al was found ($R = -0.92$ for $n = 11$), indicating that Fe substitutes for Al at the octahedral sites (and indirectly that Fe essentially is in the trivalent state in the mineral). Small amounts of Mg (0.02–0.04 *apfu*) are probably present in these positions as well. Values of F concentration are close to the detection limit in all samples, proving that F–OH substitution is negligible.

There is no appreciable Ca replacing (Ce, La) in the structure, in contrast to what is found for the associated REE silicates. Törnebohmite-(Ce) also is exceptional in that the concentration of Y_2O_3 is below detection for all samples. It is considerably enriched in La compared to the coexisting cerite-(Ce) in #A37 (Fig. 7).

The unit-cell parameters for #A37 are a 7.438(4), b 5.690(4), c 17.02(1) Å, β 111.96(8)°. Shen & Moore (1982) reported a 7.383(4), b 5.673(3), c 16.937(6) Å, β 112.04(8)° from single-crystal data; no corresponding chemical analysis was carried out, so a direct comparison is not possible.

Törnebohmite is a rare mineral globally, and few published analytical data are available for reference. According to Svyazhin (1962), törnebohmite-(La) occurs in a granite pegmatite in a fenitization zone of a nepheline syenite massif in the Urals. Wet-chemical analysis showed SiO_2 20.33, TiO_2 0.12, REE 62.88, Fe_2O_3 2.61, Al_2O_3 10.11, MgO 0.92, CaO 2.46, H_2O+ 0.78 (all in wt.%). These data yield a poor formula, and the data may be inferior owing to impurities. Kapustin

(1989) reported a fluorian variety of törnebohmite-(Ce) from Ulan-Erge, Tuva alkaline massif, with 0.7 wt.% F. That material also contains appreciable Ti (0.44 wt.% TiO_2), Th (0.39 wt.% ThO_2), Ca (0.48 wt.% CaO) and Sr (0.36 wt.% SrO).

Minerals of the gadolinite group

Gadolinite, $(REE,Y)_2FeBe_2[Si_2O_8]O_2$, is new to the Bastnäs-type deposits and the only Be mineral known there. It appears to be very rare at the subtype-1 deposits, and more widespread in the Norberg District, although mostly in microscopic amounts. Gadolinite-(Ce) was found in a single sample from Bastnäs (#03+246), in which it occurs as irregular grains up to 0.8 mm

TABLE 6. CHEMICAL COMPOSITION OF TÖRNEBOHMITE FROM BASTNÄS

Sample #	A37			LK4838					g10778			03+0246		
point	ap2	ap8	bv4	p1	p2	p3	p4	p5	bp1	bp4	bp6	B:1	B:2	B:5
La_2O_3 wt%	28.19	24.37	24.72	24.70	24.13	23.18	24.34	23.78	25.05	25.17	26.73	18.05	16.43	12.40
Ce_2O_3	29.24	31.18	31.64	31.74	31.89	30.68	31.42	31.30	31.07	30.69	29.67	31.70	29.81	29.71
Pr_2O_3	1.65	2.03	2.09	2.03	2.14	2.28	2.14	2.17	2.02	2.12	1.85	3.25	3.48	4.06
Nd_2O_3	4.56	5.58	5.35	5.45	5.70	7.06	5.64	6.14	5.59	5.74	5.69	10.34	11.42	15.45
Sm_2O_3	0.12	0.22	0.23	0.31	0.34	0.47	0.32	0.36	0.33	0.23	0.26	0.61	1.19	1.50
Gd_2O_3	0.05	0.05	0.04	0.00	0.13	0.16	0.21	0.06	0.24	0.06	0.00	0.20	0.48	0.60
Dy_2O_3	0.00	0.01	0.00	0.00	0.00	0.03	0.00	0.00	0.00	0.00	0.06	0.00	0.00	0.00
Ho_2O_3	0.07	0.00	0.05	0.04	0.00	0.00	0.03	0.00	0.00	0.00	0.00	n.d.	n.d.	n.d.
Er_2O_3	0.00	0.02	0.00	0.06	0.07	0.05	0.00	0.06	0.00	0.00	0.00	0.00	0.00	0.00
Yb_2O_3	0.02	0.03	0.03	0.03	0.00	0.05	0.00	0.01	0.00	0.04	0.00	n.d.	n.d.	n.d.
Lu_2O_3	0.00	0.00	0.01	0.00	0.01	0.00	0.02	0.00	0.00	0.02	0.03	n.d.	n.d.	n.d.
Y_2O_3	0.03	0.02	0.00	0.01	0.01	0.03	0.02	0.03	0.00	0.00	0.00	0.00	0.08	0.05
CaO	0.05	0.01	0.04	0.01	0.01	0.02	0.00	0.01	0.01	0.04	0.02	0.02	0.10	0.10
Fe_2O_3	1.24	1.60	1.90	1.25	1.15	1.18	0.97	1.10	0.94	1.99	1.50	0.92	1.05	0.76
MgO	0.37	0.15	0.34	0.17	0.19	0.21	0.20	0.22	0.16	0.21	0.17	0.62	0.33	0.31
Al_2O_3	8.75	8.60	8.22	8.92	8.93	8.93	8.98	8.87	8.85	8.04	8.42	7.61	7.61	8.29
SiO_2	23.15	22.85	22.69	22.29	21.56	22.09	22.65	22.61	22.26	21.98	22.14	22.79	22.26	22.68
P_2O_5	0.06	0.05	0.08	0.06	0.05	0.03	0.07	0.04	0.14	0.07	0.14	0.49	0.09	0.32
F	0.09	0.13	0.14	0.07	0.09	0.10	0.10	0.12	0.04	0.04	0.01	b.d.	b.d.	b.d.
O=F	-0.04	-0.06	-0.06	-0.03	-0.04	-0.04	-0.04	-0.05	-0.02	-0.02	0.00			
Total	97.61	96.85	97.52	97.11	96.35	96.52	97.06	96.82	96.69	96.41	96.72	96.61	94.34	96.23
La *apfu*	0.89	0.78	0.79	0.79	0.78	0.75	0.78	0.76	0.81	0.82	0.86	0.58	0.54	0.40
Ce	0.92	0.99	1.00	1.01	1.03	0.98	1.00	0.99	0.99	0.99	0.96	1.01	0.98	0.97
Pr	0.05	0.06	0.07	0.06	0.07	0.07	0.07	0.07	0.06	0.07	0.06	0.10	0.11	0.13
Nd	0.14	0.17	0.16	0.17	0.18	0.22	0.17	0.19	0.17	0.18	0.18	0.32	0.37	0.49
Sm	0.00	0.01	0.01	0.01	0.01	0.01	0.01	0.01	0.01	0.01	0.01	0.02	0.04	0.05
Gd	0.00	0.00	0.00	0.00	0.00	0.00	0.01	0.00	0.01	0.00	0.00	0.01	0.01	0.02
Dy	0.00	0.00	0.00	0.00	0.00	0.00	0.00	0.00	0.00	0.00	0.00	0.00	0.00	0.00
Ho	0.00	0.00	0.00	0.00	0.00	0.00	0.00	0.00	0.00	0.00	0.00			
Er	0.00	0.00	0.00	0.00	0.00	0.00	0.00	0.00	0.00	0.00	0.00	0.00	0.00	0.00
Yb	0.00	0.00	0.00	0.00	0.00	0.00	0.00	0.00	0.00	0.00	0.00			
Lu	0.00	0.00	0.00	0.00	0.00	0.00	0.00	0.00	0.00	0.00	0.00			
Y	0.00	0.00	0.00	0.00	0.00	0.00	0.00	0.00	0.00	0.00	0.00	0.00	0.00	0.00
Ca	0.00	0.00	0.00	0.00	0.00	0.00	0.00	0.00	0.00	0.00	0.00	0.00	0.01	0.01
Fe^{3+}	0.08	0.10	0.12	0.08	0.08	0.08	0.06	0.07	0.06	0.13	0.10	0.06	0.07	0.05
Mg	0.05	0.02	0.04	0.02	0.02	0.03	0.03	0.03	0.02	0.03	0.02	0.08	0.04	0.04
Al	0.88	0.88	0.84	0.91	0.93	0.92	0.92	0.91	0.91	0.83	0.87	0.78	0.81	0.86
Si	1.98	1.98	1.96	1.93	1.90	1.93	1.96	1.96	1.95	1.94	1.94	1.99	2.00	1.99
P	0.00	0.00	0.00	0.00	0.00	0.00	0.00	0.00	0.00	0.00	0.00	0.04	0.01	0.02
F	0.03	0.04	0.04	0.02	0.02	0.03	0.03	0.03	0.01	0.01	0.00			

n.d.: not determined; b.d.: below detection. Formula proportions are calculated on the basis of five cations.
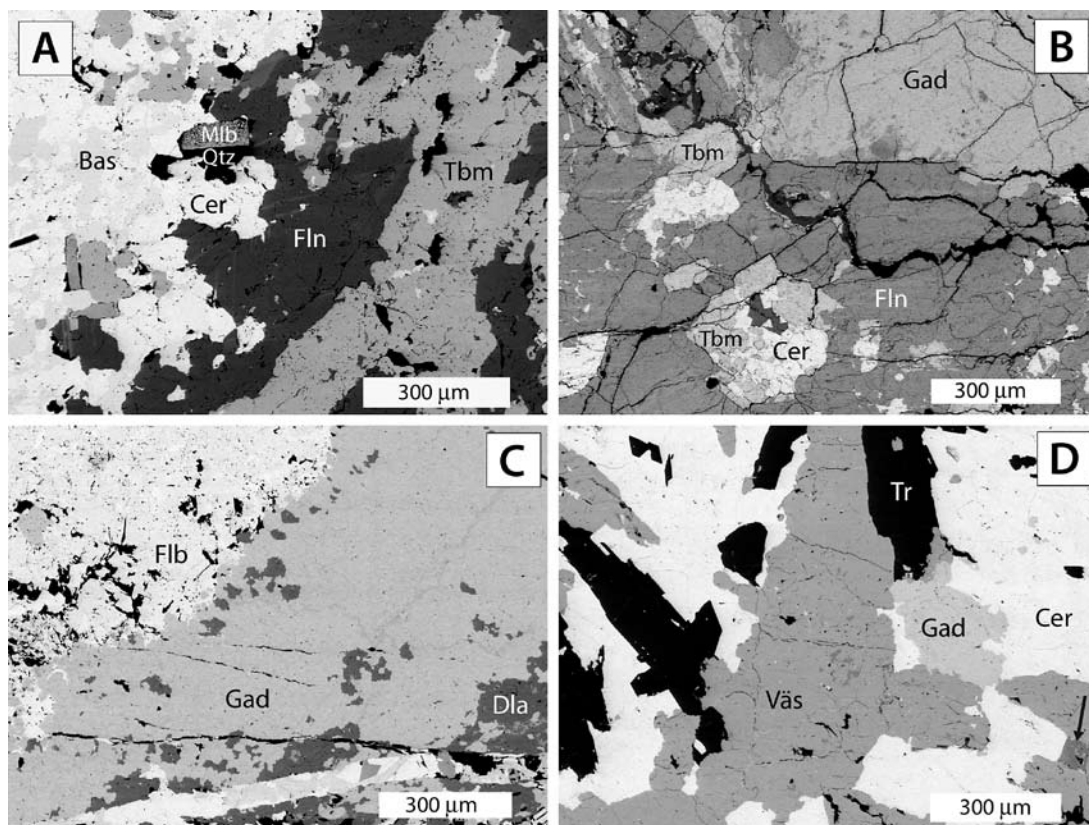
FIG. 11. BSE images of REE mineral assemblages from Bastnäs-type deposits. (A) Sample #A37, Bastnäs, with cerite (Cer), ferriallanite (Fln), törnebohmite (Tbm), bastnäsite (Bas) and molybdenite (Mlb). Quartz (Qtz) fills a small cavity. (B) Sample 03+0246, Bastnäs, with gadolinite (Gad), cerite, ferriallanite and törnebohmite. (C) Sample #970319, Malmkärra, with gadolinite, fluorbritholite (Flb) and dollaseite (Dla). (D) Sample #660298, Malmkärra, with västmanlandite (Väs), gadolinite, tremolite, cerite and magnetite (arrow).

across (Fig. 11B), in contact with törnebohmite-(Ce), ferriallanite-(Ce) and cerite-(Ce). The specimen also contains the Fe-analogue of västmanlandite-(Ce). The unit-cell parameters of gadolinite-(Ce), determined by single-crystal diffractometry, are *ca. a* 4.82, *b* 7.71, *c* 10.10 Å, β 90.12°, *V* 375 Å³.

In the subtype-2 localities, gadolinite is not restricted to a specific type of association, and a short description of each sample seems appropriate. Generally, the mineral is greenish yellow to green in thin section, without any appreciable pleochroism. In sample #970319 from Malmkärra, fine-grained masses of gadolinite-(Ce) – gadolinite-(Y), up to 2 cm wide, occur in an assemblage of mainly fluorbritholite-(Ce), västmanlandite-(Ce) and dollaseite-(Ce) (Fig. 11C). Textural features suggest that the gadolinite formed at the expense of fluorbritholite-(Ce). Sample #540033 (Malmkärra) is a specimen of tremolite–magnetite

skarn with significant dissakisite-(Ce) and fluorbritholite-(Ce). "Gadolinite-(Nd)" occurs as anhedral grains up to 100 μm in their greatest dimension, enclosed by dissakisite-(Ce). In sample #660298 (Malmkärra), anhedral grains (≤300 μm) of "gadolinite-(Nd)" occur in aggregates of cerite-(Ce), and is locally in contact with both västmanlandite-(Ce) and tremolite (Fig. 11D).

Sample #02+0126 from the Östanmossa deposit is a tremolite – magnetite – phlogopite skarn with scattered grains of molybdenite and pyrite. Solitary, subhedral crystals of gadolinite-(Y) (<1 mm) occur in a phlogopite–chlorite mass (Fig. 12A), locally in contact with magnetite. No other REE minerals have been observed in this thin section. Sample #520767 from Johannagruvan contains highly irregular grains (<200 μm) of gadolinite-(Y), partly intergrown with dollaseite-(Ce), within magnetite-bearing tremolite skarn (Fig. 12B). A vein of norbergite, 1–3 mm wide,

transects the rock just a few mm from the portion with gadolinite-(Y).

Cerium, Nd and Y are dominant in the gadolinite samples, corresponding to 70–75% of the trivalent cations present, and the compositional variations with respect to these elements are significant, probably more extensive than for any other REE mineral studied here (Table 7). Grains (in some cases only minor portions of them) corresponding to gadolinite-(Ce), gadolinite-(Y) and the Nd-dominant member ("gadolinite-Nd") have been identified (Fig. 13). Single crystals commonly show irregular growth-induced zoning in BSE mode (Fig. 12A), essentially related to variations in Ce and Y. Analytical results along a traverse (step size *ca.* 50 μm) from the periphery toward the center of an aggregate (#97319) show no correlation between composition and lateral displacement, but a pattern with clear antipathetic behavior of Ce *versus* Y is evident (Fig. 14). Gado-

linite-(Ce) is the most Y-rich phase found at Bastnäs, with Y/Ce = 0.25; the coexisting cerite-(Ce) has Y/Ce = 0.06. A few points in the analyzed grain (#03+246) actually have Nd > Ce, but on average, the phase is Ce-dominant. For gadolinite-(Y) in sample #520767 (Johannagruvan), the Y/Ce value attains 3.40, higher than in any other mineral from these deposits.

The gadolinite samples have, appropriately enough, the highest overall concentration of Gd (3.3–7.7 wt.% Gd_2O_3), although there is some overlap with the range for fluorbritholite (0.6–5.6 wt.% Gd_2O_3), a mineral that displays a similar range of Gd/Y values (0.3–0.9).

As there is an apparent lack of detectable Al in the samples, and as gadolinite is not known to incorporate lighter elements in its tetrahedral sites (*e.g.,* Demartin *et al.* 1993), the chemical formulae (Table 7) are calculated on the basis of 2 Si *apfu*. This approach reveals that all analyzed samples have a significant
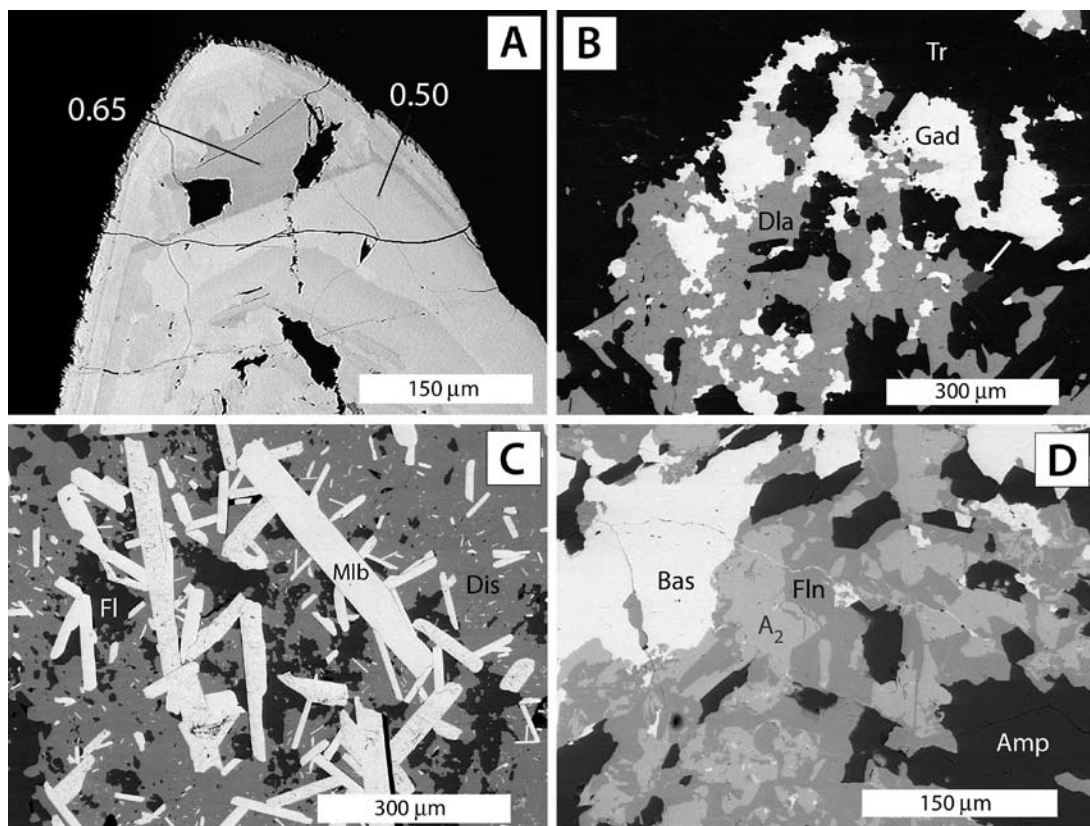
FIG. 12.   BSE images of REE mineral assemblages from Bastnäs-type deposits. (A) Part of chemically zoned crystal of gadolinite in sample #02+0126 from Östanmossa. Matrix consists of a chlorite mineral. Numbers indicate the amount of Y atoms per formula units, obtained from point analysis. (B) Sample #520767, Johannagruvan, with gadolinite (Gad), tremolite (Tr), dollaseite (Dla) and fluorapatite (arrow). (C) Sample #540025, S. Hackspikgruvan, with molybdenite (Mlb), dissakisite (Dis) and fluorite (Fl). (D) Sample #880072 from Rödbergsgruvan with bastnäsite (Bas), amphibole (Amp), ferriallanite (Fln) and the Fe-rich analogue of västmanlandite (A_2).

deficiency in Fe, with 0.72 *apfu* on average, compared to the stoichiometric value (1.00). The phenomenon is most probably related to a hingganite-type substitution ($Fe^{2+} + 2 O^{2-} = \square + 2 OH^{-}$), commonly encountered in gadolinite-group minerals (*e.g.,* Demartin *et al.* 2001), and in the present suite of samples, amounting to a molar fraction of $(REE, Y)_2Be_2[Si_2O_8](OH)_2$ in the range 0.10–0.35. The presence of some Mg (mean 0.07, maximum value 0.19 *apfu*) is clearly insufficient to compensate for the shortage in Fe. A positive ($r = 0.70$) correlation between Mg and Y, suggesting a substitution toward $Y_2MgBe_2[Si_2O_8]O_2$, a previously unrecognized "end-member" of the gadolinite group, is noteworthy. The fact that F is not detected in gadolinite, despite the

F-rich bulk composition of these rocks, indicates that F–OH substitution does not occur in the hingganite component of these minerals.

Mössbauer spectroscopy demonstrates that Fe is exclusively divalent in a sample (#970319) of gadolinite (Fig. 15). The shape of the spectrum shows a close resemblance to that of a recrystallized (annealed), originally metamict, sample of gadolinite-(Y) from Ytterby, as presented by Malczewski & Janeczek (2002). The CS values (1.04 mm/s) are identical, and in both cases, there is a distribution in the QS values related to variations of nearest-neighbor atom around the six-fold site occupied by Fe in the structure.

The samples are poor in Ca (mean 0.18 wt.%, range 0.06–0.58 wt.% CaO), indicating that the components datolite, $Ca_2B_2[Si_2O_8](OH)_2$, and homilite, $Ca_2FeB_2[Si_2O_8]O_2$, are very minor, in contrast to many specimens of gadolinite originating from alpine fissures and granitic pegmatites (Demartin *et al.* 1993, 2001, Pezzotta *et al.* 1999). This conclusion further justifies the calculation of the BeO contents (Table 7) on the stoichiometric basis of 2 Be *apfu* (*i.e.*, B-for-Be substitution is assumed to be negligible). The formula calculations give the sums $(REE + Y + Ca) \approx 1.90$ *apfu* in total. The deviation from ideality (2 *apfu*) might be due to errors in the analyses, or it might reflect a partial vacancy in the crystal structure. Note that there is no sign of metamictization in the analyzed grains, in agreement with the low concentrations of U and Th.

The unit-cell parameters for gadolinite-(Ce) – gadolinite-(Y) in #97319 were determined to be *a* 4.793(4), *b* 7.674(8), *c* 10.02(1) Å, β 90.76(9)°. The smaller unit-cell volume of this sample compared to #03+246 (368 Å^3 *versus* 375 Å^3) is consistent with its higher average Y/Ce value. Non-metamict varities of
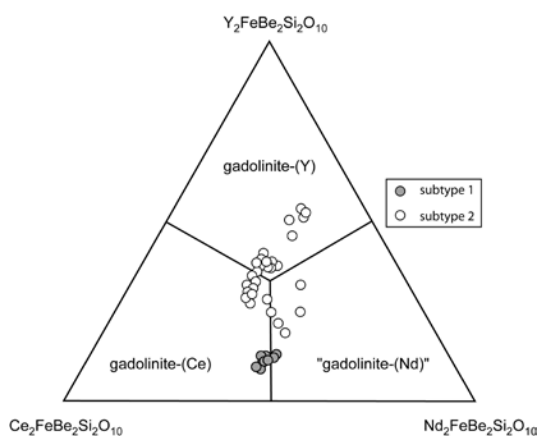
FIG. 13. Compositional diagram for the dominant REE in gadolinite.
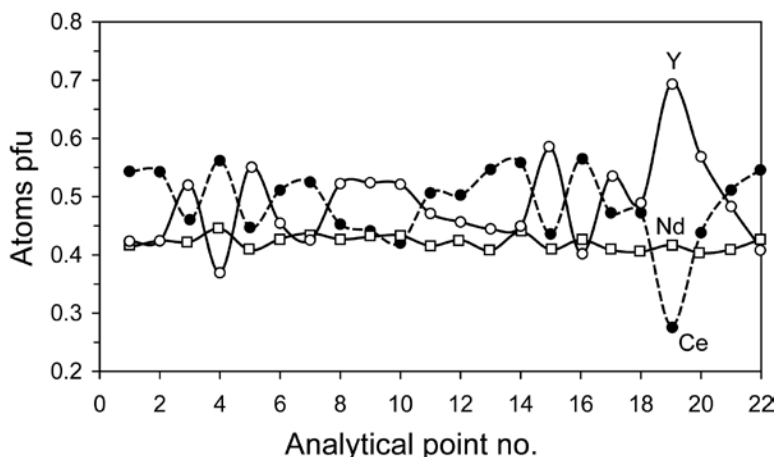
FIG. 14. Compositional profile of heterogeneous gadolinite (sample #970319 from Malm-kärra). Step size is *ca.* 6 μm.

gadolinite are relatively rare, but note that Segalstad & Larsen (1978) reported a V_{cell} of 366 Å^3 for a sample of gadolinite-(Ce) that contains a significant proportion of the datolite component. For gadolinite-(Y) with near-end-member composition, V_{cell} is equal to 652 Å^3 (Demartin *et al.* 1993).

Percleveite-(Ce)

The rare species percleveite-(Ce), ideally $Ce_2[Si_2O_7]$, was recently described from the Bastnäs deposit by Holtstam *et al.* (2003a), and only little needs to be added to their description. It occurs closely associated with mainly cerite-(Ce), in an apparent equilibrium

assemblage (sample #060375). Some bastnäsite-(Ce) has formed at the expense of both minerals, and quartz occurs in interstices and microcracks in the assemblage. Percleveite-(Ce) is enriched in Y (Y/Ce = 0.14) compared to coexisting cerite-(Ce) (Y/Ce = 0.06).

Unnamed mineral D

An unknown mineral, tentatively assigned the formula $(Y,Ce,Nd)_4MgSi_4O_{14}F_2$, was found in sample #970319 from Malmkärra. It occurs as a single grain of irregular outline, *ca.* 1.2 mm across, in contact with fluorbritholite-(Ce). The crystal is colorless, nonpleochroic and biaxial, with a large 2*V*. Owing to the specific

TABLE 7. CHEMICAL COMPOSITION OF GADOLINITE

Sample#	520767 J					540033 M		660298 M		970319 M					
point	p1	p2	p3	p4	p5	A2:1	A2:2	3:1	3:2	p1	p4	p10	p18	p19	p22
La$_2$O$_3$	1.16	1.12	1.80	1.21	1.05	1.86	2.12	3.20	3.23	4.92	4.93	2.81	3.78	1.41	4.89
Ce$_2$O$_3$	6.67	6.31	8.71	6.47	6.07	10.32	11.53	15.07	15.34	16.75	17.33	13.15	14.50	8.81	16.89
Pr$_2$O$_3$	1.78	1.89	2.14	1.77	1.74	2.54	2.54	3.26	3.04	2.64	2.86	2.50	2.43	2.16	2.72
Nd$_2$O$_3$	14.14	13.71	14.18	13.62	14.01	17.58	18.69	19.52	18.04	13.06	14.08	13.89	12.76	13.52	13.53
Sm$_2$O$_3$	6.24	5.98	5.48	5.88	6.56	6.21	6.10	4.90	4.73	3.52	3.39	4.53	3.65	5.08	3.42
Gd$_2$O$_3$	7.03	7.00	6.06	7.04	7.67	5.46	5.26	3.59	3.44	3.78	3.51	4.85	4.17	5.61	3.65
Tb$_2$O$_3$	0.33	0.20	0.17	0.23	0.19	n.d.	n.d.	n.d.	n.d.	0.00	0.00	0.15	0.07	0.40	0.00
Dy$_2$O$_3$	2.05	2.03	1.85	2.15	2.24	1.25	1.03	0.50	0.58	1.59	1.34	1.87	1.88	2.48	1.53
Ho$_2$O$_3$	0.20	0.25	0.23	0.22	0.27	0.00	0.00	0.00	0.00	0.21	0.17	0.28	0.25	0.42	0.21
Er$_2$O$_3$	0.00	0.00	0.00	0.00	0.02	0.32	0.18	0.14	0.18	0.06	0.00	0.14	0.03	0.36	0.00
Yb$_2$O$_3$	0.16	0.23	0.15	0.16	0.16	0.00	0.00	0.00	0.00	0.10	0.12	0.20	0.18	0.33	0.13
Lu$_2$O$_3$	0.00	0.00	0.00	0.00	0.00	0.00	0.00	0.00	0.00	0.00	0.00	0.00	0.00	0.00	0.00
Y$_2$O$_3$	14.57	15.19	13.07	15.19	14.68	8.71	6.60	5.31	6.03	8.98	7.84	11.22	10.33	15.09	8.74
CaO	0.28	0.28	0.29	0.29	0.58	0.24	0.09	0.09	0.06	0.17	0.21	0.20	0.23	0.37	0.22
FeO	9.81	10.08	10.09	10.02	9.14	8.67	9.20	9.77	10.08	10.30	10.44	9.68	9.76	8.23	10.17
MgO	0.49	0.61	0.80	0.65	0.41	0.39	0.63	0.45	0.15	0.67	0.58	0.58	1.44	0.21	0.79
Al$_2$O$_3$	0.00	0.00	0.00	0.00	0.00	0.00	0.00	0.00	0.00	0.00	0.00	0.00	0.00	0.00	0.00
SiO$_2$	23.11	23.14	22.86	23.15	23.34	22.39	22.43	22.42	22.41	22.57	22.59	22.91	22.48	23.17	22.62
P$_2$O$_5$	0.00	0.00	0.00	0.00	0.00	0.00	0.00	0.10	0.03	0.00	0.00	0.00	0.00	0.00	0.00
Ba	0.03	0.04	0.03	0.04	0.02	0.00	0.00	0.00	0.00	0.04	0.04	0.04	0.05	0.05	0.05
Cl	0.01	0.00	0.02	0.02	0.03	0.05	0.02	0.01	0.02	0.01	0.02	0.04	0.03	0.04	0.03
BeO*	9.62	9.63	9.52	9.64	9.72	9.32	9.34	9.33	9.33	9.40	9.40	9.54	9.36	9.65	9.42
Total	97.68	97.71	97.43	97.73	97.87	95.33	95.74	97.68	96.69	98.75	98.85	98.56	97.38	97.39	98.96
La	0.04	0.04	0.06	0.04	0.03	0.06	0.07	0.11	0.11	0.16	0.16	0.09	0.12	0.04	0.16
Ce	0.21	0.20	0.28	0.20	0.19	0.34	0.38	0.49	0.50	0.54	0.56	0.42	0.47	0.28	0.55
Pr	0.06	0.06	0.07	0.06	0.05	0.08	0.08	0.11	0.10	0.09	0.09	0.08	0.08	0.07	0.09
Nd	0.44	0.42	0.44	0.42	0.43	0.56	0.60	0.62	0.58	0.41	0.45	0.43	0.41	0.42	0.43
Sm	0.19	0.18	0.17	0.18	0.19	0.19	0.19	0.15	0.15	0.11	0.10	0.14	0.11	0.15	0.10
Gd	0.20	0.20	0.18	0.20	0.22	0.16	0.16	0.11	0.11	0.11	0.10	0.14	0.12	0.16	0.11
Tb	0.01	0.01	0.00	0.01	0.01	0.00	0.00	0.00	0.00	0.00	0.00	0.00	0.00	0.01	0.00
Dy	0.06	0.06	0.05	0.06	0.06	0.04	0.03	0.01	0.02	0.05	0.04	0.05	0.05	0.07	0.04
Ho	0.01	0.01	0.01	0.01	0.01	0.00	0.00	0.00	0.00	0.01	0.00	0.01	0.01	0.01	0.01
Er	0.00	0.00	0.00	0.00	0.00	0.01	0.01	0.00	0.00	0.00	0.00	0.00	0.00	0.01	0.00
Yb	0.00	0.01	0.00	0.00	0.00	0.00	0.00	0.00	0.00	0.00	0.00	0.01	0.00	0.01	0.00
Lu	0.00	0.00	0.00	0.00	0.00	0.00	0.00	0.00	0.00	0.00	0.00	0.00	0.00	0.00	0.00
Y	0.67	0.70	0.61	0.70	0.67	0.41	0.31	0.25	0.29	0.42	0.37	0.52	0.49	0.69	0.41
Ca	0.03	0.03	0.03	0.03	0.05	0.02	0.01	0.01	0.01	0.02	0.02	0.02	0.02	0.03	0.02
Fe^{2+}	0.71	0.73	0.74	0.72	0.66	0.65	0.69	0.73	0.75	0.76	0.77	0.71	0.73	0.59	0.75
Mg	0.06	0.08	0.10	0.08	0.05	0.05	0.08	0.06	0.02	0.09	0.08	0.08	0.19	0.03	0.10
Si	2.00	2.00	2.00	2.00	2.00	2.00	2.00	2.00	2.00	2.00	2.00	2.00	2.00	2.00	2.00
P	0.00	0.00	0.00	0.00	0.00	0.00	0.00	0.01	0.00	0.00	0.00	0.00	0.00	0.00	0.00
Ba	0.00	0.00	0.00	0.00	0.00	0.00	0.00	0.00	0.00	0.00	0.00	0.00	0.00	0.00	0.00
Cl	0.00	0.00	0.00	0.00	0.00	0.01	0.00	0.00	0.00	0.00	0.00	0.01	0.00	0.01	0.00
Be*	2.00	2.00	2.00	2.00	2.00	2.00	2.00	2.00	2.00	2.00	2.00	2.00	2.00	2.00	2.00
Σcat.	6.68	6.71	6.74	6.71	6.63	6.58	6.60	6.66	6.62	6.77	6.76	6.70	6.82	6.59	6.78

TABLE 7 (cont'd). CHEMICAL COMPOSITION OF GADOLINITE

Sample#	02+0126 Ö				03+0246 B									
point	1:1	1:2	1:3	1:4	D:1	D:2	D:3	D:4	D:5	D:6	D:7	D:9	D:10	D:11
La_2O_3 wt%	3.03	2.57	1.62	2.96	6.16	5.50	4.90	5.17	6.03	5.75	4.94	5.95	6.45	6.10
Ce_2O_3	12.81	12.20	8.25	12.46	19.05	17.77	16.48	16.44	18.44	18.15	15.73	18.66	19.06	18.83
Pr_2O_3	2.50	2.53	2.15	2.61	3.52	3.29	3.54	3.07	3.40	3.13	3.13	3.19	3.67	3.54
Nd_2O_3	13.79	14.67	13.02	13.87	18.48	18.11	18.72	18.32	17.91	17.89	18.19	18.34	17.55	18.01
Sm_2O_3	4.05	4.12	4.50	4.26	4.02	4.87	4.70	4.88	4.17	4.49	5.06	4.18	4.11	3.93
Gd_2O_3	4.05	4.13	5.10	3.96	3.47	4.20	4.34	4.61	3.52	3.73	4.86	3.56	3.46	3.30
Tb_2O_3	n.d.	n.d.	n.d.	n.d.	0.01	0.00	0.05	0.01	0.00	0.00	0.00	0.00	0.00	0.00
Dy_2O_3	1.35	1.27	2.14	1.41	0.17	0.35	0.35	0.43	0.25	0.28	0.49	0.31	0.12	0.12
Ho_2O_3	0.00	0.00	0.00	0.00	n.d.	n.d.	n.d.	n.d.	n.d.	n.d.	n.d.	n.d.	n.d.	n.d.
Er_2O_3	0.45	0.53	0.70	0.50	0.04	0.00	0.03	0.10	0.00	0.01	0.00	0.09	0.00	0.02
Yb_2O_3	n.d.	n.d.	n.d.	n.d.	n.d.	n.d.	n.d.	n.d.	n.d.	n.d.	n.d.	n.d.	n.d.	n.d.
Lu_2O_3	n.d.	n.d.	n.d.	n.d.	n.d.	n.d.	n.d.	n.d.	n.d.	n.d.	n.d.	n.d.	n.d.	n.d.
Y_2O_3	10.42	10.75	14.16	11.02	2.24	3.21	3.46	2.98	2.86	3.14	3.80	3.53	2.41	2.57
CaO	0.21	0.12	0.27	0.17	0.16	0.13	0.15	0.10	0.11	0.14	0.12	0.13	0.09	0.16
FeO	9.50	9.75	9.54	9.62	8.93	9.11	8.88	9.19	8.80	9.09	9.32	8.67	9.14	8.23
MgO	1.25	1.03	0.82	1.17	0.06	0.08	0.00	0.08	0.11	0.11	0.12	0.10	0.09	0.11
Al_2O_3	0.00	0.00	0.00	0.00	0.00	0.00	0.00	0.00	0.00	0.00	0.00	0.00	0.00	0.00
SiO_2	23.08	22.93	23.28	23.02	21.69	22.54	22.93	21.48	22.33	21.66	21.87	21.73	22.25	21.89
P_2O_5	0.07	0.09	0.07	0.05	0.06	0.05	0.05	0.04	0.00	0.03	0.03	0.00	0.00	0.11
Ba	n.d.	n.d.	n.d.	n.d.	n.d.	n.d.	n.d.	n.d.	n.d.	n.d.	n.d.	n.d.	n.d.	n.d.
Cl	0.03	0.02	0.02	0.03	n.d.	n.d.	n.d.	n.d.	n.d.	n.d.	n.d.	n.d.	n.d.	n.d.
BeO*	9.61	9.55	9.69	9.58	9.03	9.38	9.55	8.94	9.30	9.02	9.11	9.05	9.26	9.11
Total	96.20	96.24	95.33	96.69	97.10	98.61	98.14	95.83	97.22	96.61	96.77	97.48	97.68	96.03
La *apfu*	0.10	0.08	0.05	0.09	0.21	0.18	0.16	0.18	0.20	0.20	0.17	0.20	0.21	0.21
Ce	0.41	0.39	0.26	0.40	0.64	0.58	0.53	0.56	0.60	0.61	0.53	0.63	0.63	0.63
Pr	0.08	0.08	0.07	0.08	0.12	0.11	0.11	0.10	0.11	0.11	0.10	0.11	0.12	0.12
Nd	0.43	0.46	0.40	0.43	0.61	0.57	0.58	0.61	0.57	0.59	0.59	0.60	0.56	0.59
Sm	0.12	0.12	0.13	0.13	0.13	0.15	0.14	0.16	0.13	0.14	0.16	0.13	0.13	0.12
Gd	0.12	0.12	0.15	0.11	0.11	0.12	0.13	0.14	0.10	0.11	0.15	0.11	0.10	0.10
Tb	0.00	0.00	0.00	0.00	0.00	0.00	0.00	0.00	0.00	0.00	0.00	0.00	0.00	0.00
Dy	0.04	0.04	0.06	0.04	0.01	0.01	0.01	0.01	0.01	0.01	0.01	0.01	0.00	0.00
Er	0.01	0.01	0.02	0.01	0.00	0.00	0.00	0.00	0.00	0.00	0.00	0.00	0.00	0.00
Y	0.48	0.50	0.65	0.51	0.11	0.15	0.16	0.15	0.14	0.15	0.19	0.17	0.12	0.12
Ca	0.02	0.01	0.02	0.02	0.02	0.01	0.01	0.01	0.01	0.01	0.01	0.01	0.01	0.02
Fe^{2+}	0.69	0.71	0.69	0.70	0.69	0.68	0.65	0.72	0.66	0.70	0.71	0.67	0.69	0.63
Mg	0.16	0.13	0.11	0.15	0.01	0.01	0.00	0.01	0.02	0.02	0.02	0.01	0.01	0.02
Si	2.00	2.00	2.00	2.00	2.00	2.00	2.00	2.00	2.00	2.00	2.00	2.00	2.00	2.00
P	0.00	0.01	0.01	0.00	0.01	0.00	0.00	0.00	0.00	0.00	0.00	0.00	0.00	0.01
Cl	0.00	0.00	0.00	0.01										
Be*	2.00	2.00	2.00	2.00	2.00	2.00	2.00	2.00	2.00	2.00	2.00	2.00	2.00	2.00
Σ cations	6.66	6.67	6.61	6.68	6.65	6.58	6.48	6.65	6.55	6.66	6.64	6.66	6.58	6.56

n.d.: not determined. B: Bastnäs, J: Johannagruvan, M: Malmkärra, Ö: Östanmossa. The compositional data are first reported in wt%, then in *apfu*, recalculated on the basis of two atoms of Si.

orientation of the grain and its uniform extinction, the optical sign could not be determined with certainty. On the basis of the chemical data (Table 4), it seems to represent the Mg-analogue of rowlandite-(Y), nominally $Y_4Fe[Si_2O_7]_2F_2$, a triclinic mineral (Sipovalov & Stepanov 1971) normally found in granitic pegmatite environments. The analytical totals are reasonable for an anhydrous mineral, and a charge-balance calculation for the average composition, based on nine cations, gives 29.98 positive charges, in excellent agreement with the suggested formula. Further study is required for a full characterization of this apparently new species. It is one of the few phases with clear Y-dominance found at these deposits. The ratio Y/Ce is 1.89–1.99,

higher than in any other mineral in the sample [where fluorbritholite-(Ce) has 0.35 < Y/Ce < 0.58 and gadolinite-(Ce) – gadolinite-(Y) has 0.66 < Y/Ce < 1.34]. Note also the unique enrichment in the HREE (for these deposits), with >1 wt.% Yb_2O_3 and detectable amounts of Lu in the unnamed mineral. The result is a nearly complete and unusually flat chondrite-normalized REE curve (Fig. 16).

Unnamed mineral C

A tungsten-bearing REE silicate mineral occurs in a Bastnäs sample (#060375) as rare anhedral grains up to 300 μm wide. They are optically biaxial and

strongly pleochroic (rust red to nearly black). Scheelite appears as a filling of microfractures in the grains. From textural relations, it is clear that the mineral formed at the expense of associated cerite-(Ce) and percleveite-(Ce). The REE array (Table 4) is similar for the three minerals (Ce > La > Nd > Pr > Sm), but mineral C is significantly lower in Y (Y/Ce = 0.01). It is clearly exotic in combining REE, Si and W as major components. On the whole, members of the silicate class with structural W are very few (*e.g.,* welinite, the khomyakovite series), and the eudialyte-group member johnsenite-(Ce) is the only REE–W-bearing silicate mineral hitherto approved (Grice & Gault 2006). The exotic composition of mineral C and its association with percleveite-(Ce) point to unusual conditions of formation for this mineral.

The valence state of Fe and the possible presence of hydroxide in the mineral remain open questions. A tentative empirical formula, compatible with the analytical data at hand, would be $(Ce,La,Nd,Ca)_5$ $Mg(Fe,Al)_3WSi_5O_{26}$ on an anhydrous basis. The oxide sums are in the range 97.5–99.3 wt.%, assuming only Fe^{3+}.

Dollaseite-(*Ce*) – dissakisite-(*Ce*)

Dollaseite-(Ce), ideally $CeCaMg_2Al[SiO_4][Si_2O_7]$ $F(OH)$, is an important mineral for the sequestration of REE in the type-2 deposits of the Norberg District, but not known from any locality outside this area. It was originally described from Östanmossa and named "magnesium orthite" by Geijer (1927). Peacor & Dunn (1988) renamed it dollaseite-(Ce), and demonstrated its close structural relationship with the allanite subgroup; it is chemically distinguished from the other members by a charge-coupled substitution involving both cations and anions: $(Fe, Al)^{3+} + O^{2-} = Mg^{2+} +$ F^-. As shown in this work, the exchange is not always complete, and some samples actually tend to be closer to dissakisite-(Ce), $CeCaMgAl_2[SiO_4][Si_2O_7]O(OH)$, in composition. For this reason, all the REE-bearing epidote-group minerals from the subtype-2 deposits will be treated together, under the present heading.

Dollaseite-(Ce) typically occurs as dark brown aggregates, several cm wide, in a mineralized dolomite–tremolite rock. The mineral grains are normally up to 0.5 mm long and irregular in outline, but subhedral
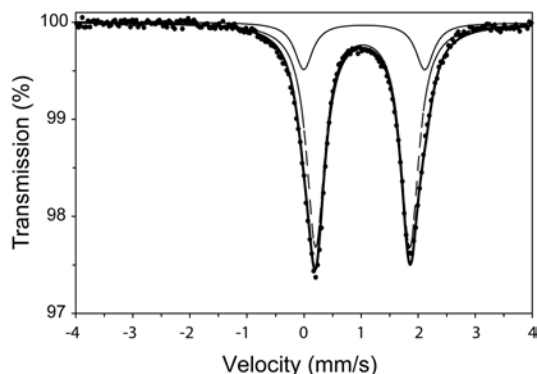
FIG. 15.   Fitted Mössbauer spectrum for gadolinite (sample #970319 from Malmkärra).
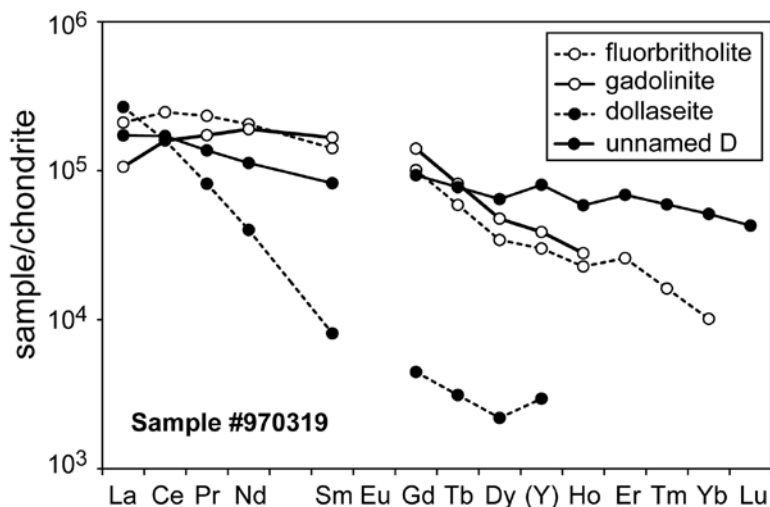
FIG. 16.   Selected chondrite-normalized patterns for coexisting REE minerals from Malmkärra.

crystals also seem to have formed in direct contact with carbonate. Dollaseite-(Ce) may occur as radiating, twinned crystals, and it is commonly associated with magnetite and norbergite. The mineral is also commonly observed as a microscopic phase in assemblages of fluorbritholite-(Ce), cerite-(Ce) and gadolinite-(Ce), as described in previous sections (Fig. 11C). In addition, a mineral closer to dissakisite-(Ce) in composition has been observed in a peculiar rock from S. Hackspik-gruvan (#540025), chiefly composed of fluorite and fluorian phlogopite. Aggregates up to 4 mm in size, consisting of small ($\leq$100 μm), irregular grains of dissakisite-(Ce) closely associated with magnetite and euhedral molybdenite crystals, occur in the mass of fluorite (Fig. 12C).

The atom proportions given for epidote-group minerals in this paper were calculated according to the procedure advocated for allanite by Ercit (2002): the sum of the octahedrally and tetrahedrally coordinated cations, Σ(Mg + Fe + Ti + Al + Si), was normalized to six atoms, and Fe^{2+} and Fe^{3+} were partitioned to balance the negative charges from O^{2-} and F^- (Table 8). The samples can be described as essentially dollaseite – dissakisite – allanite solid solutions (Fig. 17). They are generally low in Fe^{3+} (Fe^{3+} < Al, $i.e.$, the ferriallanite component is subordinate). Mössbauer data were collected for #270427 from Östanmossa (dollaseite close to the end-member composition) and #540027 from Malmkärra (dollaseite–dissakisite of approxi-mately intermediate composition). In both cases, four doublets were used to fit the spectra (Fig. 18, Table 9). On the basis of their CS values, two were attributed to Fe^{3+} and two to Fe^{2+}, both of them in octahedral coordination with oxygen. Also, for #540027, the ratio $Fe^{3+}/\Sigma Fe$ determined from the absorption area is 0.51, which is within the calculated range (0.41–0.60) for the point analyses of the sample (Table 8). For #270427, the average EMP-based value (0.25) is in good agreement with the ratio obtained by Mössbauer spectroscopy (0.22). Site assignments can be made in accordance with previous results from structure refinements of minerals with similar compositions (Peacor & Dunn 1988, Rouse & Peacor 1993) and by comparison of the hyperfine parameters with data for other epidote-group minerals (Liebscher 2004). For both samples, it is clear that Fe^{2+} prefers $M3$ over $M1$; $M3$ also is the host for most of the Fe^{3+} in #540027. For the purer dollaseite, in #270427, $M3$ is nearly fully occupied with divalent ions, but $M2$ is only partially filled with Al, and accordingly some Fe^{3+} will enter this site. A minor fraction of the Fe is probably present as Fe^{3+} in the $M1$ site of both samples, although not resolved in the spectra.

For the whole series under consideration, there is a strong positive correlation between (Mg + Fe^{2+}) and F (linear, $r = 0.95$); the dollaseite-type substitution thus seems to be the dominant exchange-mechanism in these samples. Sample #Öm0201 from Östanmossa is distinct in having Fe^{2+} > Mg, thus representing a case of allanite–dollaseite solid solution.
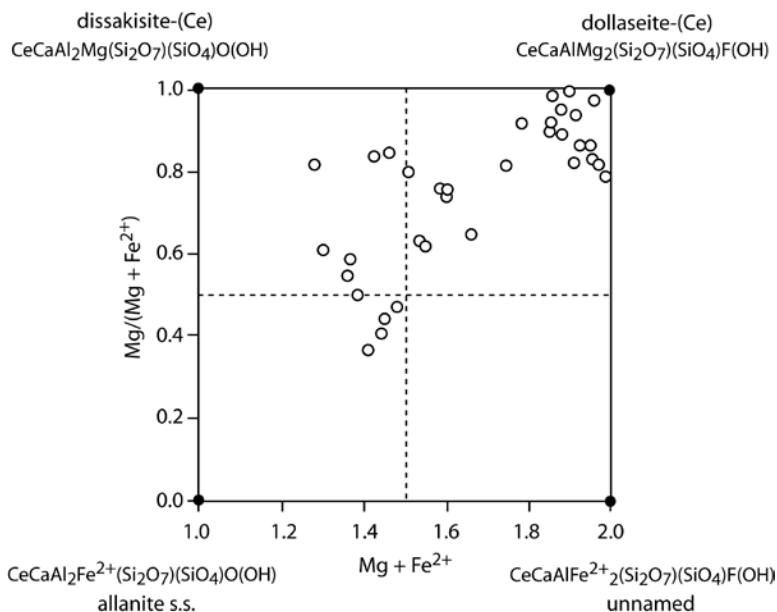
FIG. 17.   Compositional diagram for dollaseite – dissakisite – allanite from subtype-2 deposits (Norberg District). Note that Al predominates over Fe^{3+} in all samples.

The (Ca + REE) sums indicate that the structural sites hosting these cations, $A1 + A2$, are fully occupied (or nearly so). For most samples here, the REE are present in excess of the ideal value of one atom per formula unit (average Ca contents of individual samples correspond to a range of 0.87–1.03 Ca *apfu*), suggesting that some fraction of the REE enters the smaller $A1$ site. This is in agreement with the structure refinement carried out by Peacor & Dunn (1988), indicating an amount of

heavy atoms (equivalent of 0.06 Ce *apfu* from atomic scattering factors) at $A1$ in type dollaseite-(Ce). Cerium and La accounts for 66–89 at.% of the REE present; the Ce/(Ce+La) value varies from 0.48 to 0.67, implying that a few points (dollaseite in #381132) actually are La-dominant. Concentrations of Y are low throughout the sample series (range 0.1–1.6, mean 0.5 wt.% Y_2O_3), but still higher than what we found for ferriallanite (*cf.* Table 10; Holtstam *et al.* 2003b), and the chondrite-

TABLE 8. CHEMICAL COMPOSITION OF DOLLASEITE – DISSAKISITE – ALLANITE
FROM THE NORBERG DISTRICT

Sample #	270427 Ö							381132 H			
point	A p6	A p7	A p8	B p1	B p2	B p3	B p4	b p2	b p4	b p5	b p6
La_2O_3 wt%	7.14	6.70	6.64	7.41	7.55	6.84	6.87	13.50	13.25	13.70	13.02
Ce_2O_3	13.02	13.83	13.65	13.67	13.90	13.33	13.43	13.54	14.00	13.71	13.75
Pr_2O_3	1.48	1.57	1.58	1.40	1.44	1.51	1.57	0.85	0.87	0.86	0.94
Nd_2O_3	6.16	6.79	6.43	5.68	5.31	6.32	6.23	2.25	2.32	2.27	2.36
Sm_2O_3	1.01	1.01	0.96	0.93	0.77	1.08	0.89	0.18	0.09	0.14	0.11
Gd_2O_3	0.63	0.47	0.52	0.52	0.49	0.52	0.51	0.12	0.06	0.10	0.07
Dy_2O_3	0.12	0.06	0.09	0.08	0.11	0.13	0.08	0.01	0.03	0.07	0.08
Ho_2O_3	0.02	0.01	0.00	0.02	0.00	0.04	0.06	0.00	0.00	0.01	0.00
Er_2O_3	0.00	0.00	0.00	0.00	0.00	0.00	0.00	0.04	0.03	0.10	0.04
Yb_2O_3	0.07	0.00	0.01	0.00	0.03	0.03	0.04	0.00	0.01	0.03	0.00
Lu_2O_3	0.00	0.00	0.00	0.00	0.00	0.02	0.00	0.02	0.00	0.00	0.01
Y_2O_3	1.11	0.60	0.79	0.90	0.86	0.64	0.94	0.93	0.39	0.39	0.55	0.41
CaO	8.73	8.72	8.82	8.85	9.04	8.82	8.97	8.47	8.52	8.13	8.58
Fe_2O_3 *	1.26	0.12	0.85	1.09	1.00	0.49	1.08	2.77	1.71	2.09	1.65
FeO *	2.56	2.58	1.88	3.44	3.70	3.07	2.16	3.44	4.42	5.04	4.27
MgO	12.21	12.99	12.96	11.47	11.17	12.30	12.59	11.48	11.31	10.96	11.42
Al_2O_3	8.55	8.12	8.39	8.86	9.19	8.51	8.65	7.84	7.77	7.21	7.78
SiO_2	29.95	29.70	29.61	30.30	29.77	29.97	29.73	28.76	29.72	29.50	29.78
P_2O_5	0.01	0.00	0.00	0.00	0.00	0.00	0.00	0.01	0.00	0.00	0.01
Ti	0.01	0.00	0.00	0.00	0.00	0.01	0.00	0.10	0.12	0.13	0.09
Mn	0.18	0.19	0.20	0.18	0.13	0.18	0.21	0.00	0.00	0.00	0.00
F	2.99	3.27	3.20	2.86	2.78	3.12	3.12	2.85	2.87	2.80	2.96
Cl	0.00	0.00	0.00	0.01	0.00	0.00	0.00	0.00	0.02	0.01	0.01
O=F	-1.26	-1.38	-1.35	-1.20	-1.17	-1.31	-1.31	-1.20	-1.21	-1.18	-1.25
O=Cl	0.00	0.00	0.00	0.00	0.00	0.00	0.00	0.00	0.00	0.00	0.00
Total	95.95	95.35	95.22	96.40	95.82	95.91	95.69	95.42	96.28	96.22	96.08
La *afpu*	0.26	0.24	0.24	0.27	0.27	0.25	0.25	0.50	0.48	0.50	0.47
Ce	0.47	0.50	0.49	0.49	0.50	0.48	0.48	0.49	0.51	0.50	0.50
Pr	0.05	0.06	0.06	0.05	0.05	0.05	0.06	0.03	0.03	0.03	0.03
Nd	0.21	0.24	0.23	0.20	0.19	0.22	0.22	0.08	0.08	0.08	0.08
Sm	0.03	0.03	0.03	0.03	0.03	0.04	0.03	0.01	0.00	0.00	0.00
Gd	0.02	0.02	0.02	0.02	0.02	0.02	0.02	0.00	0.00	0.00	0.00
Dy	0.00	0.00	0.00	0.00	0.00	0.00	0.00	0.00	0.00	0.00	0.00
Ho	0.00	0.00	0.00	0.00	0.00	0.00	0.00	0.00	0.00	0.00	0.00
Er	0.00	0.00	0.00	0.00	0.00	0.00	0.00	0.00	0.00	0.00	0.00
Yb	0.00	0.00	0.00	0.00	0.00	0.00	0.00	0.00	0.00	0.00	0.00
Lu	0.00	0.00	0.00	0.00	0.00	0.00	0.00	0.00	0.00	0.00	0.00
Y	0.06	0.03	0.04	0.04	0.03	0.05	0.04	0.02	0.02	0.03	0.02
Ca	0.91	0.92	0.93	0.92	0.95	0.92	0.94	0.91	0.90	0.87	0.91
Fe^{3+} *	0.09	0.01	0.06	0.08	0.07	0.04	0.08	0.21	0.13	0.16	0.12
Fe^{2+} *	0.21	0.21	0.15	0.28	0.30	0.25	0.18	0.29	0.36	0.42	0.35
Mg	1.78	1.90	1.89	1.66	1.63	1.79	1.83	1.71	1.66	1.63	1.68
Al	0.98	0.94	0.97	1.02	1.06	0.98	0.99	0.92	0.90	0.85	0.94
Si	2.92	2.92	2.90	2.95	2.92	2.93	2.90	2.87	2.93	2.94	2.94
P	0.00	0.00	0.00	0.00	0.00	0.00	0.00	0.00	0.00	0.00	0.00
Ti	0.00	0.00	0.00	0.00	0.00	0.00	0.00	0.01	0.01	0.01	0.01
Mn	0.02	0.02	0.02	0.01	0.01	0.02	0.02	0.00	0.00	0.00	0.00
F	0.92	1.02	0.99	0.88	0.86	0.96	0.96	0.90	0.90	0.88	0.92
Cl	0.00	0.00	0.00	0.00	0.00	0.00	0.00	0.00	0.00	0.00	0.00
Σ cations	8.02	8.04	8.03	8.02	8.04	8.03	8.03	8.04	8.03	8.03	8.02

TABLE 8 (cont'd). CHEMICAL COMPOSITION OF DOLLASEITE – DISSAKISITE – ALLANITE
FROM THE NORBERG DISTRICT

Sample #	540025 H			540027 M				970319 M		Öm a1 Ö			
point	1:1	1:2	1:3	p2	p5	v3	v4	v3	v4	2:1	2:2	3:1	3:2
La_2O_3	8.57	8.18	8.27	8.63	8.58	8.16	7.90	9.60	9.89	6.09	6.15	6.45	6.08
Ce_2O_3	13.14	12.81	13.17	14.58	14.63	14.51	14.37	15.26	14.94	12.66	12.68	12.46	12.76
Pr_2O_3	1.40	1.17	1.03	1.27	1.34	1.35	1.28	1.12	1.22	1.45	1.44	1.41	1.59
Nd_2O_3	4.81	5.00	4.94	3.86	4.13	4.24	4.70	3.01	2.60	6.07	6.03	5.97	6.39
Sm_2O_3	0.47	0.56	0.55	0.38	0.45	0.41	0.61	0.25	0.11	0.83	0.95	0.98	0.98
Gd_2O_3	0.97	0.97	0.70	0.18	0.25	0.10	0.28	0.21	0.06	0.30	0.40	0.38	0.24
Dy_2O_3	n.d.	n.d.	n.d.	0.04	0.01	0.05	0.06	0.07	0.09	n.d.	n.d.	n.d.	n.d.
Ho_2O_3	n.d.	n.d.	n.d.	0.00	0.01	0.08	0.05	0.01	0.00	n.d.	n.d.	n.d.	n.d.
Er_2O_3	0.00	0.00	0.00	0.11	0.02	0.14	0.07	0.07	0.12	0.06	0.00	0.00	0.00
Yb_2O_3	n.d.	n.d.	n.d.	0.04	0.00	0.01	0.01	0.04	0.06	n.d.	n.d.	n.d.	n.d.
Lu_2O_3	n.d.	n.d.	n.d.	0.01	0.00	0.00	0.00	0.01	0.02	n.d.	n.d.	n.d.	n.d.
Y_2O_3	0.52	0.35	0.36	0.32	0.40	0.39	0.58	1.04	0.53	0.31	0.31	0.33	0.33
CaO	9.12	9.35	9.27	9.28	9.11	9.05	8.72	7.85	8.62	9.47	9.49	9.38	9.29
Fe_2O_3	1.33	1.60	1.84	3.89	4.92	3.45	4.93	7.61	7.11	2.66	3.04	3.84	3.23
FeO	7.24	7.25	7.05	4.86	3.27	4.49	2.97	3.50	7.67	9.26	9.58	10.41	9.98
MgO	7.35	6.57	6.62	7.12	8.26	8.18	8.40	8.19	5.39	4.52	4.23	3.31	3.83
Al_2O_3	10.38	11.25	11.11	11.04	10.35	10.03	10.24	8.01	8.43	10.75	11.00	10.66	10.38
SiO_2	31.20	31.09	31.27	29.87	30.87	30.38	30.04	30.38	30.07	29.61	29.70	28.94	29.67
P_2O_5	0.02	0.10	0.05	0.00	0.02	0.00	0.02	0.00	0.00	0.00	0.00	0.04	0.06
Ti	n.d.	n.d.		0.17	0.19	0.20	0.18	0.08	0.13	n.d.	n.d.	n.d.	n.d.
Mn	n.d.	n.d.		0.03	0.00	0.00	0.02	0.43	0.20	n.d.	n.d.	n.d.	n.d.
F	1.59	1.41	1.42	1.02	1.24	1.48	1.37	1.70	1.04	0.84	0.88	0.50	0.46
Cl	n.d.	n.d.	n.d.	0.01	0.01	0.69	0.10	0.01	0.01	n.d.	n.d.	n.d.	n.d.
O=F	-0.67	-0.59	-0.60	-0.43	-0.52	-0.62	-0.58	-0.72	-0.44	-0.35	-0.37	-0.21	-0.19
O=Cl	0.00	0.00	0.00	0.00	0.00	-0.16	-0.02	0.00	0.00	0.00	0.00	0.00	0.00
Total	97.47	97.06	97.05	96.27	97.54	96.59	96.23	97.73	97.86	94.53	95.51	94.86	95.08
La	0.31	0.29	0.30	0.32	0.31	0.30	0.29	0.35	0.36	0.23	0.23	0.25	0.23
Ce	0.47	0.46	0.47	0.53	0.52	0.52	0.52	0.55	0.55	0.47	0.47	0.47	0.48
Pr	0.05	0.04	0.04	0.05	0.05	0.05	0.05	0.04	0.04	0.05	0.05	0.05	0.06
Nd	0.17	0.17	0.17	0.14	0.14	0.15	0.17	0.11	0.09	0.22	0.22	0.22	0.23
Sm	0.02	0.02	0.02	0.01	0.02	0.01	0.02	0.01	0.00	0.03	0.03	0.04	0.03
Gd	0.03	0.03	0.02	0.01	0.01	0.00	0.01	0.01	0.00	0.01	0.01	0.01	0.01
Dy				0.00	0.00	0.00	0.00	0.00	0.00				
Ho	0.00	0.00	0.00	0.00	0.00	0.00	0.00	0.00	0.00	0.00	0.00	0.00	0.00
Er				0.00	0.00	0.00	0.00	0.00	0.00				
Yb				0.00	0.00	0.00	0.00	0.00	0.00				
Lu	0.00	0.00	0.00	0.00	0.00	0.00	0.00	0.00	0.00	0.00	0.00	0.00	0.00
Y	0.03	0.02	0.02	0.02	0.02	0.02	0.03	0.05	0.03	0.02	0.02	0.02	0.02
Ca	0.95	0.98	0.97	0.98	0.95	0.96	0.92	0.83	0.92	1.04	1.03	1.04	1.02
Fe^{3+} *	0.10	0.12	0.14	0.29	0.36	0.26	0.37	0.56	0.53	0.20	0.23	0.30	0.25
Fe^{2+} *	0.59	0.59	0.57	0.40	0.26	0.37	0.24	0.29	0.64	0.79	0.81	0.90	0.86
Mg	1.07	0.96	0.96	1.05	1.19	1.20	1.23	1.20	0.80	0.69	0.64	0.51	0.59
Al	1.19	1.29	1.28	1.29	1.18	1.16	1.19	0.93	0.99	1.29	1.31	1.30	1.26
Si	3.05	3.03	3.05	2.96	2.99	2.99	2.96	2.98	3.00	3.02	3.01	2.99	3.05
P	0.00	0.01	0.00	0.00	0.00	0.00	0.00	0.00	0.00	0.00	0.00	0.00	0.00
Ti				0.01	0.01	0.01	0.01	0.01	0.01				
Mn				0.00	0.00	0.00	0.00	0.04	0.02				
F	0.49	0.44	0.44	0.32	0.38	0.46	0.43	0.53	0.33	0.27	0.28	0.16	0.15
Cl	0.00	0.00	0.00	0.00	0.00	0.12	0.02	0.00	0.00	0.00	0.00	0.00	0.00
Σ cat.	8.02	8.01	8.00	8.05	8.00	8.02	8.00	7.94	8.01	8.07	8.06	8.10	8.09

n.d.: not determined; * Calculated values. H: S. Hackspikgruvan, M: Malmkärra, Ö: Östanmossa. The compositional data are first expressed in wt%, then in *apfu*, calculated on the basis of 6 (Fe + Mg + Mn + Ti + Al + Si) atoms.

normalized curves are steep in comparison with those of the coexisting REE minerals.

The refined unit-cell parameters for sample #540027 [*a* 8.916(4), *b* 5.732(4), *c* 10.141(5) Å, β 114.52(6)°, *V* 471.5 Å³] are very similar to those of #270427 [*a* 8.927(3), *b* 5.712(2), *c* 10.154(3) Å, β 114.48(4)°, *V* 471.2 Å³], but notably different from those of type dissakisite-(Ce) [*a* 8.905(1), *b* 5.684(1), *c* 10.113(1) Å, β 114.62(2)°, *V* 465.3 Å³ (Rouse & Peacor 1993)]. In going from dollaseite to dissakisite, we would expect a decrease in the unit-cell size by replacing Mg²⁺ with Al³⁺ (considering the sizes of these ionic species), but

the higher Fe^{2+} and Fe^{3+} contents of #540027 seem to compensate for this.

Ferriallanite-(Ce) – allanite-(Ce)

Ferriallanite-(Ce), ideally $CeCaFe^{2+}AlFe^{3+}[SiO_4]$ $[Si_2O_7]O(OH)$, is the most common REE mineral in the Bastnäs deposit next to cerite-(Ce); its occurrence has recently been described in detail by Holtstam *et al*. (2003b), with chemical data. Ferriallanite-(Ce) from Rödbergsgruvan [#880072, see description under cerite-(Ce) above] is chemically similar, except for

Y_2O_3, which is slightly elevated (0.4 wt.%) in this sample (Table 10). For the whole population of samples, the following characteristics hold: (a) a clear negative correlation ($r = –0.88$) between Fe^{2+} and Mg is related to a simple cation-exchange that is the dominant mechanism of substitution operating in ferriallanite-(Ce) (Fig. 19); (b) a less pronounced Fe^{3+}–Al substitution exists, which relates it to the hypothetical end-member $CeCaFe^{2+}Fe^{3+}_2[SiO_4][Si_2O_7]O(OH)$ (Fig. 19); (c) "oversubstitution" of REE occurs, *i.e.,* all samples have REE > 1 and Ca < 1 *apfu*; (d) the common "allanite-type" substitution, $Ca^{2+} + (Al + Fe)^{3+} \leftrightarrow REE^{3+} + (Fe$
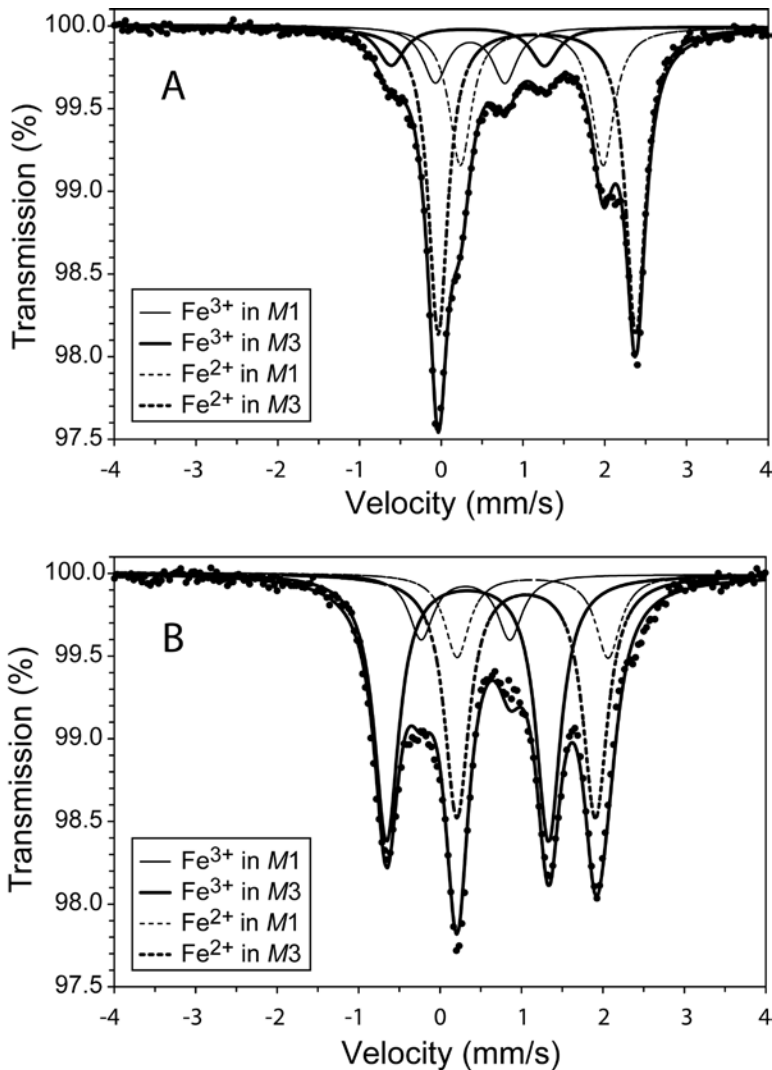
FIG. 18.   Fitted Mössbauer spectra for dollaseite–dissakisite. (A) Sample #270427 from Östanmoϭa. (B) Sample 540027 from Malmkärra.

TABLE 9. MÖSSBAUER PARAMETERS FOR DOLLASEITE AND DISSAKISITE

	CS (mm/s)	QS (mm/s)	Γ (mm/s)	Abs. area (%)
#270427				
^{M3} Fe^{3+}	0.32	1.88	0.30	10(1)
^{M1M2} Fe^{3+}	0.35	0.86	0.30	12(1)
^{M3} Fe^{2+}	1.17	2.41	0.30	52(3)
^{M1} Fe^{2+}	1.11	1.74	0.30	26(2)
#540027				
^{M3} Fe^{3+}	0.34	1.99	0.36	41(4)
^{M1} Fe^{3+}	0.31	1.09	0.36	10(1)
^{M3} Fe^{2+}	1.06	1.70	0.36	37(4)
^{M1} Fe^{2+}	1.14	1.85	0.36	12(1)

CS: centroid shift, QS: quadrupole split, Γ: line width.

$+ Mg)^{2+}$ (*e.g.,* Ercit 2002, Gieré & Sorensen 2004) does not play an important role.

Allanite-(Ce), $CeCaFe^{2+}Al_2[SiO_4][Si_2O_7]O(OH)$, seems to be confined to mineral assemblages lacking cerite-(Ce) in the subtype-1 deposits. In #884305 from Rödbergsgruvan, radial aggregates (up to 8 mm across) of allanite-(Ce) crystals occur in a coarse-grained mass of actinolite with minor quartz and a significant impregnation of molybdenite. Sample #02+0051 from Bastnäs is a layered magnetite–actinolite skarn; allanite-(Ce) occurs as irregular grains (0.1–0.3 mm) arranged in stripes partly enclosed by, and semiparallel to, the magnetite-rich layers. Minute grains of zircon and monazite-(Ce) have been found as accessory minerals in this sample. In sample #680002 from Bastnäs, dissakisite-(Ce) occurs in coarse-grained tremolite skarn, partly altered to chlorite, in contact with subhedral grains of cobaltite.

In addition to their intrinsically lower Fe^{3+} contents, allanite-(Ce) differs from ferriallanite-(Ce) in that Ca is dominant over the REE at all points. For dissakisite-(Ce) in #680002, Ca and REE are present in nearly stoichiometric amounts. A relatively large variation in the A-type cations is observed within the allanite-(Ce) samples [Ca/(Ca + REE) in the range 0.53–0.65]. As seen on BSE images, the darkest and most Ca-rich portions of the crystals are commonly concentrated along the rim and microcracks. This kind of pattern generally indicates chemical modification as a result of interaction with late-stage fluids (*e.g.,* Sorensen 1991, Poitrasson 2002). The samples of allanite, like those of ferriallanite (*cf.* Holtstam *et al.* 2003b), are very poor in actinides; thus alteration related to metamictization probably has not occurred.

The intrasample content of the octahedrally coordinated divalent cations is relatively constant, but considering all three allanite–dissakisite specimens analyzed, a large variation [$0.39 < Fe^{2+}/(Fe^{2+} + Mg) < 0.93$] is expressed, corresponding to a significant part of the allanite–dissakisite solid-solution series. Note

that allanite *sensu stricto* and dissakisite are probably more common in the Bastnäs-type deposits than indicated by the present data (as scattered microscopic grains within the amphibole skarns). For this study, we essentially selected the most REE-rich assemblages with, *e.g.,* cerite-(Ce), fluorbritholite-(Ce), and the accompanying epidote-type minerals. In terms of their chemical composition, these assemblages may not be representative for the deposits as a whole.

Västmanlandite-(Ce) and its Fe analogue

Västmanlandite-(Ce), ideally $Ce_3CaAl_2Mg_2[Si_2O_7]$ $[SiO_4]_3F(OH)_2$, is a recently approved mineral species (Holtstam *et al.* 2005). The crystal structure is based on a regular 1:1 stacking along **c** of a dollaseite-(Ce)-type module (*D*) $[CeCaMg_2Al(Si_2O_7)(SiO_4)$ $F(OH)]$ and a törnebohmite-(Ce)-type module (*T*) $[Ce_2Al(SiO_4)_2(OH)]$. Västmanlandite is found in subtype-2 deposits, and members of an isomorphic series containing higher concentrations of Fe occur in subtype 1. These minerals have been observed in a majority of the sections investigated, and can now be considered a characteristic component of the Bastnäs-type REE mineralization.

In the type specimen (#01+0081), västmanlandite-(Ce) occurs as mostly anhedral grains 0.2–3 mm in size, in close association with fluorbritholite-(Ce), dollaseite-(Ce), magnetite, tremolite and dolomite. The textural relations indicate that västmanlandite-(Ce)
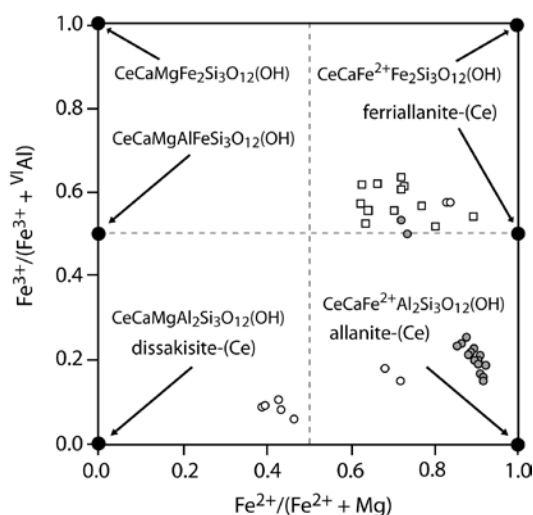
FIG. 19. Compositional diagram for allanite-(Ce) and related minerals from subtype-1 deposits. Filled symbols: Röd-bergsgruvan, open symbols: Bastnäs. Analytical results for ferrillanite-(Ce) from Bastnäs, presented in Holtstam *et al.* (2003b), are included.

largely formed at the expense of fluorbritholite-(Ce) (Holtstam *et al.* 2005). Although västmanlandite-(Ce) is subordinate in relation to dollaseite-(Ce) in most of the other samples, the close association with this mineral and fluorbritholite (exceptionally, cerite) is the rule.

In subtype-1 deposits, the grains of västmanlandite-(Ce) series occur scattered (≤0.4 mm), in direct contact with ferriallanite-(Ce) and closely associated with cerite-(Ce). In sample #52:414, this mineral has developed as a major phase largely replacing cerite-(Ce), and ferriallanite-(Ce) occurs in turn as a subordinate product of alteration along the rim and fractures in it. In the cerite-(Ce) specimen from Rödbergsgruvan (#880072), the västmanlandite-type mineral appears as irregular domains, normally <100 μm across, surrounded by ferriallanite-(Ce) forming larger aggregates (Fig. 12D). The grains have a partly corroded appearance, and to some extent seem to be replaced by the ferriallanite-(Ce).

The chemical formulae (Table 11) are normalized to 13 metal atoms, and Fe^{3+} has been calculated so as to bring cation charges to equal the negative charges

TABLE 10. CHEMICAL COMPOSITION OF ALLANITE AND RELATED MINERALS

Sample #	680002 B				880072 R		884305 R						
point	p4	p5	p6	p7	p3	p7	A:2	A:3	A tr	A tr	A tr	A tr	A tr
La_2O_3	7.89	7.90	7.83	7.95	10.77	10.94	5.36	4.62	6.01	5.35	5.11	6.38	6.35
Ce_2O_3	13.19	14.16	12.19	12.86	14.27	14.40	9.87	8.11	10.37	9.84	9.02	11.07	10.86
Pr_2O_3	1.37	1.39	1.19	1.24	0.89	0.88	1.47	0.98	1.08	1.18	1.19	1.24	1.31
Nd_2O_3	4.31	4.21	4.17	4.31	2.16	2.04	4.93	3.71	4.66	4.53	3.75	4.46	4.48
Sm_2O_3	0.36	0.31	0.49	0.48	0.15	0.13	1.00	0.74	1.06	0.88	0.65	0.85	0.95
Gd_2O_3	0.19	0.15	0.22	0.27	0.07	0.13	0.74	0.68	0.74	0.81	0.57	0.70	0.74
Dy_2O_3	0.00	0.00	0.05	0.00	0.03	0.01	0.00	0.00	0.00	0.00	0.00	0.00	0.00
Ho_2O_3	0.00	0.00	0.00	0.00	0.08	0.02	n.d.	n.d.	n.d.	n.d.	n.d.	n.d.	n.d.
Er_2O_3	0.00	0.03	0.02	0.01	0.00	0.05	0.00	0.00	0.05	0.01	0.00	0.00	0.00
Yb_2O_3	0.02	0.05	0.00	0.00	0.00	0.03	n.d.	n.d.	n.d.	n.d.	n.d.	n.d.	n.d.
Lu_2O_3	0.03	0.04	0.02	0.01	0.04	0.01	n.d.	n.d.	n.d.	n.d.	n.d.	n.d.	n.d.
Y_2O_3	0.15	0.10	0.18	0.13	0.45	0.38	0.43	0.73	0.47	0.71	0.56	0.63	0.34
CaO	9.63	9.09	10.15	9.80	8.31	8.37	10.84	12.87	10.40	11.32	12.10	9.59	10.43
Fe_2O_3 *	3.19	3.98	3.20	3.07	11.87	11.27	4.71	6.07	4.55	7.49	6.59	5.52	
FeO *	5.16	4.41	4.72	5.43	10.04	10.25	9.49	7.74	10.16	9.39	7.14	9.11	10.05
MgO	4.42	5.11	3.88	4.24	2.11	2.02	0.51	0.44	0.50	0.46	0.66	0.78	0.57
Al_2O_3	14.67	13.77	16.01	14.88	7.07	7.46	15.45	16.89	14.79	16.24	15.97	13.59	14.41
SiO_2	31.10	30.69	31.46	30.65	27.93	28.48	30.85	31.59	30.65	31.21	31.88	30.40	30.55
P_2O_5	0.02	0.00	0.00	0.00	0.02	0.01	0.05	0.01	0.06	0.06	0.00	0.12	0.01
Ti	0.47	0.53	0.30	0.39	0.02	0.03	n.d.	n.d.	n.d.	n.d.	n.d.	n.d.	n.d.
Mn	0.00	0.00	0.00	0.00	0.00	0.00	n.d.	n.d.	n.d.	n.d.	n.d.	n.d.	n.d.
F	0.32	0.49	0.16	0.30	0.46	0.43	n.d.	n.d.	n.d.	n.d.	n.d.	n.d.	n.d.
Cl	0.02	0.01	0.02	0.02	0.00	0.01	n.d.	n.d.	n.d.	n.d.	n.d.	n.d.	n.d.
O=F	-0.13	-0.21	-0.07	-0.13	-0.19	-0.18							
Total	96.37	96.21	96.20	95.91	96.54	97.17	95.70	95.21	95.22	96.54	96.09	95.51	96.59
La	0.28	0.28	0.28	0.29	0.42	0.42	0.19	0.16	0.22	0.19	0.18	0.23	0.23
Ce	0.47	0.50	0.43	0.46	0.55	0.55	0.35	0.28	0.38	0.35	0.31	0.40	0.39
Pr	0.05	0.05	0.04	0.04	0.03	0.03	0.05	0.03	0.04	0.04	0.04	0.05	0.05
Nd	0.15	0.15	0.14	0.15	0.08	0.08	0.17	0.13	0.16	0.16	0.13	0.16	0.16
Sm	0.01	0.01	0.02	0.02	0.01	0.00	0.03	0.02	0.04	0.03	0.02	0.03	0.03
Gd	0.01	0.00	0.01	0.01	0.00	0.00	0.02	0.02	0.02	0.03	0.02	0.02	0.02
Dy	0.00	0.00	0.00	0.00	0.00	0.00	0.00	0.00	0.00	0.00	0.00	0.00	0.00
Ho	0.00	0.00	0.00	0.00	0.00	0.00							
Er	0.00	0.00	0.00	0.00	0.00	0.00	0.00	0.00	0.00	0.00	0.00	0.00	0.00
Yb	0.00	0.00	0.00	0.00	0.00	0.00							
Lu	0.00	0.00	0.00	0.00	0.00	0.00							
Y	0.01	0.01	0.01	0.01	0.03	0.02	0.02	0.04	0.03	0.04	0.03	0.03	0.02
Ca	1.00	0.95	1.04	1.02	0.94	0.94	1.14	1.31	1.10	1.17	1.23	1.02	1.10
Fe^{3+} *	0.23	0.29	0.23	0.23	0.94	0.89	0.35	0.43	0.31	0.33	0.53	0.49	0.41
Fe^{2+} *	0.42	0.36	0.38	0.44	0.89	0.90	0.78	0.61	0.84	0.76	0.57	0.76	0.83
Mg	0.64	0.74	0.55	0.61	0.33	0.31	0.07	0.06	0.07	0.07	0.09	0.12	0.08
Al	1.67	1.58	1.81	1.71	0.88	0.92	1.78	1.89	1.73	1.84	1.78	1.60	1.67
Si	3.01	2.99	3.01	2.98	2.95	2.98	3.02	3.00	3.04	3.00	3.02	3.03	3.01
P	0.00	0.00	0.00	0.00	0.00	0.00	0.00	0.00	0.01	0.00	0.00	0.01	0.00
Ti	0.03	0.04	0.02	0.03	0.00	0.00							
Mn	0.00	0.00	0.00	0.00	0.00	0.00							
F	0.10	0.15	0.05	0.09	0.15	0.14							
Cl	0.00	0.00	0.00	0.00	0.00	0.00							
Σ cat.	7.97	7.96	7.96	7.99	8.07	8.06	7.99	8.00	7.99	7.99	7.96	7.95	8.00

TABLE 10 (cont'd). CHEMICAL COMPOSITION OF ALLANITE AND RELATED MINERALS

Sample #	884305 R								02+0051 B		03+0246 B	
point	A tr	A tr	A tr	A tr	A tr	A tr	A tr	A tr	p1	p2	F:1	F:2
La_2O_3 wt%	5.67	6.02	6.43	6.08	6.04	5.96	5.86	6.79	8.27	6.23	9.73	10.02
Ce_2O_3	10.43	10.86	10.59	10.15	10.23	10.65	10.51	11.33	11.16	9.03	13.57	13.48
Pr_2O_3	1.37	1.23	1.31	1.32	1.21	1.42	1.23	1.24	1.10	0.80	1.20	1.16
Nd_2O_3	4.69	4.81	4.61	4.29	4.49	5.05	4.98	4.55	3.07	2.94	2.88	2.80
Sm_2O_3	1.19	0.78	0.87	0.80	0.91	1.01	0.99	0.52	0.46	0.41	0.22	0.23
Gd_2O_3	1.02	0.81	0.54	0.65	0.64	-0.97	0.97	0.56	0.05	0.09	0.12	0.13
Dy_2O_3	0.00	0.00	0.00	0.00	0.00	0.00	0.00	0.00	0.00	0.00	0.00	0.00
Ho_2O_3	n.d.	n.d.	n.d.	n.d.	n.d.	n.d.	n.d.	n.d.	n.d.	n.d.	n.d.	n.d.
Er_2O_3	0.00	0.00	0.01	0.00	0.00	0.00	0.01	0.00	0.00	0.00	0.00	0.01
Yb_2O_3	n.d.	n.d.	n.d.	n.d.	n.d.	n.d.	n.d.	n.d.	n.d.	n.d.	n.d.	n.d.
Lu_2O_3	n.d.	n.d.	n.d.	n.d.	n.d.	n.d.	n.d.	n.d.	n.d.	n.d.	n.d.	n.d.
Y_2O_3	0.27	0.44	0.45	0.20	0.40	0.35	0.40	0.27	0.26	0.37	0.27	0.41
CaO	10.18	10.08	10.32	11.19	10.70	10.38	10.19	10.18	10.92	13.51	8.26	8.18
Fe_2O_3 *	6.16	6.50	5.13	6.13	6.17	7.92	6.28	5.77	4.69	6.78	12.49	12.26
FeO *	9.21	9.10	10.21	9.34	9.08	7.51	8.85	9.54	6.86	4.62	11.41	11.64
MgO	0.64	0.59	0.46	0.53	0.51	0.59	0.61	0.62	1.47	1.19	1.25	1.29
Al_2O_3	14.23	14.47	14.52	14.99	15.01	15.01	14.96	14.59	17.27	19.73	5.94	5.81
SiO_2	30.30	30.26	30.23	30.96	30.52	30.40	30.57	30.71	31.28	33.65	28.40	28.33
P_2O_5	0.01	0.03	0.16	0.13	0.06	0.04	0.02	0.03	0.04	0.00	0.05	0.00
Ti	n.d.	n.d.	n.d.	n.d.	n.d.	n.d.	n.d.	n.d.	n.d.	n.d.	n.d.	n.d.
Mn	n.d.	n.d.	n.d.	n.d.	n.d.	n.d.	n.d.	n.d.	n.d.	n.d.	n.d.	n.d.
F	n.d.	n.d.	n.d.	n.d.	n.d.	n.d.	n.d.	n.d.	n.d.	n.d.	n.d.	n.d.
Cl	n.d.	n.d.	n.d.	n.d.	n.d.	n.d.	n.d.	n.d.	n.d.	n.d.	n.d.	n.d.
Total	95.37	95.99	95.83	96.76	95.98	95.33	96.42	96.68	96.90	99.37	95.80	95.76
La *apfu*	0.21	0.22	0.23	0.22	0.22	0.22	0.21	0.25	0.29	0.20	0.38	0.40
Ce	0.38	0.39	0.38	0.36	0.37	0.38	0.38	0.41	0.39	0.29	0.53	0.53
Pr	0.05	0.04	0.05	0.05	0.04	0.05	0.04	0.04	0.04	0.03	0.05	0.05
Nd	0.17	0.17	0.16	0.15	0.16	0.18	0.17	0.16	0.10	0.09	0.11	0.11
Sm	0.04	0.03	0.03	0.03	0.03	0.03	0.03	0.02	0.02	0.01	0.01	0.01
Gd	0.03	0.03	0.02	0.02	0.02	-0.03	0.03	0.02	0.00	0.00	0.00	0.00
Dy	0.00	0.00	0.00	0.00	0.00	0.00	0.00	0.00	0.00	0.00	0.00	0.00
Er	0.00	0.00	0.00	0.00	0.00	0.00	0.00	0.00	0.00	0.00	0.00	0.00
Y	0.01	0.02	0.02	0.01	0.02	0.02	0.02	0.01	0.01	0.02	0.02	0.02
Ca	1.08	1.07	1.10	1.16	1.12	1.09	1.07	1.07	1.11	1.28	0.94	0.94
Fe^{3+} *	0.46	0.48	0.38	0.45	0.45	0.58	0.46	0.43	0.34	0.45	1.00	0.99
Fe^{2+} *	0.77	0.75	0.85	0.76	0.74	0.62	0.73	0.78	0.54	0.34	1.02	1.04
Mg	0.09	0.09	0.07	0.08	0.07	0.09	0.09	0.09	0.21	0.16	0.20	0.21
Al	1.67	1.69	1.70	1.71	1.73	1.73	1.73	1.69	1.93	2.06	0.75	0.73
Si	3.01	2.99	2.99	3.00	2.99	2.98	2.99	3.01	2.97	2.98	3.03	3.03
P	0.00	0.00	0.01	0.01	0.00	0.00	0.00	0.00	0.00	0.00	0.00	0.00
Σ cations	7.98	7.97	8.00	7.99	7.98	7.94	7.96	7.98	7.96	7.93	8.04	8.05

n.d.: not determined. B: Bastnäs, R: Rödbergsgruvan. The compositional data are first expressed in wt%, then in *apfu*, calculated on the basis of 6 (Fe + Mg + Mn + Ti + Al + Si) atoms.

provided by O^{2-} and F^-. Aluminum is allocated with Si to fill up the tetrahedral sites (*T*) to a sum of five cations, and then the Al-dominated *M2* site is summed to two using the Al in excess of that used for the *T* sites, plus an appropriate amount of Fe^{3+}. The remaining Fe^{3+} plus Fe^{2+} and Mg are assigned to *M1* + *M3*. This procedure is well supported by structural data (Holtstam *et al.* 2005, and unpubl. data). In the present suite, Mg and F are anticorrelated with Fe. For $^{[M1, M3]}Fe^{3+}$ *versus* F, there is a linear relationship ($r^2 = 0.95$) with a slope of −1.0 and intercept of 0.9. This is evidence of a dollaseite-type substitution, $Fe^{3+} + O^{2-} = Mg^{2+} + F^-$, operating extensively. The calculation of valences from stoichiometry and preliminary Mössbauer measurements indicate that

samples in the västmanlandite series also must contain a significant concentration of FeO, related to an extensive Fe^{2+}–Mg^{2+} substitution. To describe these compositional variations comprehensively, a diagram like the one in Figure 20 can be used, where the nominal occupancy of the Mg–Fe sites (*M1* + *M3*) has been depicted in terms of Mg/(Mg + Fe^{2+}) *versus* Fe^{3+}/(Fe^{3+} + Fe^{2+} + Mg). It now becomes clear that in the Fe-rich members, Fe^{3+} is accompanied by a roughly equal amount of Fe^{2+}, and the whole population can essentially be described as a partial solid-solution series between västmanlandite-(Ce) and an Fe analogue without F, a yet unapproved mineral species with the ideal formula $Ce_3CaAl_2Fe^{2+}Fe^{3+}[Si_2O_7][SiO_4]_3O(OH)_2$.

TABLE 11. CHEMICAL COMPOSITION OF VÄSTMANLANDITE-SERIES MINERALS

#	UU318/77 M p12	A37 B a p3	A37 B a p9	52:414 B b p3	52:414 B b p4	381132 H b p15	381132 H b p16	390477 B p9	490216 J p10	660298 M 1:1	660298 M 1:1	660298 M 1:2	880072 R p4	880072 R p6	880072 R p9	970319 M p11	970319 M v9	01+0081 M v10	01+0081 M n=3	01+0081 M B B:1	03+0029 M B B:2	03+0029 M A B:1
La_2O_3	12.75	13.80	17.56	17.51	17.73	18.46	19.02	14.04	13.56	14.38	14.00	11.54	16.93	17.39	15.09	14.61	14.58	12.86	13.65	16.06	15.92	16.79
Ce_2O_3	24.49	24.10	21.55	21.67	21.47	22.54	21.86	21.93	21.95	23.56	23.49	23.75	21.84	21.87	22.86	22.74	23.64	23.91	23.90	22.16	22.25	21.69
Pr_2O_3	2.06	1.81	1.22	1.51	1.52	1.44	1.42	1.93	1.89	2.00	2.05	2.32	1.58	1.51	1.80	1.78	1.81	2.15	2.07	1.70	1.96	1.80
Nd_2O_3	7.00	5.23	3.39	4.03	4.13	4.03	3.62	5.76	5.97	5.75	5.77	6.82	4.14	3.87	5.00	5.30	5.00	6.25	6.28	4.98	4.91	4.29
Sm_2O_3	0.70	0.28	0.18	0.25	0.30	0.21	0.10	0.44	0.47	0.46	0.41	0.42	0.24	0.28	0.47	0.53	0.43	0.66	0.42	0.22	0.46	0.37
Gd_2O_3	0.04	0.05	0.05	0.06	0.07	0.01	0.02	0.16	0.17	0.02	0.00	0.00	0.23	0.10	0.33	0.30	0.23	0.23	0.15	0.47	0.39	0.37
Dy_2O_3	0.00	0.14	0.00	0.04	0.00	0.00	0.10	0.01	0.00	0.00	0.00	0.00	0.08	0.02	0.17	0.06	0.19	0.07	0.01	0.00	0.00	0.00
Ho_2O_3	n.d.	0.00	0.00	0.12	0.00	0.01	0.00	0.00	0.00	0.02	n.d.	n.d.	n.d.	0.04	0.00	0.00	0.00	0.15	0.02	n.d.	n.d.	n.d.
Er_2O_3	0.00	0.00	0.02	0.00	0.00	0.04	0.00	0.00	0.12	0.00	0.00	0.00	0.02	0.05	0.00	0.08	0.21	0.07	0.00	0.00	0.00	0.00
Yb_2O_3	n.d.	0.00	0.00	0.02	0.00	0.02	0.01	0.01	0.08	n.d.	n.d.	n.d.	0.00	0.00	0.06	0.03	0.05	0.02	0.03	n.d.	n.d.	n.d.
Lu_2O_3	n.d.	0.00	0.03	0.03	0.00	0.02	0.00	0.00	0.02	n.d.	n.d.	n.d.	0.02	0.01	0.01	0.00	0.02	0.00	0.00	n.d.	n.d.	n.d.
$Y2O3$	0.26	0.06	0.01	0.06	0.06	0.12	0.12	0.09	0.11	0.12	0.19	0.20	0.25	0.26	0.83	0.73	0.99	0.56	0.18	0.11	0.20	0.14
CaO	4.03	4.57	4.74	4.53	4.53	4.72	4.67	4.57	4.63	4.72	4.76	4.73	4.44	4.34	4.22	4.19	4.11	4.29	4.65	4.79	4.87	4.74
Fe_2O_3 *	1.81	7.02	8.34	7.38	6.63	1.73	2.44	6.58	6.71	0.00	1.38	3.56	5.81	6.20	1.64	0.59	1.71	3.02	3.04	3.35	2.92	1.82
FeO *	1.18	4.55	4.36	3.34	4.08	1.14	0.62	3.98	4.01	2.36	3.31	4.95	3.59	3.45	2.29	2.64	1.88	1.91	0.82	3.04	2.17	3.07
MgO	6.14	1.86	1.06	2.08	1.97	6.36	6.37	2.21	2.07	5.96	4.75	2.51	3.08	3.14	5.55	6.13	6.13	5.56	5.51	3.72	4.52	4.32
Al_2O_3	8.35	7.47	8.07	8.26	8.28	8.84	8.80	8.16	8.14	9.35	8.69	8.75	8.01	7.81	8.49	8.44	8.37	8.22	8.58	8.94	8.86	8.73
SiO_2	27.41	26.12	25.48	25.67	26.25	26.77	26.19	26.42	26.24	28.00	27.53	27.12	25.91	25.69	26.70	27.23	26.90	26.65	26.61	27.36	27.67	27.25
P_2O_5	0.00	0.08	0.01	0.06	0.09	0.04	0.00	0.18	0.11	0.08	0.16	0.13	0.01	0.03	0.07	0.14	0.19	0.23	0.05	0.06	0.04	0.04
Ti	n.d.	0.02	0.05	0.07	0.03	0.02	0.04	0.03	0.04	n.d.	n.d.	n.d.	0.01	0.03	0.03	0.06	0.03	0.00	0.04	n.d.	n.d.	n.d.
F	1.04	0.30	0.12	0.21	0.20	1.59	1.59	0.21	0.24	1.39	1.10	0.53	0.72	0.71	1.27	1.41	1.33	1.16	1.06	0.64	0.77	0.90
Cl	n.d.	0.02	0.02	0.02	0.02	0.03	0.01	0.02	0.02	n.d.	n.d.	n.d.	0.01	0.01	0.03	0.09	0.03	0.02	0.00	n.d.	n.d.	n.d.
O=F	-0.44	-0.13	-0.05	-0.09	-0.08	-0.67	-0.67	-0.09	-0.10	-0.58	-0.46	-0.22	-0.30	-0.30	-0.53	-0.59	-0.56	-0.49	-0.45	-0.27	-0.32	-0.38
O=Cl		0.00	0.00	0.00	0.00	-0.01	0.00	0.00	0.00				0.00	0.00	-0.01	-0.02	-0.01	0.00	-0.01			
Total	96.82	97.35	96.20	96.81	97.27	97.44	96.36	96.63	96.46	97.55	97.11	97.10	96.66	96.47	96.37	96.47	97.26	97.49	96.60	97.35	97.58	95.97
La *apfu*	0.87	0.97	1.24	1.23	1.23	1.24	1.30	0.98	0.95	0.96	0.95	0.79	1.18	1.22	1.03	0.99	0.99	0.87	0.93	1.09	1.08	1.16
Ce	1.66	1.68	1.51	1.51	1.48	1.51	1.48	1.51	1.52	1.56	1.58	1.62	1.51	1.52	1.56	1.53	1.59	1.61	1.62	1.50	1.49	1.48
Pr	0.14	0.13	0.09	0.10	0.10	0.10	0.10	0.13	0.13	0.13	0.14	0.16	0.11	0.10	0.12	0.12	0.12	0.14	0.14	0.11	0.13	0.12
Nd	0.46	0.36	0.23	0.27	0.28	0.26	0.24	0.39	0.40	0.37	0.38	0.45	0.28	0.26	0.33	0.35	0.33	0.41	0.42	0.33	0.32	0.29
Sm	0.04	0.02	0.01	0.02	0.02	0.01	0.01	0.03	0.03	0.03	0.03	0.03	0.02	0.02	0.03	0.03	0.03	0.04	0.03	0.01	0.03	0.02
Gd	0.00	0.00	0.00	0.00	0.00	0.00	0.00	0.01	0.01	0.00	0.00	0.00	0.01	0.01	0.02	0.02	0.01	0.01	0.01	0.03	0.02	0.02
Dy	0.00	0.01	0.00	0.00	0.00	0.00	0.01	0.00	0.00	0.00	0.00	0.00	0.00	0.00	0.01	0.00	0.01	0.00	0.00	0.00	0.00	0.00
Ho		0.00	0.00	0.01	0.00	0.00	0.00	0.00	0.00				0.00	0.00	0.00	0.00	0.00	0.01	0.00			
Er	0.00	0.00	0.00	0.00	0.00	0.00	0.00	0.00	0.01	0.00	0.00	0.00	0.00	0.00	0.00	0.00	0.01	0.00	0.00	0.00	0.00	0.00
Yb		0.00	0.00	0.00	0.00	0.00	0.00	0.00	0.00				0.00	0.00	0.00	0.00	0.00	0.00	0.00			
Lu		0.00	0.00	0.00	0.00	0.00	0.00	0.00	0.00				0.00	0.00	0.00	0.00	0.00	0.00	0.00			
Y	0.03	0.01	0.00	0.01	0.01	0.01	0.01	0.01	0.01	0.01	0.02	0.02	0.03	0.03	0.08	0.07	0.10	0.05	0.02	0.01	0.02	0.01
Ca	0.80	0.93	0.97	0.92	0.92	0.92	0.92	0.92	0.94	0.91	0.94	0.95	0.90	0.88	0.84	0.83	0.81	0.85	0.92	0.95	0.95	0.95
Fe^{2+} *	0.18	0.72	0.70	0.53	0.64	0.17	0.09	0.63	0.64	0.36	0.51	0.77	0.57	0.55	0.36	0.41	0.29	0.29	0.13	0.47	0.33	0.48
Fe^{3+} *	0.25	1.00	1.20	1.06	0.94	0.24	0.34	0.93	0.96	0.00	0.19	0.50	0.83	0.89	0.23	0.08	0.24	0.42	0.43	0.47	0.40	0.26
Mg	1.69	0.53	0.30	0.59	0.55	1.73	1.75	0.62	0.59	1.61	1.30	0.70	0.87	0.89	1.54	1.68	1.68	1.53	1.52	1.02	1.23	1.20
Al	1.82	1.67	1.83	1.85	1.84	1.90	1.92	1.81	1.82	1.99	1.88	1.92	1.79	1.75	1.86	1.83	1.81	1.79	1.88	1.95	1.91	1.92
Si	5.06	4.96	4.89	4.88	4.95	4.89	4.83	4.98	4.97	5.06	5.06	5.06	4.90	4.88	4.96	5.01	4.94	4.91	4.94	5.05	5.07	5.08
P	0.00	0.01	0.00	0.01	0.01	0.01	0.00	0.03	0.02	0.01	0.02	0.02	0.00	0.00	0.01	0.02	0.03	0.04	0.01	0.01	0.01	0.01
Ti		0.00	0.01	0.01	0.00	0.00	0.01	0.00	0.01				0.00	0.00	0.00	0.01	0.00	0.00	0.01			
F	0.61	0.18	0.07	0.13	0.12	0.92	0.93	0.13	0.14	0.79	0.64	0.31	0.43	0.43	0.75	0.82	0.77	0.68	0.62	0.37	0.44	0.53
Cl		0.01	0.01	0.01	0.01	0.01	0.00	0.00	0.01				0.00	0.00	0.01	0.03	0.01	0.01	0.00			

n.d.: not determined. B: Bastnäs, H: S. Hackspikgruvan, J: Johannagruvan, M: Malmkärra, R: Rödbergsgruvan. The full dataset is presented in Holtstam *et al.* (2005). *: calculated. The compositional data are first expressed in wt%, then in *apfu*, calculated on the basis of 13 cations.

All samples of this mineral series are Ce-dominant, with Ce/(Ce + La) values in the range 0.53–0.67 for västmanlandite-(Ce) and 0.55–0.63 for the Fe-rich members. There is a consistent deficit in their Ca contents relative the ideal formula (0.90 Ca *apfu* present, on average); as shown for the type specimen of västmanlandite-(Ce), a minor fraction of the REE atoms are accommodated at the Ca site in the *D* module, whereas there is no evidence of Ca replacing REE at other sites (Holtstam *et al.* 2005). Although it shows a considerably higher overall REE concentration than the associated dollaseite and ferriallanite, the chondrite-normalized pattern of västmanlandite-(Ce) and its iron-rich counterpart mimic those of the epidote-group minerals (*e.g.*, Fig. 7).

DISCUSSION AND PRELIMINARY CONCLUSIONS

Although the Bastnäs-type deposits have been recognized for a long time, they still seem unique, without good analogues from other parts of the world. Deposits with similar assemblages of minerals, however, do occur. Cerite-(Ce) is known from about ten occurrences outside Sweden (Förster 2000, Chakhmouradian &

Zaitsev 2002, Konev *et al.* 2005). Fluorbritholite seems to be equally rare, although this might partly be related to the fact that the fluorine-component of "britholite" is not always recognized in routine analytical work. Other species characteristic of the Bastnäs-type deposits are even rarer than cerite and fluorbritholite. Dollaseite-(Ce) has, so far, remained unique to the REE deposits in the Norberg District. Västmanlandite-(Ce) has recently been found as a rock-forming mineral in the "Tornebohmitovaya" carbonatite vein at the Biraia Fe–REE deposit, eastern Siberia, associated with törnebohmite-(Ce), bastnäsite-(Ce), ferriallanite-(Ce), and biraite-(Ce) in carbonate matrices (P.M. Kartashov, pers. commun., 2004). In the type locality for ferriallanite-(Ce), an alkaline granitic pegmatite at Ulyn Khuren, Altai Mountains, Mongolia, percleveite-(Ce) has been found associated with zircon and ferriallanite-(Ce); this assemblage has formed metasomatically by alteration of REE-rich eudialyte-group minerals (P.M. Kartashov, pers. commun., 2005).

With very few exceptions, the REE silicates mentioned are found elsewhere within intrusions (alkaline or cabonatitic) or closely associated with such rocks in exocontact zones. In the Bastnäs-type deposits, the REE mineralization bears no direct spatial relationship to magmatic systems, although Geijer (1961) proposed a genetic link to the intrusive processes forming the early (orogenic) granitic rocks in Bergslagen. The Swedish deposits thus remain quite unique in being essentially exoskarns in carbonate protoliths of sedimentary origin. A common feature is mineral formation at relatively high temperatures (Holtstam *et al.* 2006) by carbonate–silica reactions.

The Trimouns talc deposit, Midi-Pyrénées, France, is interesting in this context, as it contains characteristic rare species, both Ce- and Y-dominant, like dissakisite-(Ce), parisite-(Ce), törnebohmite-(Ce), gadolinite-(Y) and hingganite-(Y), associated with a dolomitic rock (de Parseval *et al.* 1997). The proposed genetic mechanism includes the release of REE from primary allanite during large-scale formation of chlorite and talc.

The division of Bastnäs-type deposits into two subtypes was proposed on the basis of preliminary mineral analyses (Holtstam & Andersson 2002). In subtype 1, the Rödbergsgruvan and Bastnäs deposits, REE mineral assemblages are dominated by cerite-(Ce), ferriallanite-(Ce) and bastnäsite-(Ce). In subtype 2, represented by deposits in the Norberg District, cerite-(Ce) is relatively rare; instead fluorbritholite-(Ce) and Y-dominant species occur. The main gangue mineral is tremolite–actinolite in the Bastnäs-type deposits. In addition, norbergite, chondrodite, fluorophlogopite and fluorite occur in close association with the REE minerals in subtype-2 deposits, where sulfide mineralization is less prominent than in subtype 1.

The proposed division now appears to be well justified. For all mineral groups compared, the most Y-rich average compositions are found in subtype-2 deposits,
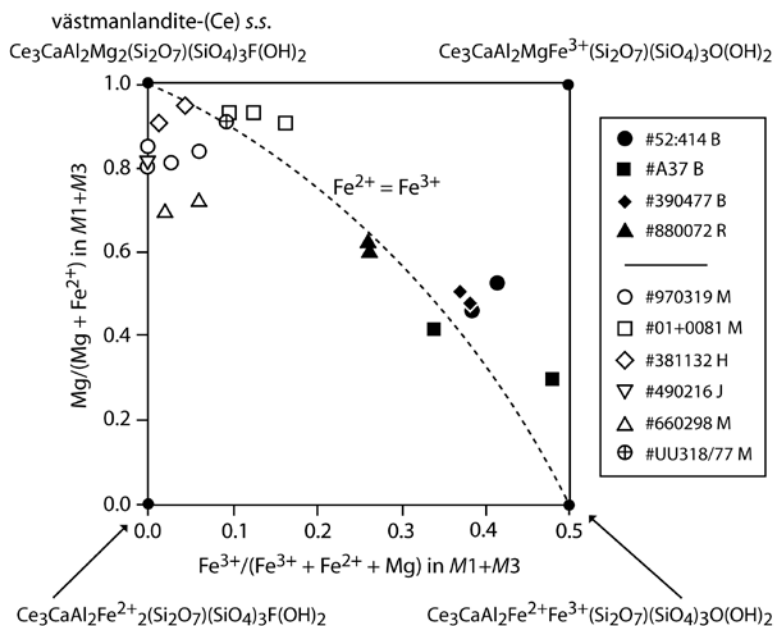
FIG. 20.   Compositional diagram for västmanlandite and isotypic minerals. Filled symbols: subtype 1 (Bastnäs, Rödbergsgruvan), open symbols: subtype 2 (Norberg District).

and this also holds for most of the HREE. In addition, a characteristic dichotomy is observed for the epidote and västmanlandite groups of minerals: members dominated by Fe (ferriallanite and the Fe-analogue of västmanlandite) are restricted to the type-1 deposits, whereas Mg- and F-rich members (dollaseite and väst-manlandite) belong to subtype 2. Thus, in general, the type-1 deposits are enriched in La, Ce, Fe, relative to the type-2 deposits, which in turn are enriched in Y, Mg, Ca, and F, which have governed the development of characteristic parageneses.

A preliminary genetic interpretation of the two subtypes that explains some of the prominent differences involves two factors. 1) There are variations in the concentration of F in the REE-bearing mineralizing fluids. High initial concentrations are assumed for subtype 2, where characteristic F-rich assemblages with fluorite and norbergite have developed. It is an established fact that the stability of HREE and Y complexes with fluoride in hydrothermal fluids is greater than that of the LREE (Haas *et al.* 1995, Bau & Dulski 1995). 2) Differences occur in the fluid:rock ratio. Lower values were associated with the subtype-2 deposits, where there are significant carbonate remnants in the REE-bearing skarn assemblages. This can to some extent explain the generally higher Mg-contents, where the element is obtained from primary dolomite. Probably for the same reason, minerals with Ca in their ideal formula also seem to be favored in subtype 2 (*e.g.,* fluorbritholite, parisite), compared to subtype 1 (*e.g.,* fluocerite, törnebohmite).

Paragenetic sequences determined from textural relations in type-1 deposits indicate that cerite is normally the first REE mineral to crystallize, and also has the highest REE contents. The REE thus initially entered the carbonate rock as components within a Si- and F-rich aqueous fluid (carrying also some Cl, incorporated in the cerite; *cf.* Table 3a). Assuming dolomite as the reactant carbonate, a generalized mass-balance reaction for the initial formation of cerite may take the form [where (fl) implies availibility in the aqueous fluid phase, and Ln^{3+} denotes REE and Y]:

$$0.8 \text{ CaMg(CO}_3)_2 + 10 \text{ Ln}^{3+}(fl) + 7.275 \text{ SiO}_4^{4-}(fl) +$$
dolomite
$$2.1 \text{ HF}(fl) + 0.1 \text{ Fe}^{3+}(fl) + 0.95 \text{ H}_2\text{O} =$$

$$\text{Ln}_{8.4}\text{Ca}_{0.8}\text{Mg}_{0.7}\text{Fe}^{3+}_{0.1}\text{Si}_7\text{O}_{24}\text{F}_{1.5}(\text{OH})_4\text{O}_{1.5} +$$
cerite
$$1.6 \text{ LnCO}_3\text{F} + 0.275 \text{ SiO}_2 + 0.1 \text{ Mg}^{2+}(fl)$$
bastnäsite   quartz
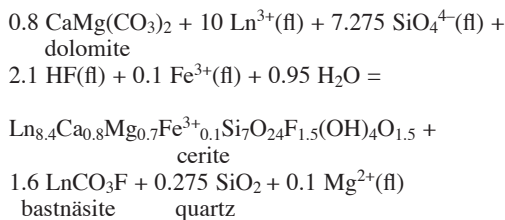
where no significant open-system mobilization of Mg and Fe is required. The formation of associated bastnäsite and minor quartz is supported texturally. Thus it is likely that the REE were transported into the carbonate horizons complexed mainly by anions with F and Si (and probably Cl, to a minor extent). The anion ligands

containing F are very efficient complexing agents of REE in hydrothermal solutions over a wide range of pH values, whereas Cl-containing ligands should be important only at acidic conditions (Wood 1990, Haas *et al.* 1995). Silicon occurs mainly as H_4SiO_4 in acid to neutral aqueous solutions (Dove & Rimstidt 1994), but the behavior of the REE cations with anion complexes of Si appears to be virtually unknown, and if occurring in solutions together with F, ligands of F will be more efficient in complexing cations (Robertson & Barnes 1978). The latter authors determined a high stability of the complex SiF_6^{2-} at acidic conditions, and it may have played some role as a complexing agent in the fluids responsible for Bastnäs-type mineralization.

Subsequently, the cerite was altered mainly to ferriallanite (in cases preceded by the Fe-rich analogue to västmanlandite) + törnebohmite + bastnäsite by the reaction with a fluid carrying major amounts of Si, Fe, Al, F, Ca, and CO_2 (the latter two from reactions with carbonate), that can be schematically given as:

$$\text{Ln}_{8.4}\text{Ca}_{0.8}\text{Mg}_{0.7}\text{Fe}^{3+}_{0.1}\text{Si}_7\text{O}_{24}\text{F}_{1.5}(\text{OH})_4\text{O}_{1.5}$$
cerite
$$+ 2.8 \text{ CaCO}_3 + 7.9 \text{ Fe}^{2+/3+}(fl) +$$
calcite

$$0.1 \text{ Mg}^{2+}(fl) + 3.8 \text{ Al}^{3+}(fl) + 8.5 \text{ SiO}_4^{4-}(fl)$$
$$+ 1.3 \text{ HF}(fl) =$$

$$4 \text{ Ln}_{1.1}\text{Ca}_{0.9}\text{Fe}_2^{2+/3+}\text{Mg}_{0.2}\text{Al}_{0.8}\text{Si}_3\text{O}_{12}\text{F}_{0.1}(\text{OH})_{0.9} +$$
ferriallanite

$$0.76 \text{ Ln}_{2.1}\text{Al}_{0.8}\text{Mg}_{0.05}\text{Fe}_{0.05}^{3+}\text{Si}_2\text{O}_8(\text{OH}) +$$
törnebohmite
$$2.8 \text{ LnCO}_3\text{F} + 2 \text{ SiO}_2 + 0.95 \text{ H}_2\text{O}$$
bastnäsite   quartz
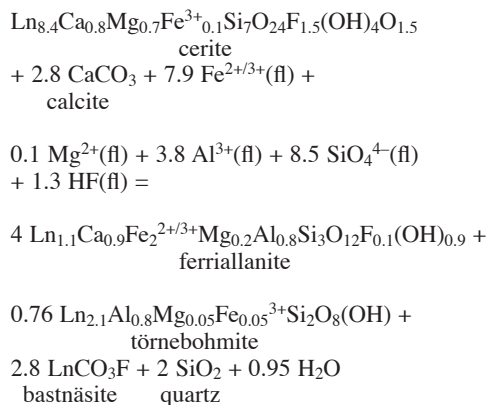
Similarly, this mass-balance reaction indicates that the main complexing anions are F^- and Si-bearing species. Carbonic species probably also are active in redistributing the REE. In some cases, the ferriallanite is in textural equilibrium with bastnäsite, whereas in other cases, it is partly replaced together with törnebohmite.

In type-2 deposits, the primary REE phase is normally fluorbritholite (also richest in REE), likewise suggesting Si- and F-rich early fluids, possibly also carrying some Cl. If the Ca content is considered to be derived by a reaction between the REE-bearing fluid and the host carbonates, a tentative mass-balance reaction may appear as:

$$1.25 \text{ CaMg(CO}_3)_2 + 3.5 \text{ Ln}^{3+}(fl) + 3 \text{ SiO}_4^{4-}(fl) +$$
dolomite
$$0.7 \text{ HF}(fl) + 0.03 \text{ HCl}(fl) =$$

$$\text{Ln}_{3.5}\text{Ca}_{1.25}\text{Si}_3\text{O}_{12}\text{F}_{0.7}(\text{OH})_{0.27}\text{Cl}_{0.03} +$$
fluorbritholite
$$1.25 \text{ Mg}^{2+}(fl) + 2 \text{ CO}_2(fl) + 0.23 \text{ H}_2\text{O}$$
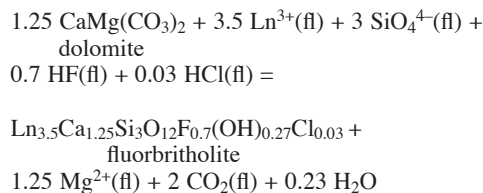
If the reacting carbonate is dolomite, the excess Mg released may be available for the britholite-alteration reaction considered below. Textural relations indicate that the fluorbritholite is altered primarily to västmanlandite, dissakisite–dollaseite, gadolinite, and fluorocarbonates, suggesting the addition of Si, Al, Fe, Be, F, Mg, Ca, and CO_2 (the latter three presumably from reaction with carbonate), schematically (omitting gadolinite):

4 $Ln_{3.5}Ca_{1.25}Si_3O_{12}F_{0.7}(OH)_{0.27}Cl_{0.03}$ +
    fluorbritholite
4.6 $CaCO_3$ + 8.45 Mg^{2+}(fl) +
  calcite

6.2 $Fe^{2+/3+}$(fl) + 8.35 Al^{3+}(fl) + 13 SiO_4^{4-}(fl) +
5.3 HF(fl) =

2 $Ln_{3.15}Ca_{0.85}Mg_{1.6}Fe^{2+}_{0.4}Fe^{3+}_{0.2}Al_{1.8}$
$Si_5O_{19}F_{0.75}(OH)_{2.25}$ +
västmanlandite

5 $Ln_{1.1}Ca_{0.9}Mg_{1.05}Fe^{2+}_{0.5}Fe^{3+}_{0.5}Al_{0.95}$
$Si_3O_{11}F_{0.4}(OH)_{1.6}$ +
dissakisite–dollaseite

1.1 $Ln_2Ca(CO_3)_3F_2$ + 2.3 CaF_2 + 1.3 CO_2(fl) +
    parisite   fluorite
0.12 HCl(fl)
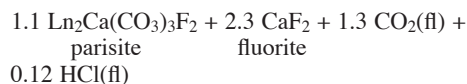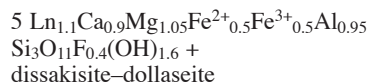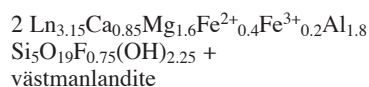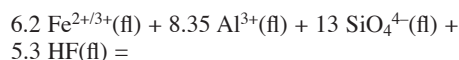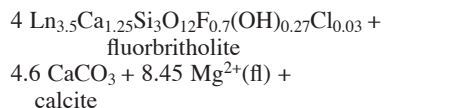
The fluids responsible for further alteration in type-2 deposits must thus also have been dominated by F and Si as complexing agents (supplemented by CO_2 released from reacting carbonates). Fluorine is known to be an efficient complexing agent for Al, Fe, and Mg in hydrothermal waters (*e.g.,* Robertson & Barnes 1978). The occurrence of fluorite in association with the secondary REE minerals confirms a high activity of F. The presence of phases such as mineral E suggests that a significant amount of Cl also was available here, but not generally incorporated in the major minerals.

In both type-1 and type-2 deposits, the initial precipitation of the REE silicates (cerite and fluorbritholite, respectively) was accomplished by a reaction between relatively acidic solutions, carrying major amounts of REE complexed mainly by ligands of F and Si, and the carbonate host-rocks. This reaction released CO_2, raised the pH, and triggered the crystallization of the REE phases. The initial fluids that entered the carbonate horizons were poor in Ca, preventing the precipitation of stable fluorite and keeping the F activity high, promoting the complexing of the other cations in the fluid (*cf.* Salvi & Williams-Jones 1996, Williams-Jones *et al.* 2000). Where the fluid reacted with the carbonates, fluorite and fluorocarbonate crystallization lowered the activities of F and CO_2, promoting the precipitation of the REE silicates (*e.g.,* Gieré 1996). The secondary assemblages are characterized by an additional supply of major rock-forming elements (Fe and minor Al in type 1, whereas Mg, Al, and Fe were added in type 2) and a dilution of the primary REE concentration. This dilution must have been accomplished by reactions between the primary REE minerals and gangue minerals such as carbonates, amphibole and magnetite, aided by the changing hydrothermal fluids. The fluid also contained an appreciable amount of S, as shown by the associated sulfides. However, sulfur must have played only a subordinate role in complexing the REE in the presence of F (Wood 1990, Gieré 1993).

Element fractionation

For some of the minerals analyzed here, there is obviously a strong crystallographic control on the incorporation of REE; bastnäsite and the epidote-group minerals display little variation in their chondrite-normalized patterns, and for cerite, the variations are moderate. Because of its flexible apatite-type structure, fluorbritholite is a very variable mineral in terms of REE composition. Together with gadolinite, it has proved useful as an indicator of REE fractionation within this type of deposit.

The median values of La/Ce and La/Nd obtained for the present datasets (a total of 202 analyses presented in the tables, unnamed minerals not included), 0.48 and 1.0, are similar to those obtained on the basis of element abundances in the average upper crust, 0.47 and 1.2, respectively (Henderson 1996). There is, however, a large spread, 0.16–1.4 for La/Ce and 0.08–10 for La/Nd, respectively, indicating substantial fractionation of these elements on a local scale within the Bastnäs-type deposits. To a significant extent, this fractionation is dependent on crystal-chemical properties of the individual minerals. The generally low values in gadolinite are clearly related to structural features; the 8-coordinated REE sites more easily accept the intermediate-size ions, in comparison to most other mineral species found here, in which REE coordination numbers are higher (9 to 10). However, wide variations also occur for specific minerals, even within a single sample or grain, indicating changing compositions of the fluid during crystallization. The sample from the Östanmossa deposit, where "fluorbritholite-(Y)" occurs in a carbonate vein transecting dollaseite-bearing amphibole skarns (#430644), is notable in this respect. The HREE and Y seem to have become enriched in the fluid phase toward the later stages of REE mineralization.

Smith *et al.* (2000) have discussed fractionation of La and Nd during hydrothermal mineral-forming processes, using data from the Bayan Obo REE deposit in China. According to their model, variations in the relative proportions of these elements are primarily related to REE speciation in the fluids and temperature conditions. At high temperatures (>250°C) and in a CO_2-rich fluid, La-bearing fluoride complexes have a higher association-constant than, for example, for Nd, promoting the observed fractionation. In an aqueous

fluid, the stability of the REE complexes tends to increase with atomic number for the REE. Bastnäsite is the mineral in our suite that shows the widest ranges in La/Nd, starting from about crustal values and going to the maximum ratios encountered. Preliminary fluid-inclusion data for bastnäsite from Bastnäs (Holtstam & Broman 2002, Holtstam *et al*. 2006) indeed show that mineral formation involved carbonic fluids at temperatures up to 400°C, at a stage of fluid immiscibility. The rapidly changing conditions that would prevail in boiling hydrothermal fluids provide an explanation for the large compositional variations found on the micro-scale of some bastnäsite grains.

Positive Y anomalies, expressed as exceptionally high Y/Dy values (Dy^{3+} being the ion most similar to Y^{3+} in terms of ionic radius) of up to 100, are commonly encountered in F-rich mineral assemblages, particularly in pegmatite parageneses. Such anomalies have been ascribed to fractionation of Y over the REE during fluid transport, related to the significantly higher (experimentally determined) stability-constants for YF^{2+} complexes (Gramaccioli *et al*. 1999). For those mineral analyses given in the present work, where both the Y and Dy concentrations are significantly above the detection level (94 of 202), the average Y/Dy value is 10.7 (range 4–22), *i.e.*, close to the values for the continental crust, 9.8, and average chondrite, 10.3 (Henderson 1996). There is a good linear correlation ($r^2 = 0.76$) for Y *versus* Dy in our data, with a slope of *ca*. 9, and thus no strong fractionation of Y relative the HREE is indicated for the samples from the Bastnäs-type deposits. In our opinion, some yet unknown conditions in the mineral-forming fluids were essentially different from those responsible for Y–F mineralization in the pegmatite environments.

The Bastnäs-type deposits, although economically insignificant by modern standards, share many characteristics with the genetically diversified, intrusion-related Fe oxide – Cu – Au – REE deposits of the Olympic Dam type (Holtstam & Ensterö 2002, Holtstam & Broman 2002). In contrast to the previously recognized members of this class, in which U and Th typically are associated with the HREE (*e.g.,* Lottermoser 1995), the Bastnäs-type deposits show depletion of actinides. Although small amounts of uraninite associated with asphalt (which probably is a late impregnation) occur in the Bastnäs mines, our data here have revealed exceptionally low U and Th contents (below the detection limit of the EMP) in gadolinite, fluorbritholite and the allanite-group minerals. These phases are normally significantly enriched in the actinides, and as a consequence commonly metamict, which is not the case here. As U and Th are expected to be transported in a similar fashion as the REE in hydrothermal fluids (Smith *et al*. 2002), the lack of these elements might be dependent on the nature of the source or fluid composition in the case of the Bastnäs-type deposits. The explanation to the enigmatic deficiency of U and Th in the Bastnäs-type deposits could tentatively be sought in the earlier stages of the development of the mineralizing fluid. Uranium and Th may have been fractionated from the REE, as has been observed in some cases (*e.g.,* Lira & Ripley 1990). If the hydrothermal fluids were rich in Si, U and Th, silicates such as uranothorite may have precipitated early owing to their higher stability, *i.e.,* before the fluids reached the carbonate rocks acting as traps for the REE.

References

ALLEN, R.L., LUNDSTRÖM, I., RIPA, M., SIMEONOV A.H. & CHRISTOFFERSON, H. (1996): Facies analysis of a 1.9 Ga, continental margin, back-arc, felsic caldera province with diverse Zn–Pb–Ag–(Cu–Au) sulphide and Fe oxide deposits, Bergslagen region, Sweden. *Econ. Geol*. **91**, 979-1008.

AMBROS, M. (1983): Beskrivning till berggrundskartan Lindesberg NO. *Sver. Geol. Undersök*. **Af 141**, 1-75 (in Swedish).

AMBROS, M. (1988): Beskrivning till berggrundskartorna Avesta NV och SV. *Sver. Geol. Undersök.,* **Af 152-153**, 1-84 (in Swedish).

ANDERSSON, U.B. & ÖHLANDER, B. (2004): The late Svecofennian magmatism. *In* The Transscandinavian Igneous Belt (TIB) in Sweden; a Review of its Character and Evolution (K. Högdahl, U.B. Andersson & O. Eklund, eds.). *Geol. Surv. Finland, Spec. Pap*. **37**, 102-104.

ARDEN, K.M & HALDEN, N.M. (1999): Crystallization and alteration history of britholite in rare-earth-element-enriched pegmatitic segregations associated with the Eden Lake Complex, Manitoba, Canada. *Can. Mineral*. **37**, 1239-1253.

ATENCIO, D., BEVINS, R.E., FLEISCHER, M., WILLIAMS, C.T. & WILLIAMS, P.A. (1989): Revision of the lanthanite group and new data for specimens from Bastnäs, Sweden, and Bethlehem, USA. *Mineral. Mag*. **53**, 639-642.

BAU, M. & DULSKI, P. (1995): Comparative study of yttrium and rare-earth element behaviours in fluorine-rich hydrothermal fluids. *Contrib. Mineral. Petrol*. **119**, 213-223.

BERZELIUS, J.J. (1825): Kohlensaures cereroxydul. *Z. Mineral.* **2**, 209.

BEUKES, G.J., DE BRUIYN, H. & VAN DER WESTHUIZEN, W.A. (1991): Fluocerite and associated minerals from the Baviaanskranz granite pegmatite near Kakamas South Africa. *S. Afr. J. Geol.* **94**, 313-320.

BEVINS, R.E., ROWBOTHAM, G., STEPHENS, F.S., TURGOOSE, S. & WILLIAMS, P.A. (1985): Lanthanite-(Ce), $(Ce,La,Nd)_2(CO_3)_3 \cdot 8H_2O$, a new mineral from Wales, UK. *Am. Mineral.* **70**, 411-413.

BOYNTON, W.V. (1984): Geochemistry of the rare earth elements: meteorite studies. *In* Rare Earth Element Geochemistry (P. Henderson, ed.). Elsevier, Amsterdam, The Netherlands (63-114).

CARLBORG, H. (1923): Ekonomisk-teknisk beskrivning. *In* Riddarhytte malmfält i Skinnskattebergs socken i Västmanlands län. Kungl. Kommerskollegium & Sveriges Geologiska Undersökning. Victor Pettersson, Stockholm, Sweden (in Swedish).

CHAKHMOURADIAN, A.R. & ZAITSEV, A.N. (2002): Calcite – amphibole – clinopyroxene rock from the Afrikanda Complex, Kola Peninsula, Russia: mineralogy and a possible link to carbonatites. III. Silicate minerals. *Can. Mineral.* **40**, 1347-1374.

CRONSTEDT, A.F. (1751): Rön och försök giorde med trenne järnmalms arter. *K. Vetenskaps Akademiens Handlingar* **12**, 226-232.

DAL NEGRO, A., ROSSI, G. & TAZZOLI, V. (1977): The crystal structure of lanthanite. *Am. Mineral.* **62**, 142-146.

DELLA VENTURA, G., WILLIAMS, C.T., CABELLA, R., OBERTI, R., CAPRILLI, E. & BELLATRECCIA, F. (1999): Britholite–hellandite intergrowths and associated REE-minerals from the alkali-syenitic ejecta of the Vico volcanic complex (Latium, Italy); petrological implications bearing on REE mobility in volcanic systems. *Eur. J. Mineral.* **11**, 843-854.

DEMARTIN, F., MINAGLIA, A. & GRAMACCIOLI, C.M. (2001): Characterization of gadolinite-group minerals using crystallographic data only: the case of hingganite-(Y) from Cuasso al Monte, Italy. *Can. Mineral.* **39**, 1105-1114.

DEMARTIN, F., PILATI, T., DIELLA, V., GENTILE, P. & GRAMACCIOLI, C.M. (1993): A crystal-chemical investigation of alpine gadolinite. *Can. Mineral.* **31**, 127-136.

DE PARSEVAL, P., FONTAN, E. & AIGOUY, T. (1997): Composition chimique des minéraux de terres rares de Trimouns (Ariège, France). *C.R. Acad. Sci. Paris, Ser.* **Ua 324**, 625-630.

DOVE, P.M. & RIMSTIDT, J.D. (1994): Silica–water interactions. *In* Silica (P.J. Heaney, ed.). *Rev. Mineral.* **29**, 259-308.

ENSTERÖ, B. (2003): *En mineralogisk studie av sulfidparageneser i Nya Bastnäsfältets lantanidmalmer, Riddarhyttan, Bergslagen.* M.Sc. thesis, Stockholm University, Stockholm, Sweden.

ERCIT, T.S. (2002): The mess that is "allanite". *Can. Mineral.* **40**, 1411-1419.

FÖRSTER, H.-J. (2000): Cerite-(Ce) and thorian synchysite-(Ce) from the Niederbobritzsch granite, Erzgebirge, Germany: implications for the differential mobility of the *LREE* and Th during alteration. *Can. Mineral.* **38**, 67-79.

GEIJER, P. (1921): The cerium minerals of Bastnäs at Riddarhyttan. *Sver. Geol. Undersök* **C304**, 1-24.

GEIJER, P. (1923): Geologisk beskrivning. *In* Riddarhytte malmfält i Skinnskattebergs socken i Västmanlands län. Kungl. Kommerskollegium & Sveriges Geologiska Undersökning. Victor Pettersson, Stockholm, Sweden (in Swedish).

GEIJER, P. (1927): Some mineral associations from the Norberg district. *Sver. Geol. Undersök* **C343**, 1-32.

GEIJER, P. (1936): Norbergs berggrund och malmfyndigheter. *Sver. Geol. Undersök* **Ca24**, 1-162.

GEIJER, P. (1961): The geological significance of the cerium mineral occurrences of the Bastnäs type in central Sweden. *Arkiv Mineral. Geol.* **3**, 99-105.

GEIJER, P. & MAGNUSSON, N.H. (1944): De mellansvenska järnmalmernas geologi. *Sver. Geol. Undersök* **Ca 35**, 1-654 (in Swedish).

GIERÉ, R. (1993): Transport and deposition of REE in H_2S-rich fluids: evidence from accessory mineral assemblages. *Chem. Geol.* **110**, 251-268.

GIERÉ, R. (1996): Formation of rare earth minerals in hydrothermal systems. *In* Rare Earth Minerals, Chemistry, Origin and Ore Deposits (A.P. Jones, F. Wall & C.T. Williams, eds.). *The Mineralogical Society Ser.* **7**. Chapman & Hall, London, U.K. (105-150).

GIERÉ, R. & SORENSEN, S.S. (2004): Allanite and other REE-rich epidote minerals. *In* Epidotes (A. Liebscher & G. Franz, eds.). *Rev. Mineral. Geochem.* **56**, 431-493.

GRAMACCIOLI, C. M., DIELLA, V. & DEMARTIN, F. (1999): The role of fluoride complexes in REE geochemistry and the importance of 4*f* electrons: some examples in minerals. *Eur. J. Mineral.* **11**, 983-992.

GRICE, J.D. & GAULT, R.A. (2006): Johnsenite-(Ce), a new member of the eudialyte group from Mont Saint-Hilaire, Quebec, Canada. *Can. Mineral.* **44**, 105-115.

GU JIEXIANG, CHAO, G.Y. & TANG SUREN (1994): A new mineral – fluorbritholite-(Ce). *J. Wuhan Univ. of Technol.* **9**(3), 9-14.

HAAS, J.R., SHOCK, E.L. & SASSANI, D.A. (1995): Rare earth elements in hydrothermal systems: estimates of standard partial molal thermodynamic properties of aqueous com-

plexes of the rare earth elements at high pressures and temperatures. *Geochim. Cosmochim. Acta* **59**, 4329-4350.

HALLBERG, A. (2003): Styles of hydrothermal alteration and accompanying chemical changes in the Sången formation, Bergslagen, Sweden, and adjacent areas. *In* Economic Geology Research and Documentation **2**, 2001-2002. *Sver. Geol. Undersök.*, *Rapp. Medd.* **113**, 4-35.

HENDERSON, P. (1996): The rare earth elements: introduction and review. *In* Rare Earth Minerals. Chemistry, Origin and Ore Deposits (A.P. Jones, F. Wall & C.T. Williams, eds.). *The Mineralogical Society Ser.* **7**. Chapman & Hall, London, U.K. (1-19).

HISINGER, W. (1838): Analyser av några svenska mineralier. 2. Basiskt fluor-cerium från Bastnäs. *Kungl. Vetenskaps-Akademiens Handlingar* **187**, 1-9.

HISINGER, W. & BERZELIUS, J.J. (1804): *Cerium, en ny Metall, funnen i Bastnäs Tungsten från Riddarhyttan i Westman-land.* Henrik A. Nordström, Stockholm, Sweden.

HOLTSTAM, D. & ANDERSSON, U.B. (2002): Rare earth mineral-ogy of Bastnäs-type Fe–REE(–Cu–Mo) deposits in Berg-slagen, Sweden. *Int. Mineral. Assoc., 18th Gen. Meeting* (*Edinburgh*), *Abstr.*, 282.

HOLTSTAM, D., ANDERSSON, U. & MANSFELD, J. (2003b): Ferriallanite-(Ce) from the Bastnäs deposit, Västmanland, Sweden. *Can. Mineral.* **41**, 1233-1240.

HOLTSTAM, D. & BROMAN, C. (2002): Lanthanide mineralizations of Bastnäs type: overview and new data. *GFF* **124**, 230-231.

HOLTSTAM, D., BROMAN, C., MANSFELD, J. & ANDERSSON, U.B. (2006): Tracking ore-forming fluids in Bastnäs-type REE deposits. *Twenty-Seventh Nordic Geological Winter Meeting* (*Oulu*). *Bull. Geol. Soc. Finland, Spec. Issue* **1** (s. 53), *suppl.* s. 2.

HOLTSTAM, D. & ENSTERÖ, B. (2002): Does the Bastnäs REE deposit in central Sweden belong to the Fe oxide–Cu–U–Au–REE class of ores? *Twenty-Fifth Nordic Geological Winter Meeting* (*Reykjavík*), *Abstr. Vol.*, 83.

HOLTSTAM, D., GRINS, J. & NYSTEN, P. (2004): Håleniusite-(La) from the Bastnäs deposit, Västmanland, Sweden: a new REE oxyfluoride mineral species. *Can. Mineral.* **42**, 1097-1103.

HOLTSTAM, D., KOLITSCH, U. & ANDERSSON, U.B. (2005): Västmanlandite-(Ce) – a new lanthanide- and F-bearing sorosilicate mineral from Västmanland, Sweden: descrip-tion, crystal structure, and relation to gatelite-(Ce). *Eur. J. Mineral.* **17**, 129-141.

HOLTSTAM, D., NORRESTAM, R. & ANDERSSON, U.B. (2003a): Percleveite-(Ce), a new lanthanide disilicate mineral from Bastnäs, Skinnskatteberg, Sweden. *Eur. J. Mineral.* **15**, 725-731.

IMAOKA, T. & NAKASHIMA, K. (1994): Fluocerite in a peral-kaline rhyolite dyke from Cape Ashizuri, Shikoku Island, southwest Japan. *Neues Jahrb. Mineral., Monatsh.*, 529-539.

JERNBERG, P. & SUNDQVIST, T. (1983): A versatile Mössbauer analysis program. *Inst. of Physics Rep., Univ. Uppsala* **UUIP-1090**.

KAPUSTIN, YU.L. (1989): Cerite and törnebohmite from fenites in the alkaline Tuva massifs. *Zap. Vses. Mineral. Obsh-chest.* **118**(4), 47-56 (in Russ.).

KONEV, A., PASERO, M., PUSHCHAROVSKY, D., MERLINO, S., KASHAEV, A., SUVOROVA, L., USHCHAPOVSKAYA, Z., NAR-TOVA, N., LEBEDEVA, Y. & CHUKANOV, N. (2005): Biraite-(Ce), $Ce_2Fe^{2+}(CO_3)(Si_2O_7)$, a new mineral from Siberia with a novel structure type. *Eur. J. Mineral.* **17**, 715-721.

LAHTI, S.I. & SUOMINEN, V. (1988): Occurrence, crystallogra-phy and chemistry of the fluocerite – bastnaesite – cerianite intergrowth from the Fjaelskaer Granite, southwestern Finland. *Bull. Geol. Soc. Finland* **60**, 45-53.

LIEBSCHER, A. (2004): Spectroscopy of epidote-group miner-als. *In* Epidotes (A. Liebscher & G. Franz, eds.). *Rev. Mineral. Geochem.* **56**, 125-170.

LIFEROVICH, R.P. & MITCHELL, R.H. (2006): Apatite-group minerals from nepheline syenite, Pilansberg alkaline com-plex, South Africa. *Mineral. Mag.* **70**, 463-484.

LINDH, A. & PERSSON, P.-O. (1990): Proterozoic granitoid rocks of the Baltic shield - trends of development. *In* Mid-Proterozoic Laurentia–Baltica (C.F. Gower, T. Riv-ers & A.B. Ryan, eds.). *Geol. Assoc. Can., Spec. Pap.* **38**, 23-40.

LIRA, R. & RIPLEY, E.M. (1990): Fluid inclusion studies of the Rodeo de Los Molles REE and Th deposit, Las Chacras batholith, central Argentina. *Geochim. Cosmochim. Acta* **54**, 663-671.

LOTTERMOSER, B.G. (1995): Rare earth element mineralogy of the Olympic Dam Cu–U–Au–Ag deposit, Roxby Downs, South Australia: implications for ore genesis. *Neues Jahrb. Mineral., Monatsh.*, 371-384.

LUNDSTRÖM, I. & KOARK, H.J. (1979): Beskrivning till berg-grundskartan Lindesberg SV. *Sver. Geol. Undersök.* **Af 126**, 1-75 (in Swedish).

MALCZEWSKI, D. & JANECZEK, J. (2002): Activation energy of annealed, metamict gadolinite from ^{57}Fe Mössbauer spec-troscopy. *Phys. Chem. Minerals* **29**, 226-232.

MANDARINO, J.A. & BACK, M.L. (2004): *Fleischer's Glossary of Mineral Species.* The Mineralogical Record, Tucson, Arizona.

MOORE, P.B. & SHEN, J. (1983): Cerite, $RE_9(Fe^{3+},Mg)$ $(SiO_4)_6(SiO_3)(OH)(OH)_3$; its crystal structure and relation to whitlockite. *Am. Mineral.* **68**, 996-1003.

Ni, Yunxiang, Hughes, J.M. & Mariano, A.N. (1993): The atomic arrangement of bastnäsite-(Ce), Ce(CO$_3$)F, and structural elements of synchisite-(Ce), röntgenite-(Ce), and parisite-(Ce). *Am. Mineral.* **78**, 415-418.

Ni, Yunxiang, Post, J.E. & Hughes, J.M. (2000): The crystal structure of parisite-(Ce), Ce$_2$CaF$_2$(CO$_3$)$_3$. *Am. Mineral.* **85**, 251-258.

Noe, D.C., Hughes, J.M., Mariano, A.N., Drexler, J.W. & Kato, A. (1993): The crystal structure of monoclinic britholite-(Ce) and britolite-(Y). *Z. Kristallogr.* **206**, 233-246.

Novak, G.A. & Colville, A.A. (1989): A practical interactive least-squares cell-parameter program using an electronic spreadsheet and a personal computer. *Am. Mineral.* **74**, 488-490.

Oberti, R., Ottolini, L., Della Ventura, G. & Parodi, G.C. (2001): On the symmetry and crystal chemistry of britholite: new structural and microanalytical data. *Am. Mineral.* **86**, 1066-1075.

Pakhomovsky, Y.A., Men'shikov, Y.P., Yakovenchuk, V.N., Ivanyuk, G.Yu., Krivovichev, S.V. & Burns, P.C. (2002): Cerite-(La), (La,Ce,Ca)$_9$(Fe,Ca,Mg)(SiO$_4$)$_3$ [SiO$_3$OH]$_4$(OH)$_3$, a new mineral from the Khibina alkaline massif: occurrence and crystal structure. *Can. Mineral.* **40**, 1177-1184.

Pan, Yuanming & Fleet, M. (2002): Compositions of the apatite-group minerals: substitution mechanisms and controlling factors. *In* Phosphates - Geochemical, Geobiological, and Materials Importance (M.L. Kohn, J. Rakovan & J.M. Hughes, eds.). *Rev. Mineral. Geochem.* **48**, 13-49.

Peacor, D.R. & Dunn, P.J. (1988): Dollaseite-(Ce) (magnesium orthite redefined): structure refinement and implications for F + M^{2+} substitutions in epidote-group minerals. *Am. Mineral.* **73**, 838-842.

Pezzotta, F., Diella, V. & Guastoni, A. (1999): Chemical and paragenetic data on gadolinite-group minerals from Baveno and Cuasso al Monte, southern Alps, Italy. *Am. Mineral.* **84**, 782-789.

Poitrasson, F. (2002): In situ investigations of allanite hydrothermal alteration: examples from calc-alkaline and anorogenic granite of Corsica (southeast France). *Contrib. Mineral. Petrol.* **142**, 485-500.

Pouchou, J.L. & Pichoir, F. (1991): Quantitative analysis of homogeneous or stratified microvolumes applying the model "PAP". *In* Electron Probe Quantitation (K.F.J. Heinrich & D.E. Newbury, eds.). Plenum Press, New York, N.Y. (31-75).

Robertson, C.E. & Barnes, R.B. (1978): Stability of fluoride complex with silica and its distribution in natural water systems. *Chem. Geol.* **21**, 239-256.

Romer, R.L. & Smeds, S.-A. (1997): U–Pb columbite chronology of post-kinematic Palaeoproterozoic pegmatites in Sweden. *Precamb. Res.* **82**, 85-99.

Rouse, R.C. & Peacor, D.R. (1993): The crystal structure of dissakisite-(Ce), the Mg analogue of allanite-(Ce). *Can. Mineral.* **31**, 153-157.

Salvi, S. & Williams-Jones, A.E. (1996): The role of hydrothermal processes in concentrating high-field strength elements in the Strange Lake peralkaline complex, northeastern Canada. *Geochim. Cosmochim. Acta* **60**, 1917-1932.

Segalstad, T.V. & Larsen, A.O. (1978): Gadolinite-(Ce) from Skien, southwestern Oslo region, Norway. *Am. Mineral.* **63**, 188-195.

Shen, J. & Moore, P.B. (1982): Törnebohmite, RE$_2$Al(OH)[SiO$_4$]$_2$: crystal structure and genealogy of RE(III)Si(IV) = Ca(II)P(V) isomorphisms. *Am. Mineral.* **67**, 1021-1028.

Sipovalov, Yu. & Stepanov, A.V. (1971): X-ray structural study of rowlandite. *Issled. Oblast. Khim. Fiz. Metod. Anal. Syr'ya*, 189-192 (in Russ.).

Smith, M.P., Henderson, P. & Campbell, L. (2000): Fractionation of the REE during hydrothermal processes: Constraints from the Bayan Obo Fe–REE–Nb deposit, Inner Mongolia, China. *Geochim. Cosmochim. Acta* **64**, 3141-3160.

Smith, M.P., Henderson, P. & Jeffries, T. (2002): The formation and alteration of allanite in skarn from the Beinn an Dubhaich granite aureole, Skye. *Eur. J. Mineral.* **14**, 471-486.

Sorensen, S. (1991): Petrogenetic significance of zoned allanite in garnet amphibolites from a paleo-subduction zone: Catalina schist, southern California. *Am. Mineral.* **76**, 589-601.

Strunz, H. & Nickel, E.H. (2001): *Strunz Mineralogical Tables. Chemical-Structural Classification System* (9th ed.). Schweizerbarts'sche, Stuttgart, Germany.

Styles, M.T. & Young, B.R. (1983): Fluocerite and its alteration products from the Afu Hills, Nigeria. *Mineral. Mag.* **47**, 41-46.

Svyazhin, N.V. (1962): Törnebohmite from the alkaline area of the Ural. *Zap. Vses. Mineral. Obshchest.* **91**, 97-99 (in Russ.).

Trägårdh, J. (1988): Cordierite–mica–quartz schists in a Proterozoic volcanic iron ore-bearing terrain, Riddarhyttan area, Bergslagen, Sweden. *Geologie en Mijnbouw* **67**, 397-409.

Trägårdh, J. (1991): Metamorphism of magnesium-altered felsic volcanic rocks from Bergslagen, central Sweden. A transition from Mg-chlorite to cordierite-rich rocks. *Ore Geol. Rev.* **6**, 485-497.

VAN WAMBEKE, L. (1977): The Karonge rare earth deposits, Republic of Burundi: new mineralogical–geochemical data and origin of the mineralization. *Mineral. Deposita* **12**, 373-380.

WILLIAMS-JONES, A.E., SAMSON, I.M. & OLIVO, G.R. (2000): The genesis of hydrothermal fluorite–REE deposits in the Gallinas Mountains, New Mexico. *Econ. Geol.* **95**, 327-342.

WOOD, S.A. (1990): The aqueous geochemistry of the rare-earth elements and yttrium. 2. Theoretical predictions of speciation in hydrothermal solutions to 350°C at saturation water pressure. *Chem. Geol.* **88**, 99-125.